Master's thesis

NTNU
Norwegian University of Science and Technology
Faculty of Medicine and Health Sciences
Department of Clinical and Molecular Medicine

Ingrid Aass Roseth

Genetic Engineering for Revealing Underlying Mechanisms of Inflammatory Bowel Diseases

Master's thesis in Molecular Medicine
Supervisor: Atle van Beelen Granlund
May 2020

NTNU
Norwegian University of
Science and Technology

Ingrid Aass Roseth

Genetic Engineering for Revealing Underlying Mechanisms of Inflammatory Bowel Diseases

Master's thesis in Molecular Medicine
Supervisor: Atle van Beelen Granlund
May 2020

Norwegian University of Science and Technology
Faculty of Medicine and Health Sciences
Department of Clinical and Molecular Medicine

NTNU
Norwegian University of
Science and Technology

Abstract

IBD is a group of chronic, inflammatory disorders affecting the gastrointestinal tract. It consists primarily of the diseases ulcerative colitis and Crohn's disease. The underlying mechanisms are still largely unknown. However, it is accepted that the etiology is inflicted by genetics, environmental factors and microbial dysbiosis. The prevalence is increasing world-wide, both in developed and developing countries. IBD is considered as an incurable disease, and the current treatments are merely maintaining remission and relief of symptoms. Deeper insight into the causes and molecular mechanisms of IBD pathology are demanded for development of new treatment options and for targeting the disease in the individual patient with higher precision.

Organoid culture has emerged as a complex and disease-relevant research model the last decade. Stem cells derived from patient biopsies can be cultured and lead to establishment of 3D "mini-organs". Compared to cancer cell lines, intestinal organoids can to a greater extent resemble the *in vivo* composition of epithelial cells. Organoid cultures have great potential in disease modeling and discovery of gene functions by utilizing gene editing tools, such as CRISPR/Cas9 technology. However, organoids are difficult to manipulate, and development of standardized protocols are required. Lipocalin-2 (*LCN2)* is a gene highly upregulated in active IBD. It is described as an antimicrobial peptide and acute phase protein mediating host resistance towards luminal antigens. However, its contribution as a positive or negative mediator in the events of proliferation, migration and cell junction formation remains controversial.

In the current thesis, our main aim was to establish a functional and standardized procedure for gene editing in patient derived colonic organoids, more specifically we focused on the establishment of a stable *LCN2* KO cell line. HT-29 cancer cell line was used for initial experiments to establish a method which could later be applied on intestinal organoids. Gene delivery strategies such as electroporation, lipofection and lentiviral transduction were evaluated for their potential in meditating efficient transfection of nucleic acids. Furthermore, we tested transient fluorescent plasmids, siRNAs, CRISPR-plasmids and -lentiviral particles for generation of GFP-fluorescent- and LCN2-depleted cells.

Electroporation resulted in both reduced cell viability and low transfection efficiency, while lipofection on the other hand, enabled plasmid delivery in cancer cells. To improve liposomal transfection of organoids we evaluated different experimental parameters, such as disruption of the Matrigel, reagent concentrations and FCS supplementation. Despite improvements, gene editing of organoids through electroporation and liposomal transfection remained

challenging. siRNA knockdown in organoids did also not result in satisfactory results. Evaluation of these methods demonstrated lentiviral transduction as the most efficient, based on eGFP expression and western blot analysis of Cas9-transduced HT-29 cells. These results suggest that lentiviral transduction could be a more efficient gene editing strategy for organoids. However, viral transduction of organoids remains to be evaluated.

Even though we did not succeed in establishing a stable organoid or HT-29 KO cell line, we evaluated the effect of siRNA depletion of LCN2 on proliferation, migration and cell adhesion. xCELLigence, a technology measuring cellular impedance, was used to analyze HT-29 cells transfected with LCN2- or scramble siRNA. Results showed an increased cell spreading or proliferation in cells depleted of LCN2. Seen together with previous findings, these results suggest that LCN2 may not be a positive regulator of proliferation itself, but rather involved in cellular organization and cell junction formation. This should be explored in future research. Furthermore, the establishment of *LCN2* KO organoids should be further pursued as this would be a valuable tool in examination of LCN2's role upon growth and differentiation processes.

Sammendrag

Inflammatorisk tarmsykdom, også kalt IBD, er en samlebetegnelse på kronisk betennelse i tarmen. IBD består i hovedsak av ulcerøs kolitt og Crohns sykdom. De underliggende årsakene er i stor grad ukjent, men både genetikk, miljøfaktorer og tarmflora spiller inn i sykdomsdannelsen. Forekomsten av IBD øker globalt, både i vestlige land og utviklingsland. Det finnes ingen kur mot IBD, og medisinsk behandling kan kun opprettholde remisjon og lette symptomer. En dypere innsikt i årsakene og de molekylære mekanismene underlagt IBD-patologi er avgjørende for utvikling av nye behandlingsalternativer, samt medisinsk oppfølging tilpasset hver enkelt pasient.

Organoider eller “mini-tarmer” er cellemodeller utviklet det siste tiåret. Stamceller hentet fra pasientprøver kan isoleres og dyrkes til multicellulære 3D-strukturer. Sammenliknet med kreftcellelinjer, er organoider mer komplekse cellemodeller som i større grad kan etterlikne arkitekturen og sammensetning av celler sett *in vivo* hos pasienter. Genredigering, som ved hjelp av CRISPR/Cas9, kan i sammen med organoid-kultur ha stort potensiale for å avdekke funksjonen til gener viktig i sykdomssammenheng. Organoider er imidlertid svært vanskelig å manipulere, og det er et behov for standardiserte prosedyrer for genredigering av disse cellene. Lipocalin-2 (*LCN2*) er et gen kraftig oppregulert ved aktiv IBD. Det er kjent som et antimikrobielt peptid og akutt-fase protein som beskytter verten mot luminale antigener. LCN2 er videre rapportert involvert i prosesser slik som celledeling, migrasjon og dannelse av celleforbindelser. LCN2s rolle i disse prosessene er omstridt.

Hovedmålet for denne masteroppgaven var å etablere en funksjonell og standardisert prosedyre for genredigering i pasient-deriverte organoider, mer spesifikt å etablere en *LCN2* knockout cellelinje. Kreftcellelinjen HT-29 ble brukt i innledende forsøk for testing av metoder, før metodedesign så ble anvendt på organoid-kultur. Elektroporering, liposomal transfeksjon og lentiviral transduksjon ble evaluert for effektivitet av genopptak og inkorporering av nukleinsyrer. Disse metodene ble testet med fluorescerende plasmider, siRNA, CRISPR-plasmider og CRISPR-Lentivirus for etablering av GFP-fluorescerende- eller LCN2-depriverte celler.

Elektroporering førte til redusert levedyktighet hos cellene, samt lav transfeksjonseffektivitet. Liposomal transfeksjon var derimot velfungerende for plasmid-opptak i HT-29 kreftceller. Med mål om å øke effektiviteten av liposomal transfeksjon i organoider, ble ulike eksperimentelle variabler slik som fravær av Matrigel, FCS tilskudd og reagens-konsentrasjoner evaluert. Til tross for forbedringer viste både elektroporering og liposomal transfeksjon seg å ha lav effektivitet i organoider. Vi oppnådde heller ikke suksess med siRNA knockdown i organoidene. Evaluering av disse ulike metodene demonstrerte lentiviral

transduksjon som den mest effektive, basert på eGFP uttrykk og western blot analyser av Cas9-transduserte HT-29 celler. Disse resultatene antyder at transduksjon kan være den mest effektive metoden for genredigering også i organoider. Dette gjenstår å undersøke.

Til tross for at vi ikke lyktes med å etablere en stabil organoid- eller HT-29 KO cellelinje, har vi evaluert effekten av LCN2-fravær i HT-29 celler. xCELLigence ble brukt for å vurdere LCN2 sin rolle i celledeling, migrasjon og celleadhesjon. xCELLigence måler cellular impedans og ble brukt for målinger av HT-29 celler transfektert med enten LCN2- eller scramble siRNA. Våre resultater viste en økt cellespredning eller celledeling i LCN2-depriverte celler. Sett i sammenheng med tidligere funn, kan det tyde på at LCN2 ikke er en positiv regulator av celledeling i seg selv, men heller involvert i vevsorganisering og dannelse av celleforbindelser. Dette bør undersøkes i framtidige studier. Videre bør etablering av *LCN2* KO organoider følges opp, da dette vil være et verdifullt redskap for å avdekke LCN2 sin rolle i vekst og differensieringsprosesser.

Acknowledgements

This master's thesis was conducted at the Inflammatory Bowel Diseases (IBD) Research Group at Centre of Molecular Inflammation Research (CEMIR), Department of Clinical and Molecular Medicine, The Faculty of Medicine and Health Sciences at the Norwegian University of Science and Technology.

First and foremost, I wish to thank my supervisor, Atle van Beelen Granlund, for the guidance and constant encouragement throughout this period. In addition to assisting me in the lab, he has gladly taken the time to answer all my questions. He has introduced me to scientific thinking, included me in discussions, as well as giving me the freedom to explore different experimental methods. I appreciate the trust.

Furthermore, I would like to thank the rest of the IBD group, for including me in the Monday meetings and in the lunchroom. Feeling as a part of the group have been a great motivation for me. I would especially like to thank Helene Kolstad Skovdahl and Zekarias Ginbot for introducing me to the work with organoid culture, and their patience during this training.

Also, I would like to thank my family for motivating and supporting me, with a special thanks to my sister, Kristin. Working within the field of molecular medicine herself, she has been a mainstay for me during the work of this thesis, but also in life in general. Lastly, I would like to thank my roommates, for being my family number two during these years in Trondheim.

Table of Contents

Abbreviations

IBD: Inflammatory Bowel Diseases

GI: gastrointestinal

UC: ulcerative colitis

CD: Crohn's disease

EIM: extraintestinal manifestation

5-ASA: 5-aminosalisylic acid

TNFα: tumor necrosis factor alpha

IL-23: interleukin 23

HCl: hydrochloride acid

SCFAs: short chain fatty acids

ISC: intestinal stem cell

IELs: intraepithelial lymphocytes

M cell: Microfold cell

AMP: antimicrobial peptide

LCN2/ NGAL: Lipocalin-2 / Neutrophil Gelatinase-associated Lipocalin

GF: growth factor

Wnt: wingless

LP: lamina propria

IgA: immunoglobulin A

GWAS: genome-wide association study

SNP: single nucleotide polymorphism

ATG16L1: Autophagy-related 16-like 1

IRGM: Immunity-related GTPase family M

NOD2: Nucleotide-binding oligomerization domain containing 2

IL-10: interleukin 10

CARD9: caspase recruitment family member 9

MUC2: mucin 2

CDH1: E-Cadherin

NSAIDs: non-steroidal anti-inflammatory drugs

MMP-9: metalloprotease-9

EMT: epithelial to mesenchymal transition

ZO: zonula occludens

KO: knock out

UACL: Ulcer-associated cell lineage

STAT3: signal transducer and activator of transcription 3

TF: transcription factor

Tcf3: transcription factor 3

NF-κB: nuclear factor kappa-light-chain-enhancer of activated B cells

IL-1β: interleukin 1β

IL-17: interleukin 17

IL-22: interleukin 22

TGFα: transforming growth factor alpha

Poly(I:C): polyinosinic:polycytidylic acid

PRR: pattern recognition receptor

TLR3: Toll-like receptor 3

TLR4: Toll-like receptor 4

LPS: lipopolysaccharide

PSCs: pluripotent stem cells

iPSCs: induced pluripotent stem cells

ASCs: adult stem cells

LGR5+: Leucine-rich repeat-containing G-protein coupled receptor 5

RSPOs: R-spondin proteins

LRP5/6: low-density lipoprotein receptor-related protein 5/6

Axin/APC/GSKβ:

BMP: bone morphogenic protein

TGF-β: transforming growth factor β

EGF: epidermal growth factor

FABP1: fatty acid binding protein 1

CGA: glycoprotein hormones, alpha polypeptide

DSB: double stranded break

CRISPR: Clustered Regularly Interspaced Short Palindromic Repeats

Cas9: crispr associated protein 9

sgRNA: single guide RNA

PAM: protospacer adjacent motif

crRNA: crispr RNA

tracrRNA: trans-activating crispr RNA

NHEJ: non-homologous end joining

HDR: homology directed repair

MCS: multiple cloning site

PCR: polymerase chain reaction

mRNA: messenger RNA

siRNA: short interfering RNA

RISC: RNA induced silencing complex

(e)GFP: (enhanced) green fluorescent protein

PBS: phosphate buffer saline

FCS: fetal calf serum

EDTA: ethylenediaminetetraacetic acid

BSA: bovine serum albumin

MG-A: minigut A

MG-B: minigut B

MG-C: minigut C

MG-E: minigut E

LB: lysogeny broth

amp: ampicillin

TAE: tris-acetate-EDTA

R-buffer: resuspension buffer

GAPDH: glyceraldehyde 3-phosphate dehydrogenase

PFA: paraformaldehyde

PES: polyethersulfone

DMSO: dimethyl sulfoxide

PCV: pellet-cell-volume

LDS: lithium dodecyl sulfate

DTT: dithiothreitol

meOH: methanol

HIV-1: human immunodeficiency virus 1

HR: homologous recombination

CtIP: Ct-BP interacting protein

CTNNB1: catenin beta 1

CMV: cytomegalovirus

Elf1α: elongation factor 1 alpha

ESC: embryonic stem cell

PGK: phosphoglycerate kinase 1

CBA: hybrid CMV enhancer/chicken β-actin

WT: wildtype

HGF: hepatocyte growth factor

c-Met: tyrosine-protein kinase Met

MAPK: mitogen-activated protein kinase

PI3: phosphoinositide 3-kinase

DEG: differential expressed gene

LRP2: low density lipoprotein-related protein 2

A2M: alpha-2-macroglobulin

TGFB1: transforming growth factor beta 1

Introduction

Diagnose and Prevalence of IBD

Inflammatory bowel disease (IBD) is a collective term of chronic, inflammatory disorders affecting the gastrointestinal (GI) tract. Primarily, the term includes the diseases ulcerative colitis (UC) and Crohn's disease (CD), which are characterized by periods of inflammation and remission[1]. Patients suffering from IBD often experience abdominal pain, bloody diarrhea, vomiting, fever, fatigue and weight loss, due to malnutrition[2]. UC and CD share many of these clinical aspects, but can be separated based on location, distribution and depth of inflammation. UC is restricted to the large intestine (colon), and identified as a diffuse chronic injury, where inflammation is restricted to mucosa and submucosa. The ulcerations of UC are often large. On the other hand, CD can affect any area of the GI tract from esophagus to rectum. The pattern of inflammation is discontinuous, often alternating between healthy, unaffected areas to inflamed ones. CD is also characterized by deeper ulcerations than what is usually seen in UC. These ulcers can give rise to transmural lesions such as fissures and fistulas, reaching serosa and further underlying tissue[3,4]. IBD-patients can also experience extraintestinal manifestations (EIMs), most commonly musculoskeletal or dermatological manifestations, such as *arthritis* and *pyoderma gangrenosum* or *Erythema nodosum*, respectively[5].

The burden of IBD is increasing worldwide, and 6.8 million cases of IBD were reported globally in 2017[6]. The highest reported incidents are within Europe and North America, with more than 1.5 and 3.5 million people affected,respectively[6-9]. The substantially higher prevalence in the western world indicate that environmental factors and the western lifestyle impacts disease development. However, reported incidents of IBD have also increased in other parts of the world, in both developing and newly industrialized countries. Whether the higher incident rates in developed countries are solely influenced by lifestyle, or also by differences in quality and capacity of health care systems, are aspects that should be considered when discussing prevalence and environmental factors. Despite differences across regions, IBD rises as a global disease and challenge, both socially and economically. The direct annual costs of IBD in Europe are estimated to 5.6 billion Euro[8].

Treatment Options

Due to heterogeneity and phenotypic variations between IBD patients, ensuring the correct diagnosis and treatment regime remains a challenge. Conventional drugs such as 5-aminosalisylic acid (5-ASA) and corticosteroids can in milder cases induce remission, or can be effective in case of acute flares[10,11]. However, in some cases, biological drugs such as anti-tumor necrosis factor alpha (TNFα), α4β7 integrin- and interleukin-23 receptor (IL-23R)

inhibitors have become natural choices. Some of these drugs are still under development and evaluated for side-effects. Even though these drugs can relieve symptoms and optimally achieve remission, IBD is still considered incurable. Furthermore, a significant part of patients are not responding to available treatment, or they lose responsiveness after some years of therapy, leading to requirement of surgical intervention[12]. Alternative therapies, such as fecal transplantations and regenerative therapy are under investigation, but requires further research[13-15].

The Digestive System

The digestive process can be divided into five key steps; ingestion, digestion, absorption, compaction and defecation. Food is transported from the oral cavity to esophagus through the pharynx, and through peristaltic movements of smooth muscle cells, food enters the stomach. The stomach is largely sterile due to gastric juice consisting of hydrochloride acid (HCl) and proteases such as pepsin[16]. The low pH kills most bacteria, as well as chemically digesting and disrupting matrix and peptide bonds of meat and plant material[17]. Processed content is then transported into the small intestine. Most of the digestion, as well as absorption, occurs in this part of the bowel. The small intestine is further divided into the *duodenum, jejunum* and *ileum,* with an overall length of approximately six meters[18]. As an adaption to absorption, the small intestine is characterized by a highly folded structure, composed of projections called *villi.* Each epithelial cell has *microvilli* as well, increasing the surface area further[17]. Together, these folding structures and projections leads to a surface area of 200-300 m^2. The small intestine is connected to the large intestine, the colon, through the caecum (with the appendix). The colon is further subdivided into *ascending*-, *transverse-, descending* and *sigmoid colon,* before reaching the rectum and anus. The colon is mainly involved in water and salt reabsorption and compaction of waste products[18].

The GI tract is the organ system in the body exposed to the highest load of bacteria, fungi and viruses, and harbors in total approximately 10^{14} microbes[19]. The concentration of microbes increases along the system, from nearly zero in the stomach, to a high load in the colon[20]. A diverse gut microbiota is crucial for maintaining homeostasis and health. Commensal bacteria contribute by metabolizing indigestible food components, providing nutrients and beneficial short chain fatty acids (SCFAs), stimulating and modulating immune responses, as well as preventing pathogenic infections[21,22]. Nevertheless, a physical barrier is crucial, preventing microorganisms and pathogens from the gut lumen to enter the internal environment[23]. This physical barrier consists of mucus and a single, interconnected epithelial layer[21]. The epithelial cells are kept together by different types of cell junctions, such as adherens junctions, desmosomes and tight junctions, together forming apical junctional

complexes[23]. The tight junctions are the most important ones for excluding luminal content, by forming a branching network on the apical side of the cells[23].

The epithelial monolayer is organized in a crypt-villus like structure **(Figure 1**)[24]. Intestinal stem cells (ISCs) and secretory Paneth cells are located in the crypts, with absorptive enterocytes in the villi[25]. Mucus-producing Goblet cells and enteroendocrine cells are scattered throughout the monolayer. The epithelium is also interspaced with intraepithelial lymphocytes (IELs), as well as low numbers of Tuft-, Cup- and Microfold cells (M-cells)[24,26].The function of these three cell types is not fully discovered, but Tuft cells are believed to have chemosensory properties and M-cells involved in luminal antigen sampling, thus contributing to host resistance[26,27]. The intestinal epithelium is constantly renewed, with an average lifespan of 4-5 days[28]. All the various types of epithelial cells differentiate from the ISC progenitor. Enterocytes are the most abundant cell type, functioning in nutrient uptake. The goblet cells usually contain large vacuoles of the glycosylated protein mucin, which is the main constituent of the mucus-layer. Both Paneth cells and enteroendocrine cells are secretory epithelial cells, secreting antimicrobial peptides (AMPs) and hormones, respectively. Some of the hormones secreted regulate digestion and absorption, while other hormones can be secreted after encountering pathogens through innate immune receptors[24]. Examples of secreted AMPs are defensin and lipocalin-2 (LCN2)[29,30]. They can modulate interactions between host and microbiota, as well as the innate immune system. The Paneth cells also contribute to maintenance of the stem cell niche by production of growth factors (GFs), such as Wingless (Wnt) proteins[26,31]. Under homeostatic conditions, these cells are only expressed in the small intestine; however, metaplastic Paneth cells are commonly seen in the colon during active inflammation[25,32].

Beneath the epithelial monolayer lies the lamina propria (LP), a loose network of connective tissue[33]. It consists of capillaries, lymph vessels, mesenchymal cells, as well as a large portion of immune cells. Immune cells abundant in the LP are macrophages, neutrophils, mast cells and dendritic cells, but also B- and T- lymphocytes[19,34]. Antibody-producing plasma cells secrete several grams of immunoglobulin A (IgA) every day[35]. The epithelial monolayer and LP constitute the mucosa. Submucosa, a second layer of connective tissue, connects LP to the underlying muscular layer, muscularis externa. Muscularis externa is made up by smooth muscle cells and is responsible for peristaltic movements, the driving force of moving food components through the GI tract. Lastly, the muscularis is surrounded by serosa, a thin layer of connective tissue[36].

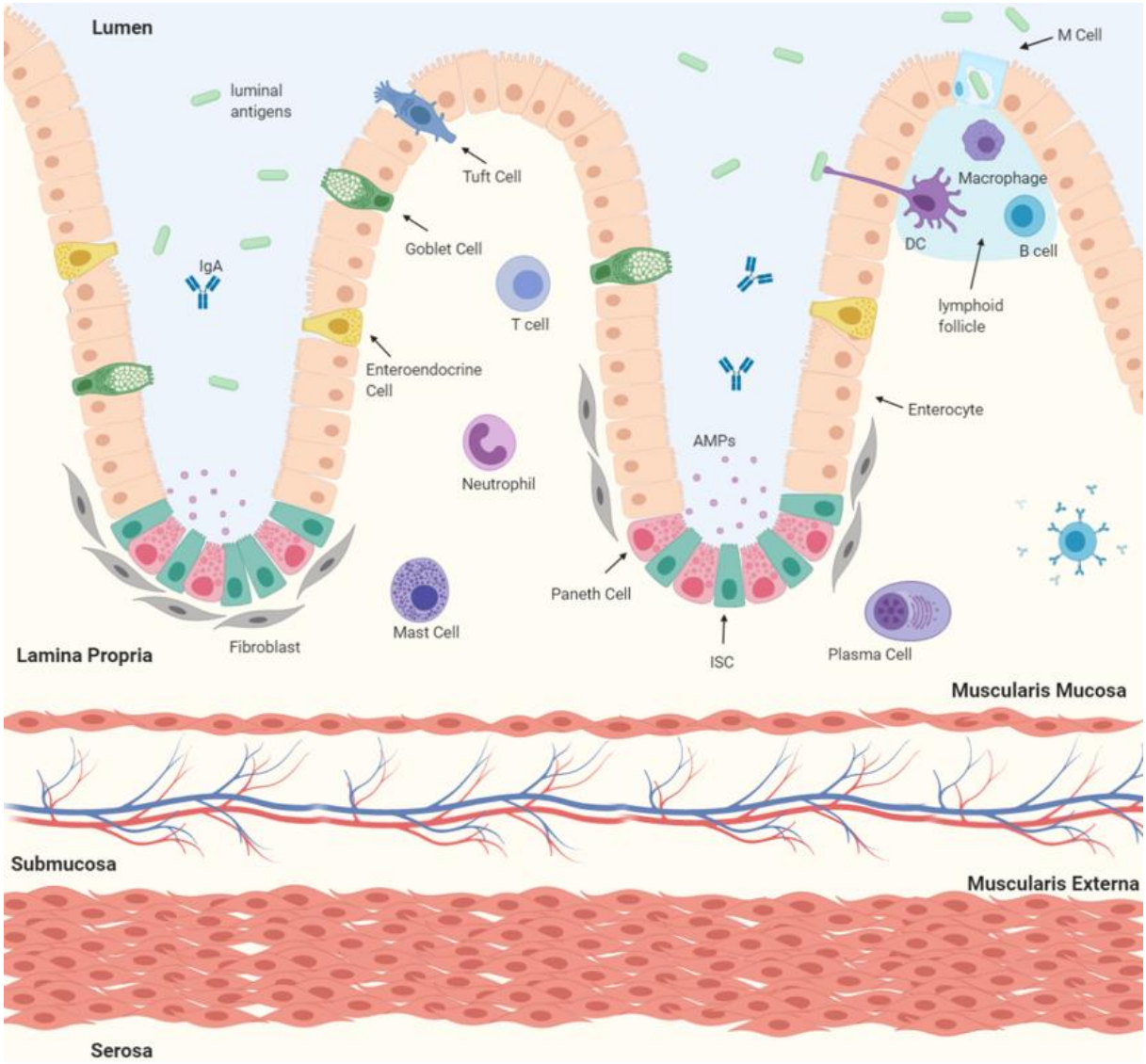

Figure 1: The intestinal epithelial layer represents a physical and chemical barrier against luminal antigens and potential pathogens. The epithelial monolayer is kept together by cell junctions and consists of several types of epithelial cells with specialized functions. Intestinal stem cells differentiate into enterocytes, secretory Paneth cells and enteroendocrine cells, as well as mucus-producing Goblet cells. The monolayer is also interspersed with a low number of Tuft-, M and Cup Cells. Below the monolayer lies the lamina propria, consisting of lymphoid aggregates, as well as lymph- and blood vessels, mesenchymal- and immune cells. The epithelial layer and lamina propria constitute the mucosa. The second layer of connective tissue, submucosa, lies adjacent to the further underlying muscularis externa and serosa. Figure created with BioRender.

Etiology

IBD is a multifactorial disease, where the innate immune system is believed to be the main driver of inflammation. Inflammation can be initiated by an aberrant response towards commensal bacteria, a normal response towards specific pathogens, or an possible autoimmune response towards self-antigens[37-39]. Although the full picture remains obscure, it is commonly accepted that IBD etiology is inflicted by both genetic, micro-biotic and environmental factors[40]. Genome-wide association studies (GWAS) have discovered more than 240 risk loci or single nucleotide polymorphisms (SNPs) associated with IBD[41]. SNPs have been observed in genes involved in the innate immune system, autophagy or the epithelial barrier function, amongst others. Some of the genes characterized are believed to be of special importance in IBD-development, such as Autophagy-related 16-like 1 (*ATG16L1*), Immunity-related GTPase Family M (*IRGM*), nucleotide-binding oligomerization domain containing 2 (*NOD2),* interleukin-10 *(IL-10),* caspase recruitment family member 9 (*CARD9*), mucin 2 (*MUC2*) and E-cadherins (*CDH1*)[42,43]. Many of the disease-related genes are common for both UC and CD, while others are specific for each entity[42,44].

Despite the discovery of large numbers of risk loci, less than 30% of the disease risk can be explained by genetics[45]. This suggests that both microbiota and environmental factors are important players. Imbalance of the microbiota is seen in a majority of IBD patients, characterized by a higher microbial load, but loss of diversity[46,47]. Upon dysbiosis, studies have shown a loss of the phyla *Firmicutes* and *Bacteroidetes,* and an increase in *Proteobacteria,* such as species of the family *Enterobacteriaceae*[22,46]*.* Alterations appear to influence both fermentation products and the immune balance[22]. Although the importance of the microbiome is fully accepted, the actual contribution is difficult to determine due to individual variations in flora between patients, as well as a range of differences in types of specimen and experimental procedures[48]. The environmental contribution consists of a wide range of factors, and it is also believed that many have not yet been identified. Cigarette smoking is one of the most heavily studied, and smokers are twice as likely to develop CD as non-smokers. In UC, however, smoking seems to have a protective role against disease[43,49]. In addition, antibiotics, non-steroidal anti-inflammatory drugs (NSAIDs), stress, diet and pollution are some of the most studied features[43,49]. The “hygiene hypothesis” has also been suggested as a cause of disease[43]. Improved sanitary conditions cause a more limited exposure to antigens. Antigen exposure is important for priming and shaping the immune system, leading to immune tolerance and appropriate responses[50].

Lipocalin-2

LCN2, also known as neutrophil gelatinase-associated lipocalin (NGAL), 24p3 or siderocalin, is a member of the lipocalin-superfamily. LCN2 is a 25 kDa, small secreted glycoprotein, located on the chromosomal locus 9q34.11[51]. It exists in its monomeric form, but can also form a dimer (50 kDa), or complex with the proteolytic extracellular matrix protease, metalloprotease-9 (MMP-9)[52]. LCN2 was first discovered in the granules of neutrophils, but has been shown to be expressed by a variety of cell types, as for example endothelial and epithelial cells. In the intestine, Paneth cells are responsible for secretion of LCN2. The 198 aa long peptide is characterized as an acute phase protein and an AMP[30,52]. LCN2 exerts its role as AMP through sequestering of iron in competition with enterobacteria. These bacteria secrete chelating compounds specialized in sequestration of iron, important for bacterial survival[51-53]. Thus, lipocalin-2 modulates immune responses and host resistance to pathogenic infections.

In addition to its role as an iron scavenger, LCN2 has been implicated in a range of functions, such as in transport of hydrophobic molecules, apoptosis, differentiation processes, and to have a role in proliferation, migration and wound healing[54-58]. LCN2 is also studied in connection with cancer, and reports on its role are conflicting. A range of studies suggests that LCN2 is a mediator of metastasis, contributing to epithelial to mesenchymal transition (EMT)[59-61]. Other studies imply that LCN2 functions as a negative regulator of these phenomena[62-64]. In brain endothelial cells, LCN2 was seen to restore the homeostatic levels of CDH1 and zonula occludens (ZO) proteins after TNFα treatment, thereby restoring barrier function[65]. CDH1- and ZOs are essential for the maintenance of adherens junctions and tight junctions, respectively. The conflicting roles of LCN2 among studies might be due to different contribution, dependent on disease and context. In the gut, LCN2 has mainly been shown to regulate microbiota and protect against gut inflammation and colitis. Mice studies comparing IL-10 knock out (KO) mice and LCN2/IL-10 double KO mice showed a more rapid onset of colitis and exacerbated inflammation in mice deficient of LCN2[54,63]. However, in other settings, LCN2 seems to favor inflammation by induction of proinflammatory cytokines and recruitment of immune cells[66-68]. This tendency has been implicated in metabolic disorders such as obesity and type 2 diabetes mellitus, as well as in skin inflammation and atherosclerotic diseases[51,66].

At the IBD Research Group at CEMIR, NTNU, LCN2 have been studied the recent years regarding its role in IBD[29,55,69,70]. Studies conducted on a cell lineage important for wound healing and regeneration after ulcerations, Ulcer-associated cell lineage (UACL), showed that LCN2 was one of the ten most upregulated genes in active disease compared to inactive disease and healthy controls[55]. These findings strengthen the theory of LCN2 as a mediator

of proliferation, migration and/or differentiation. Another study conducted on mice reported similar findings, where overexpression of the STAT3-dependent transcription factor (TF), transcription Factor 3 (Tcf3), led to downstream LCN2 secretion[56]. This TF is involved in wound healing and accelerated migration of keratinocytes. Furthermore, the study showed that wound healing in STAT3-deficient skin was rescued by supplementation of recombinant LCN2. Nevertheless, the exact role and to which extent LCN2 is involved in repair remains to be elucidated. Due to high levels of secreted LCN2 during active inflammation, the protein is also examined for its potential as a clinical marker for IBD activity[29].

It is believed that LCN2 is regulated through the NF-kB signaling pathway, stimulated with cytokines such as IL-1β, IL-17, IL-22, TGF-α and several others[54,71]. Further, poly(I:C), a ligand for the pattern recognition receptor (PRR) Toll-like receptor 3 (TLR 3) were shown to induce LCN2 expression in epithelial cells[29]. The same induction of gene expression was seen with engagement of Toll-like receptor 4 (TLR 4) after stimulation with the bacterial lipoglycan, lipopolysaccharide (LPS)[52,54].

Organoid Culture

IBD research is highly dependent upon animal models or *in vitro* studies with cancer cell lines. Such model systems have been crucial for advances within molecular medicine. Nevertheless, there are some inherit limitations. Animal models have the disadvantage of not reflecting the human physiology and genetics completely, which might lead to differences in the pathological responses. 16S rRNA sequencing have also revealed significant differences between microbiota of mice and humans, which as mentioned, is an important part of IBD pathogenesis[72]. In IBD research, colon carcinoma cell lines such as HT-29 and Caco-2 have been widely used. They are convenient model systems due to their resilience and ability to divide forever. However, these cells have also transformed characteristics and physiological properties that might differ from normal epithelial cells. In addition, enrichment of one cell type is often common for these cell lines[73,74], thus not reflecting the actual composition of cell types and the *in vivo* environment[75].

During the last decade, advances in stem cell biology have led to the development of organoid cultures. Organoids are self-organizing 3D “mini organs” derived from stem cells, which can be grown and expanded long term[76]. These structures bear great promise as an improved model system, as they can reflect the genetics, architecture and composition of cells found *in vivo* **(Figure 2)***[77,78].* Organoids can be established from pluripotent or induced pluripotent stem cells (PSCs/iPSCs), or from multipotent and tissue specific adult stem cells (ASCs)[76]. Different types of stem cells will further be reflected in the grown organoids, and choices should be made dependent on the actual study. In IBD-research, establishment of organoids from ASC is beneficial. These can be directly isolated from patient biopsies and have further shown to be both genetically stable and to preserve the region specificity seen *in vivo* in patients[75,79]. These features are promising for future use in personalized medicine, as well as in studies of genetic and epigenetic alterations in the epithelial layer. However, using ASCs will provide organoids that are solely epithelial, thus the interplay between epithelial-, mesenchymal-, and immune cells cannot be explored, without co-culture with cells from other sources. These types of studies are possible by using PSCs, but they are on the other hand prone to genomic instability and acquirement of genetic and epigenetic changes during the reprogramming processes[75,80].

Intestinal organoids have been established from both mouse and human stem cells[78,81]. ASCs are isolated from intestinal crypts and can be selected upon by the epithelial stem cell marker, Leucine-rich repeat-containing G-protein coupled receptor 5 (LGR5+), or simply by selecting for growing organoids. By providing the right conditions of culture medium and matrices, these stem cells can grow and organize into 3D-structures[77]. Canonical Wnt signaling is of major importance for maintenance and proliferation of an undifferentiated stem

cell niche. The signaling pathway initiates by binding of Wnt-ligand to the Frizzled receptor and is further augmented by R-spondin proteins (RSPOs) and their Low-density lipoprotein receptor-related protein 5/6 (LRP5/6) receptor. Together, these events stabilize the TF β-catenin, which translocate to nucleus and initiate expression of downstream genes. Without Wnt and RSPOs, β-catenin is degraded by the Axin/APC/GSKβ-complex. The Wnt-pathway is also negatively controlled by bone morphogenetic protein (BMP)- and transforming growth factor β (TGF-β)-signaling. TGF-β signaling does not directly affect ISC proliferation, but initiates differentiation processes, thus reducing the number of stem cells available for organoid growth. All together, the understanding of these pathways form the foundation for determining the essential components of intestinal organoid culture media. To sustain the ISC pool, supplementation of Wnt-ligands and RSPOs are necessary, as well as antagonists of BMP- and TGF-β, such as Noggin and A83-01. Other factors which have shown to be beneficial for organoid growth are epidermal growth factor (EGF), Gastrin, Notch, Nicotinamide and Prostaglandin E2. These factors are involved in inducing growth and proliferation by different mechanisms. To prevent anoikis, a type of programmed cell death executed by anchorage-dependent cells, the factors Y-27632 or Thiazovivin can be supplemented. This is especially important after passage or other procedures that are stressful to the cells. Lastly, for organoids to grow in 3D, the ISCs have to be embedded in specific matrices. Typically, for intestinal organoids Matrigel (Corning Life Sciences) is used, which is a gel consisting of extracellular matrix proteins crucial for regulation of genes, proliferation and differentiation of the cells[77,82,83].

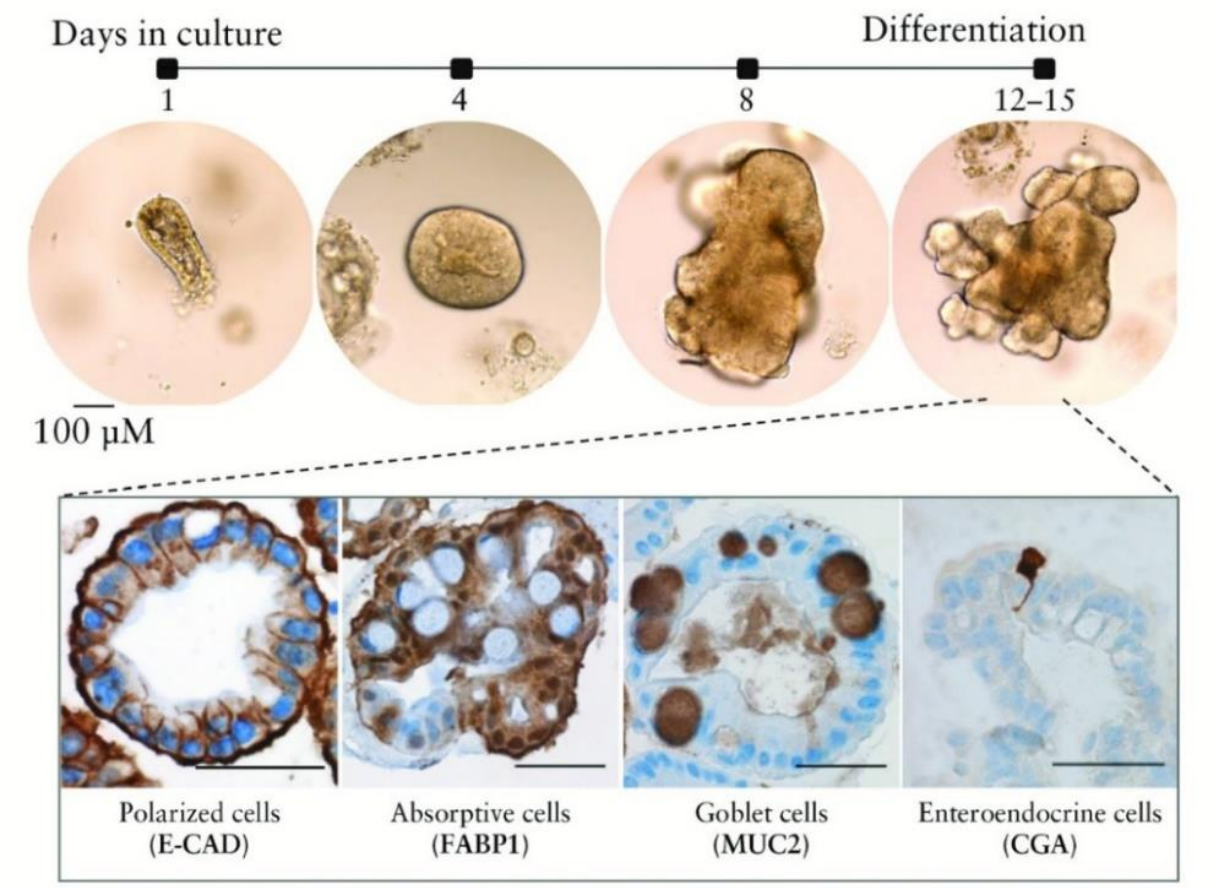

Figure 2: Organoids expands from isolated intestinal crypts. They maintain a spheroid phenotype, consisting mainly of intestinal stem cells s as long as cultured in organoid medium with high levels of Wnt and RSPOs, as well as other growth factors. Upon differentiation, the organoids develop into a budded phenotype, consisting of differentiated epithelial cells with specialized functions. Immunohistochemistry show the presence of polarized cells, absorptive enterocytes, mucus-producing goblet cells and enteroendocrine cells by staining for CDH1, Fatty Acid Binding Protein 1 (FABP1), MUC2 and Glycoprotein hormones, alpha polypeptide (CGA), respectively. Figure taken from Østvik A., E. *et al.*[84]

CRISPR/Cas9

Genetic engineering can be defined as the procedures for manipulating and creating specific alterations in the genome[85]. It is often based on the use of different types of nucleases making double stranded breaks (DSBs) in the DNA, and the subsequent endogenous repair mechanisms of the cell[86]. Over the last decade, the discovery of the CRISPR/Cas9 system has revolutionized the field of genome engineering by providing a more specific and effective tool for generating genomic alterations. It bears great promise of advances within basic biological and medical research, as well as in production of scientific and commercial products or treatment of genetic diseases.

CRISPR stands for Clustered Regularly Interspaced Short Palindromic Repeats, which was first discovered in bacteria and archaea as an adaptive immune response against viral infections[87]. As the name implies, the CRISPR region was discovered to contain fragments of viral DNA interspaced with identical, repetitive sequences. CRISPR arrays, together with the CRISPR-associated protein 9 (Cas9) nuclease, enables bacteria to recognize and cleave viral DNA upon secondary infections[88]. This feature have been exploited by researchers, and in 2013 it was published how Cas9-RNA complexes could mediate site-specific genome engineering in eukaryotic cells, as well as in bacterial cells[88]. Despite a wide range of bacterial CRISPR-systems, the type II CRISPR/Cas9 system have become the dominating system within gene editing, due to its convenience and simplicity[88]. The key factors in CRISPR/Cas9 gene editing are the Cas9 nuclease, a single guide RNA (sgRNA) and the presence of a 2-6 bp long sequence called protospacer adjacent motif (PAM)[89]. The Cas9 nuclease is capable of cleaving DNA and create a DSB. However, in order to be located at the target site, it needs to be “guided” by the sgRNA[90]. This sgRNA is an engineered fusion of crispr RNA (crRNA) that is made up by ~20 bp homologous to the target region, and a trans-activating crispr RNA (tracrRNA) that function as a scaffolding link between the crRNA and the Cas9 nuclease. In nature, these two RNAs exist separately[89]. CRISPR/Cas9 mediated editing of a specific region requires a PAM region just downstream of the target region for Cas9 to specifically bind and cleave the target. Advances within CRISPR/Cas9 technology has led to development of many Cas9 homologues with different PAM requirements, thus widening the possibilities of engineering many genomic loci[91]. Upon binding to the sgRNA and target DNA, Cas9 undergoes conformational changes creating a channel that binds the RNA-DNA hybrid. This change is believed to help double stranded DNA unwinding and invasion of guide RNA[88].

Following a DSB of DNA, the cell repair machinery will try to repair the break. This may occur through two different mechanisms; either by non-homologous end joining (NHEJ) or homology directed repair (HDR). NHEJ is error prone, leading to random insertions, deletions

or duplication of base pairs, and often a disrupted gene function[81,92]. This is one way of creating a gene KO. On the other hand, HDR allows for insertion of a specific sequence based on a donor template. This template must contain homology arms in order to be inserted[81]. HDR opens up for insertion of reporter genes, such as fluorescent tags or antibiotic resistance[93]. Thus, this makes it easier to select and verify positively altered clones. However, HDR as a method has low efficiency and results are sometimes more difficult to achieve. Homologous recombination (HR) happens in the G2 and S-phase of the cell cycle, and is thus dependent upon cells in active cell cycle for initiation[81].

Plasmids and RNA Interference

Plasmids are extrachromosomal, small, circular and double stranded DNA molecules naturally existing in bacterial cells[94]. Plasmids do not contain essential genes for bacterial survival, but advantageous genes such as antibiotic resistance[95]. The sizes of various plasmids can differ considerably, ranging from thousands to hundreds of thousand base pairs. Plasmids have been widely used as gene vectors for cloning, genetic transfer and manipulation of genes[94]. Recombinant plasmids contain functional regions such as a replication origin, a drug-resistant gene and often a selection marker, a promotor region and a region for DNA inserts. These plasmids often further contain multiple cloning sites (MCS) for easy insertion of additional DNA, as well as primer binding sites as an initiating point for PCR amplification[94]. By transformation, plasmids can be introduced into bacteria for amplification and subsequently isolated for use in gene editing of target cells. *E. coli*-derived plasmids are widely used and have been optimized as gene delivery vectors[96].

RNA interference is another tool facilitating post transcriptional suppression of gene expression[97]. This mechanism for gene silencing is based on double or single stranded RNAs involved in the degradation or inhibition of messenger RNAs (mRNAs). Short interfering RNAs (siRNAs) of 21-23 bp, are recognized by the RNA induced silencing complex (RISC), a multicomponent feature[98]. RISC search the cytoplasm for complementary RNA sequences, resulting in mRNA degradation or inhibition of translation, thus loss of protein expression[94,97,99].

Transfection and Transduction

The delivery of CRISPR/Cas9 or other technologies of genome engineering into target cells is called transformation or transfection and transduction for bacterial cells and eukaryotic cells, respectively[100]. The downstream applications can vary from production of recombinant proteins to exploration of gene regulation and gene function by enhancing or inhibiting gene expression, as well as for use in gene therapy. Chemical and physical methods exist for nucleic acid delivery, amongst them electroporation and lipofection. The delivery of nucleic acids can be transient or lead to the development of stably transfected host cells[100].

Electroporation is a physical transfection method. The cells and DNA to be taken up are suspended in a conductive solution and surrounded by an electrical circuit[101]. The mixture of cells and DNA is then exposed to an optimized voltage, where the pulse can last for microseconds or milliseconds depending on cell type transfected[101]. The number of pulses may also vary. Exposure to electric current is believed to create pores in the cells' phospholipid bilayer, as well as increased electric potential across the membrane, facilitating uptake of negatively charged molecules (**Figure 3**)[100].

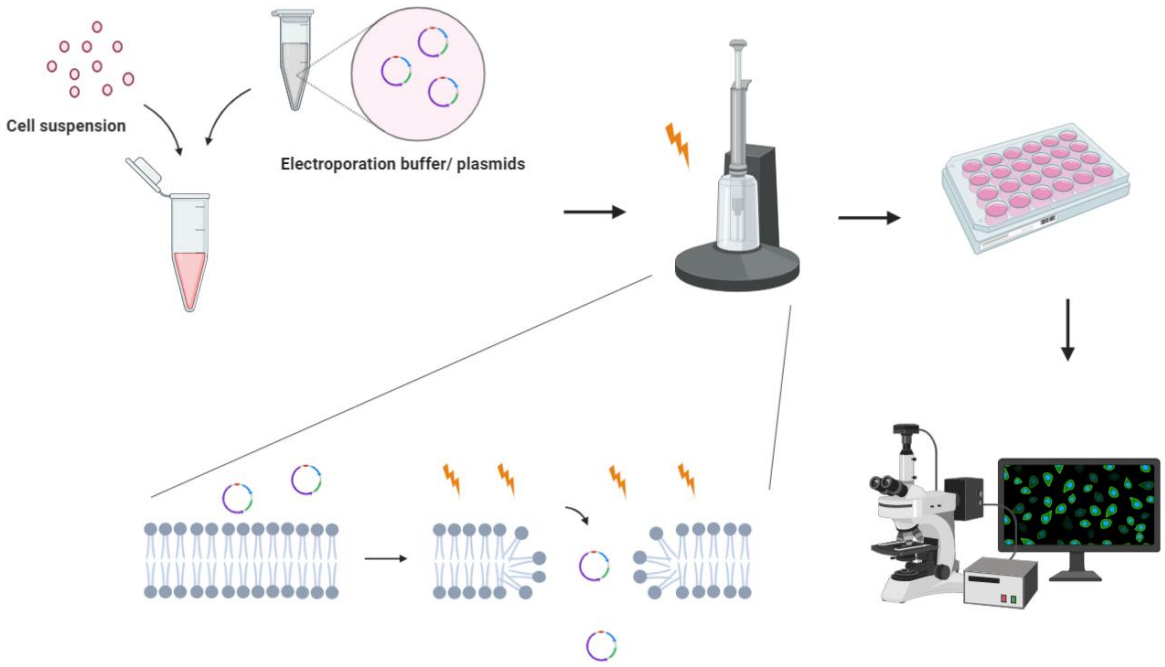

Figure 3: Electroporation is a physical transfection method facilitating cell uptake of exogenous nucleic acids by voltage exposure. Exposure creates transient pores in the cell phospholipid bilayer, enabling DNA uptake. Figure created with BioRender.

A chemical method for cell transfection is lipofection[100]. Here, liposomes are used for transporting exogenous DNA into a cell. Liposomes are made up by lipids, which are hydrophobic, fat-soluble molecules. Fat, oil and wax are all lipid components. Prior to transfection, DNA and the lipid-solution are incubated in order to create a vesicular liposome structure around the DNA. The mixture containing DNA-liposome complexes can then be added to the cells to be transfected (**Figure 4**). The uptake can either occur through direct fusion with the cell membrane, or by endocytosis. The procedure is made possible due to the hydrophobic nature of the phospholipid bilayer[102].

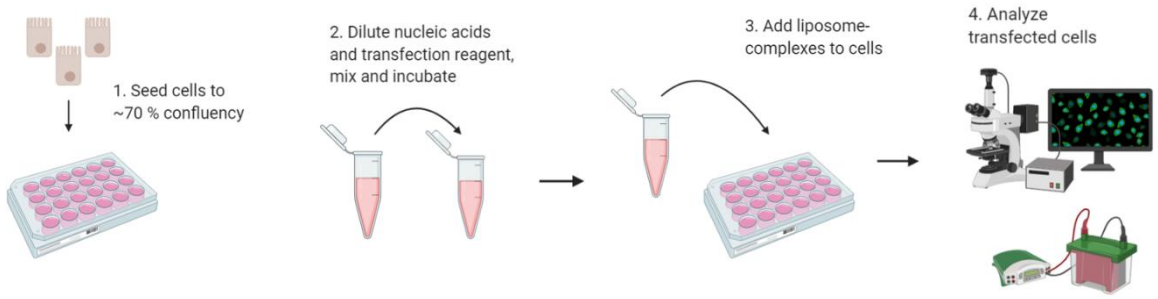

Figure 4: Lipofection is a chemical transfection method. Fat-soluble molecules, liposomes, are used for transport of exogenous nucleic acids into the cell. DNA and lipids are incubated in order to create vesicular structures around the DNA. The complex-containing solution can then be supplemented to the cell culture medium, where complexes fuse directly with cell membrane or can be taken up by endocytosis. Figure created with BioRender.

Viral transduction is a biological transfection method using viruses to infect cells of interest[100]. The viral vectors contain a sequence of interest, which leads to transgenic expression and establishment of stable cell lines.

Lentivirus is a type of retrovirus, expressing reverse transcriptase. This feature gives lentiviruses the ability to reverse transcribe their RNA genome into cDNA copies that can further be integrated into a host genome by specific protease- and integrase proteins[103]. Lentiviruses are so-called complex retroviruses, having key features that makes it possible to infect non-dividing cells, as well as mitotic ones[104].

The use of lentiviruses in experimental settings are divided into several steps. In order to create lentivirus particles equipped to infect target cells, they need to be produced and assembled within a packaging cell line. The mammalian cell line HEK293T is often used for this purpose. An expression plasmid with sequence of interest, and two or three packaging plasmids are transfected into HEK293. The cells are allowed to incubate for 2-3 days, during which viruses replicate and assemble into infectious viral particles. The particles are released

from the cells into the cell culture medium. Viral supernatants can then be transferred to target cells (**Figure 5**)[105].

An Infection by lentivirus starts with binding of viral glycoproteins to cellular receptors on the target cells and subsequent fusion with the cell membrane[105]. The reverse transcription of viral RNAs occurs in the cytoplasm before being transported into the nucleus. Next, the viral enzyme integrase cleaves the host genome. The enzyme also removes nucleotides from the reverse transcribed cDNA, creating 3'overhangs that facilitates ligation. The integrated sequence will then be replicated, transcribed and translated by the host's machinery[106].

Due to safety reasons, two types of experimental lentiviruses have been developed; the second and third generation, which divides the viral structural components between two or three packaging plasmids, respectively. The lentiviruses also contain a deletion in the 3'LTR region, leading to self-inactivation after primary infection[105].

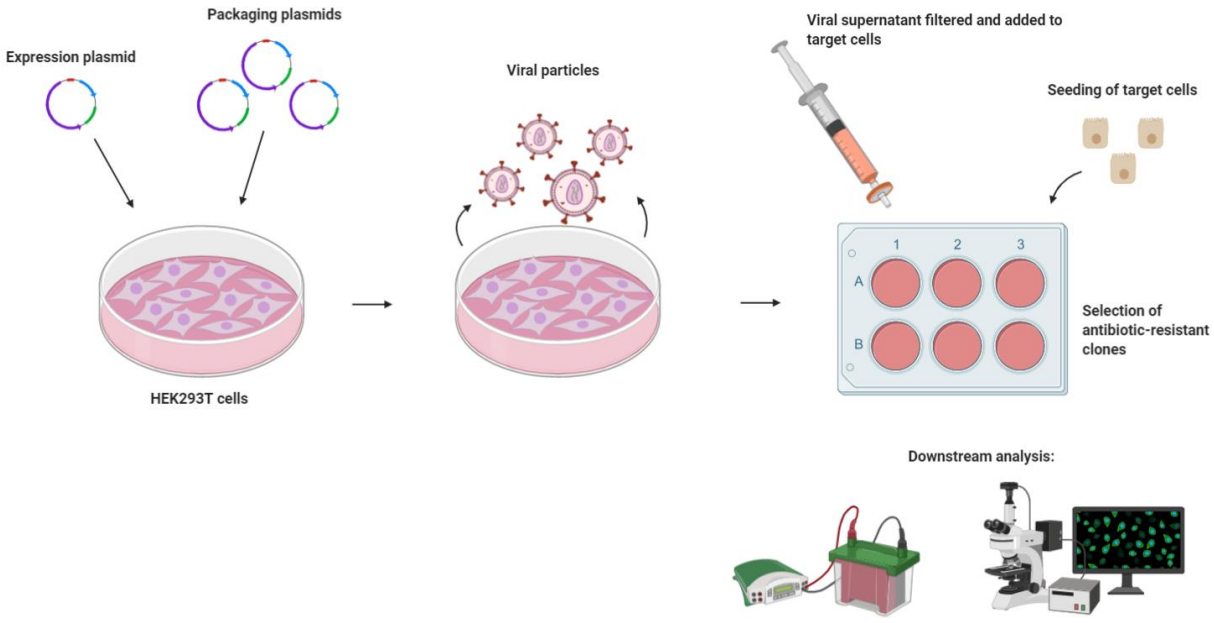

Figure 5: Lentiviral transduction is a biological transfection method, based on the production of infectious viral particles containing construct of interest. Transduction exploits lentiviruses mechanisms of action for integrating their own genetic material. The viral particles are produced in a packaging cell line (HEK293T), before viral-containing medium is harvested and added to target cells. Figure created with BioRender.

Aims and Hypotheses

The aim of this project was to establish an easy and functional procedure for genetic engineering of patient-derived intestinal colonic organoids. Organoids may be crucial for future understanding of the underlying mechanisms of IBD pathophysiology by resembling architecture and composition of epithelial cells, as well as preserving the region specificity seen *in vivo* in patients. Furthermore, organoid culture can reveal the roles of candidate genes involved in disease development in connection with gene editing tools, such as CRISPR/Cas9. *LCN2* is one such gene shown highly upregulated in active IBD. LCN2's role as an AMP by iron sequestering is well known, but its contribution in events such as proliferation, migration, cell adhesion and differentiation remain to be elucidated.

The main objectives were:

1. To establish a stable *LCN2* KO cell line of patient-derived colonic organoids by exploring the various gene delivery and gene editing options available. The method designs were first applied on the cancer cell line HT-29, before evaluated in organoid culture. Efficiency of various delivery strategies and gene delivery vectors were assessed by fluorescent microcopy and western blot protein analysis.

2. To investigate the contribution of LCN2 in the events of migration, proliferation, and cell adhesion. We hypothesized that LCN2 knockout would diminish growth. These features were evaluated by xCELLigence and cell counting of HT-29 cells transfected with LCN2 siRNAs. Protein knockdown was evaluated by western blot analysis.

Materials and Methods

Cell Culture

The colorectal adenocarcinoma cell line, HT-29 (ATCC® HTB-38), was cultured in McCoy's 5A cell culture medium (Sigma Aldrich), with 10% fetal calf serum (FCS), and 0,05% Gentamicin (Invitrogen). HT-29 was split 1:8 every 5-7 day. HEK293T (ATCC ® CRL-3216) kidney cell line was cultured in Dulbecco's modified eagle medium (DMEM) (Life Technologies), supplemented with 10% FCS and 1% Penicillin-Streptomycin (Sigma Aldrich). Cells were split 1:30 twice a week. Both cell lines were cultured in humidified 5 % CO_2 at 37 ^{o}C. The complete list of medium recipes is listed in **Table 1-2, Appendix 6**. Prior to subculture, the cells were washed with Phosphate Buffer Saline (PBS) (Life Technologies). Cells were dissociated for 5-10 and 2-4 min. in 5% CO_2 at 37 ^{o}C for HT-29 and HEK293T, respectively, with Trypsin/Ethylenediaminetetraacetic acid (EDTA) (Lonza). Inverted light microscope was used for concurrent evaluation of cell detachment. Trypsin was inactivated by addition of complete growth medium. For counting, the Invitrogen Countess cell counter with Trypan blue staining was used for estimation of cell viability and concentration (cells/mL).

Organoid Culture

Intestinal colonic organoids were established by isolation of epithelial crypts from human colon pinch biopsies taken during colonoscopy, according to a protocol based on Sato *et a*l.[82,107]. The epithelial crypts containing adult stem cells (ASCs) were resuspended and embedded in Matrigel (Corning Life Science) and overlaid with Minigut-D (MG-D) culture medium. The MG-D culture medium consisted of Minigut-C (MG-C) (described below), CHIR99021 (STEMCELL Technologies) and Thiazovivin (STEMCELL Technology).

When established, intestinal colonic organoids were cultured in MG-C, composed of Advanced Dulbecco's Modified Eagle Medium/F12 (DMEM/F12) (Life Technologies), supplemented with Wnt- and R-spondin conditioned medium (ATCC CRL-2647, 293T-HA-Rspo-Fc (Calvin Kuo)), 1% bovine serum albumin (BSA) (Sigma Aldrich), 1x GlutaMAX (Life Technologies), 10mM HEPES (Life Technologies), penicillin-streptomycin (100 U/mL), 1x N2 (Thermo Fischer), 1x B27 (Thermo Fischer), as well as the factors Noggin (PeproTech), Nicotinamide (Sigma Aldrich), N-Acetyl-L-cysteine (Sigma Aldrich), A-83-01 (Sigma Aldrich), SB202190 (Sigma Aldrich), 15- Gastrin 1 (Sigma Aldrich) and Human EGF (PeproTech). The medium was renewed every second day. Directly after passage, MG-C medium was also added Y-27632 (STEMCELL Technologies) (1 µl/mL MG-C), resulting in Minigut-E (MG-E). The complete list of all medium recipes and constituents are listed in **Table 3-10, Appendix**

6. Organoids were embedded and grown in Matrigel and incubated in humidified 5% CO_2 at 37 ^oC. All media were sterile filtered through a 0,2 µM filter before use.

Prior to subculturing of organoids, Matrigel was thawed on ice for minimum 2 hrs., 24-well plates were pre-heated to 37 ^oC, pipette tips frozen, and centrifuge cooled down to 4 ^oC. Minigut-B was supplemented with FCS (50 µl FCS/mL) and placed on ice. TrypLE Express (Life Technologies) and Minigut-E was prepared by adding 1 µl Y-27632/mL and heated to 37 ^oC.

Old growth media were removed from organoids grown in 24-well plates. Cell culture plates were then placed on ice, Matrigel containing organoids was overlaid with ice cold Mg-B + FCS (1 mL) and resuspended. The content was transferred from wells into a collection tube (50 mL). Additional Mg-B + FCS (500 µL) was added to each well in order to collect as many organoids as possible. The collection tube was then centrifuged at 85-200 x g, at 4^oC for 5 min, before the supernatant was discarded. The cell pellet was resuspended in TrypLE Express and incubated for 10 min in a 37^oC water bath. To induce shear stress, organoids were further dissociated by pipetting up and down 10 times with a syringe equipped with a 18-G fill blunt needle. Cells were then checked in light microscope for single cell suspension, followed by centrifugation at 500 x g at RT for 5 min. The supernatant was subsequently removed, and cells resuspended in Mg-B + FCS (1 mL). Cell concentration was determined by Invitrogen Countess cell counter with Trypan blue staining. A volume corresponding to 5000-10 000 cells/well was transferred and resuspended in matrigel (50 µl) by using pre-chilled tips. The cell/Matrigel suspension was added in the middle of each well on pre-heated 24-well plates. Plates were then incubated at 37^oC, 5% CO_2 for 20 min. to solidify the Matrigel before overlaid with Mg-E (500 µL). The medium was refreshed every second day, the first time after passage with Mg-E, before exchanged with MG-C. Organoids were passaged every 10-14 day, depending on their growth.

Bacterial Cloning and Isolation

Competent bacteria, D5Hα *E. coli*, and DNA plasmids were placed on ice. LB- medium and agar plates (described in **Table 11-12, Appendix 6**) containing ampicillin (amp) (100 µg/mL) were placed in 37 ^oC.

Competent bacteria (50 µL) were mixed with plasmid DNA (50-100 ng), and incubated on ice for 30 min. The bacteria/plasmid suspension was then exposed to 42 ^oC for 45-50 sec, before rapidly placed on ice for 2 min. Preheated LB-medium (180 µL) and bacteria were further incubated on a 37 ^oC heat block for 1 hr. The bacterial suspension was diluted 1:10 by adding 20 µl to 180 µl fresh LB-medium. Diluted bacteria (180 µl) was plated on agar-plates. The agar plates were wrapped in parafilm and placed at 37 ^oC upside down overnight.

Plasmid amplification was conducted the following day. Depending on required amounts, LB-medium (3 mL or 100 mL) and amp (100 µg/mL) were added to a Falcon tube (5 mL) or an Erlenmeyer flask (500 mL). A pipette tip was sterilized by the flame of a Bunsen burner before used to pick a single bacterial colony from the agar plates, that had been incubated overnight. The tip containing bacteria was dropped into the LB-medium and incubated at 37 ^{o}C for ~18 hrs. while shaking at 256 rpm. A clean pipette tip was used as negative control. Before further plasmid isolation, approximate bacterial concentration was measured by OD600 spectrophotometer (Fischer Scientific), with LB-medium used as a blank. The OD-value should be between 1-4.

Plasmid isolation was performed with PureYield™ Plasmid Miniprep System (Promega) and ZymoPURE™ II Plasmid Midiprep Kit (Zymo Research). Both miniprep and midiprep plasmid isolations were conducted in accordance to manufacture's protocols. The principles behind bacterial transformation and plasmid isolation are explained in **Appendix 1,** and the various plasmids that were isolated are listed in **Appendix 7.**

Restriction Digest Assay

The CRISPR LCN2 Human Gene Knockout Kit (OriGene), consisting of the plasmids Guide 1 (G1), Guide 2 (G2), Scramble (S) and Donor (D), were evaluated in Genome Compiler based on sequence information provided by the manufacturer. The program was used to find restriction sites, and suitable restriction enzymes were selected based on sequence information. The restriction enzymes used, and the following sequences are listed in **Table 1**. Restriction digest was conducted with FastDigest buffer 10X (Thermo Fischer) (2 µl) and FastDigest enzyme (1 µl) (Thermo Fischer). Mastermix added Plasmid DNA (0,6 µg) was prepared in accordance with the manufacture's protocol and placed on ice. The principles behind restriction digest assay are explained in **Appendix 1,** while additional information concerning the CRISPR/Cas9 LCN2 KO plasmids is described in **Appendix 2.**

Table 1: Restriction enzymes used for restriction digestion of CRISPR/Cas9 LCN2 KO plasmids; G1, G2, S and D. EcoRI FastDigest enzyme was used for G1-2 and S in all three experiments, while D was digested with EcoRI, EcoRI/BamHI and BamHI/XbaI. The following expected fragments are listed for all plasmids and restriction enzymes.

	Digestion 1		**Digestion 2**		**Digestion 3**	
Plasmid	Restriction enzymes	Sequences (bp)	Restriction enzymes	Sequences (bp)	Restriction enzymes	Sequences (bp)
G1	EcoRI	1128	EcoRI	1128	EcoRI	1128
		6876		6876		6876
G2	EcoRI	1128	EcoRI	1128	EcoRI	1128
		6876		6876		6876
S	EcoRI	1128	EcoRI	1128	EcoRI	1128
		6876		6876		6876
D	EcoRI	1103	EcoRI	1103	XbaI	1738
		5962	BamHI	5963	BamHI	5328

Gel Electrophoresis

TAE-buffer 1X (50 mL) was supplemented with agarose (0,5 g) and heated in a microwave oven until the agarose was solubilized. The gel was then cooled to approximately 60 ^{o}C and transferred to a 50 mL tube and mixed with Gelred Nucleic Acid Stain (Biotium) (5 µl). The tube was inverted a few times before transferred to the gel electrophoresis chamber. The gel was allowed to set for ~20-30 min. Gel Loading Dye Purple (6X) (Biolabs) was diluted and added to both samples and to READY-LOAD^{TM} 1Kb Plus DNA Ladder (Invitrogen). Thereafter, the gel electrophoresis chamber was filled with TAE-buffer (1X) until the gel was completely covered, and ladder (5 µl) and samples (10 µl) were loaded into the wells. The gel was run at 90 V for 1-1.5 hrs., and afterwards imaged by Gel Logic 212 PRO (Carestream Molecular Imaging).

Electroporation

The electroporation procedure was conducted both on the HT-29 cancer cell line and the colonic organoids. For both of these, cells were dissociated to single cell suspension, and counted as earlier described for passage of HT-29 cells and organoids. Volumes representing 5,6 x 10^4 and 1 x 10^5 cells per electroporation reaction for HT-29 and organoids respectively, were transferred to new vials and centrifuged at 400 x g for 5 min. The supernatants were removed, and cell pellets resuspended in PBS (1 mL) before centrifuged once more.

Transfection by electroporation was carried out with the NEON transfection system (Invitrogen). Electroporation experiments were run several times, with both CRISPR/cas9 LCN2 KO plasmids and pCMV-LifeAct plasmid (ibidi). Additional information regarding pCMV-LifeAct is found in **Appendix 2.** For each experiment, the desired plasmids were prepared in Eppendorf tubes and mixed with Resuspension-buffer (R-buffer) (Invitrogen). The mixture of plasmids and R-buffer were then used to resuspend the cell pellet. The Neon device was set up according to manufacturer's instructions, and electro parameters were set in order to obtain the highest transfection efficiency without losing more cell viability than necessary. Different set ups and optimizations were run for the different experiments, and variants are listed in **Table 1, Appendix 4.**

The cell/plasmid suspension (10 µl) was loaded into the NEON tip and exposed to electric pulses in the NEON transfection station. After electroporation, the HT-29 cell suspension was transferred to wells on a 24-well plate containing preheated growth medium (500µl) without antibiotics. For organoids, the cell suspension from the NEON pipette was diluted in MG-B + FCS (1:10), and diluted cell suspension (10 µl (1 x10^4 cells)) was then added to Matrigel (50 µl) and plated in the middle of a pre-heated 24-well plate with chilled pipette tips. The plate

was placed in 5% CO_2 at 37 ^oC for 20 min. for Matrigel to solidify, before overlaid with MG-E (500 µl). Both HT-29 and organoids were incubated 18-48 hrs. before evaluation of transfection efficiency by EVOS FL Auto 2 fluorescence microscope (Thermo Fischer Scientific).

Lipofection

Lipofection was conducted on both HT-29 cells and colonic organoids. Various lipofection transfection reagents were tested, such as Lipofectamine 2000 (Invitrogen), Lipofectamine Stem Reagent (Invitrogen), Accell Delivery Media (Dharmacon) and RNAiMAX (Invitrogen). Both plasmids and siRNAs were transfected using lipofection, including CRISPR/cas9 LCN2 KO plasmids, pCMV-LifeAct plasmid, Accell red fluorescent non-targeting control- and GAPD positive control siRNA (Dharmacon), in addition to ON-TARGETplus LCN2- and GAPDH-siRNA (Dharmacon). The alternative procedures performed in each experiment, such as plasmid- and transfection reagent concentrations, presence of FCS or other experimental alterations, are listed in **Table 2, Appendix 4.**

Lipofectamine 2000

For HT-29 cells, 50 -100 000 cells were seeded in a 24-well plate one day prior to transfection, in order to obtain 70-90 % confluency. Cells were overlaid with McCoy's 5A medium (500 µl), supplemented with 10% FCS and 0,05% Gentamicin. The following day, plasmid DNA (0,5 – 2 µg) was diluted in serum-reduced Opti-MEM medium (Life Technologies) (50 µl). In a separate tube, Lipofectamine 2000 (2 - 5 µl) was diluted in serum-reduced Opti-MEM (50 µl). The amounts are presented per well. Diluted plasmid- and Lipofectamine 2000 were incubated in room temperature for 5 min, before mixed (1:1). Thereafter, plasmids/Lipofectamine was incubated for 20 min at room temperature to allow complex formation. Complexes (100 µl) were subsequently added to each well and incubated 18- 48 hrs. in humidified 5 % CO_2 at 37 ^oC. Transfection efficiency was evaluated by EVOS FL Auto 2.

Colonic organoids were cultured 10-12 days prior to transfection. DNA and Lipofectamine 2000 were diluted and prepared similarly as described for HT-29. Old medium was removed from the organoids, and the DNA/lipofectamine mixture (100 µl) was mixed with of Opti-MEM ± FCS (10%) (400 µl). Organoids were incubated at 5% CO_2 at 37 ^oC until the following day. Medium was then refreshed (500 µl MG-C), and the transfection efficiency evaluated by EVOS FL Auto 2.

To facilitate contact between lipofection complexes and organoids in the following experiments, the Matrigel was disrupted. Disruption was conducted by adding ice cold MG-B + FCS to the wells, with further vigorous resuspension of organoids. Cell suspension was

then centrifuged at 200 x g at 4 ^{o}C for 5 min. The supernatant was removed, and intact organoids resuspended in Opti-MEM ±FCS (10%) (400 µ/well) and transferred to wells in 24-well low-attachment plates. DNA/lipofectamine (100 µl) was then added and the cell suspension incubated for 4-6 hrs. before re-plated in Matrigel (50 µl). Matrigel was overlaid with MG-E (500 µl) after 20 min of solidification.

Lipofectamine Stem Cell Reagent

The Lipofectamine stem reagent was tested on organoids only, with the same procedure as described earlier. Plasmids were diluted to a final amount of 2 µg/well and mixed with diluted Lipofectamine stem reagent (1-2 µl). Complexes were incubated in serum-free Opti-MEM for minimum 10-15 min. Both intact organoids and single cell suspension free of Matrigel were centrifuged and supernatant removed, before subsequent resuspension in Opti-MEM containing FCS (10 %). Plasmid/Lipofectamine stem complexes were added to the cells and incubated 6-7 hrs. in 5% CO_2 at 37 ^{o}C. Organoids were then collected and re-plated in Matrigel (50 µl) on a 24-well plate, and overlaid with MG-E (500 µl) after 20 min solidification.

Accell Delivery Media

Organoids were transfected with Accell siRNA red fluorescent non-targeting control and GAPDH positive control. The organoids were prepared for transfection as previously described. The Accell delivery excludes the need of transfection reagent, but require high siRNA concentrations. Various concentrations of Accell siRNA red fluorescent non-targeting control (1 µM and 30 nM) and GAPDH positive control (30-, 100-, 250-, 500- & 1 µM) was diluted directly into Accell Delivery Media, and organoids incubated for 5-6 hrs. Post transfection, organoids were re-embedded in Matrigel and overlaid with MG-E (500 µl).

RNAiMAX

To optimize siRNA knockdown, HT-29 cells were transfected with RNAiMAX and ON-TARGETplus LCN2 siRNA. The procedure was carried out in accordance with the manufacture’s protocols, using the recommended siRNA concentration (12,5 nM/well). Assessment of the optimal timepoint for protein knockdown was conducted by harvesting and pelleting cells at different timepoints (48-, 72- and 96 hrs.).

Nuclear Staining and Paraformaldehyde Fixation of Organoids

Nuclear staining of organoids transfected with pCMV-LifeAct were accomplished by supplementing MG-C with Hoechst 33342 (Thermo Fischer) (1:250, 1:500, 1:1000). Organoids were incubated 10-15 min before nuclear staining was inspected in LEICA 3 SP8 STED 3X confocal microscope. Following microscopy, organoids were fixed in paraformaldehyde (PFA) for preservation. A 4% PFA solution was supplemented with sucrose (2%). To avoid disintegration of Matrigel, the PFA with sucrose was heated to 37 ^{o}C. The culture medium was exchanged for PFA (1 mL), before incubated over night with the lid on, shielded from light. PFA was removed the following day, and the culture plate covered in foil and placed at 4 ^{o}C for storage.

Antibiotic Titration - Puromycin

50 000 HT-29 cells/well were seeded in a 24-well plate. A puromycin-stock of 10 µg/mL was prepared, and cells added puromycin in the range 0.5 -10 µg/mL. The different concentrations were run in triplicates, and the medium changed every 2-3 days. Cells were frequently monitored for cell viability/death in light microscope. The serial dilution of puromycin-stock, as well as plate-set up are shown in **Table 1-2, Appendix 3.**

Lentiviral Particle Production and Transduction

Prior to viral transduction, glycerol stocks of bacteria containing lenti- LCN2 sgRNAs and cas9- plasmids were grown on agar plates, amplified, and plasmids isolated as earlier described. HEK293T cells were passaged at least two times before utilized in transfection and packaging of viral particles. Information regarding lentivirus-plasmid constructions and target sequences are described in **Appendix 2.**

One day prior to transfection, HEK293T cells (6 x 10^5) were seeded in 60 mm dishes with DMEM supplemented with FCS (10%) without antibiotics. On the day of transfection, the expression plasmids, Cas9 and eGFP positive control (GeneCopoeia) (1 µg), and Lenti-pac HIV mix (GeneCopoeia) (1 µg) were diluted in Opti-MEM (100 µl). EndoFectin^{TM} transfection reagent (GeneCopoeia) (6 µl) was diluted in Opti-MEM (100 µl) in a separate tube. Subsequently, the diluted EndoFectin was added dropwise to the diluted plasmids. The adding sequence should not be reversed. The plasmid/EndoFectin mixture was incubated 10-25 min in RT to allow complex formation. The complexes were added directly to the cells, with swirling of the dish to distribute the mixture evenly. The cell dishes were incubated in 5% CO_2 at 37 ^{o}C overnight. Within 16 hrs., medium was changed to McCoy's 5a supplemented with FCS (5%), Gentamicin (0,05%) and TiterBoost^{TM} (GeneCopoeia) (1:500).

Approximately 36 hrs. post transfection, HT-29 cells (3 x 10^5) were transferred in cell culture medium (390 µl) to one well on a 6-well plate together with Hexadimethrine bromide (Sigma

Aldrich) (2 mg/mL) (13,5 µl), resulting in a working concentration of ~10 µg/mL. Virus supernatant (~2,5 mL) from HEK293T cells was filtered through a 0,45 µM polyethersulfone (PES) low protein-binding filter and added to target cells. Fresh medium (3 mL) supplemented with TiterBoost were added to HEK293T cells for further virus production. The same procedure was conducted after ~48- and 60 hrs., including addition of hexadimethrine bromide to HT-29 cells at all three timepoints. After additional 8 hrs., the virus-containing medium was removed from HT-29 cells and replaced with fresh, complete growth medium. After 2-3 days, puromycin (1 µg/mL) was added to transduced cells for selection of positively altered clones. Puromycin selection was carried out for 7 days. Cells transduced with Cas9-lentiviral particles were harvested and resuspended in freezing medium (FCS + 10% dimethyl sulfoxide((DMSO)) and stored at -80^{o}C before placed in liquid nitrogen. A fraction of cells was harvested for western blot analysis. Cells transduced with eGFP positive control were visualized in fluorescent microscope/EVOS FL Auto 2.

Western Blot

Prior to western blotting, cells were harvested, pelleted and lysed for protein extraction. Cell suspensions were centrifuged at 400 x g, 5 min RT, before removal of supernatant. The pellets were resuspended in PBS (1 mL), before repeating centrifuge-step and supernatant removal. Cell pellets were snap frozen in liquid nitrogen and stored at -80 ^{o}C. For organoids, the supernatant was removed, and organoids and matrigel disrupted by supplementation of Cell Recovery Solution (Corning Life Science) (500 µl), before transfer of content to appropriate tubes. Wells were washed again with the same volume of Cell Recovery Solution, to collect as many organoid cells as possible. Tubes were then placed on ice at an angle, on an orbital shaker for 1 hr. Next, tubes were centrifuged at 500 x g, 5 min at 4 ^{o}C, before the supernatant was removed, and cells washed once more in Cell Recovery Solution. Thereafter, cells were washed carefully with PBS x 3 with centrifugation between each wash-step. During the washing procedure, cell pellets were not resuspended, in order to avoid cells sticking to the pipette tip. Pellets were then snap frozen in liquid nitrogen and stored at -80 ^{o}C.

Triton-X lysis stock buffer I and II were prepared according to **Table 13-14, Appendix 6** and complete buffer I and II supplemented protease inhibitors as described in **Table 15, Appendix 6.** Cell pellets were thawed on ice and resuspended in one pellet-cell-volume (PCV) of ice-cold buffer I. Next, one PCV of buffer II was added to cell suspension and resuspended. Cell lysates were placed on a shaker (900-1100 rpm) at 4 ^{o}C for 2 hrs., before centrifuged at 13 000 rpm in a microcentrifuge for 15 min at 4 ^{o}C. The supernatant was recovered, and protein concentration measured by Bradford assay, before lysates were stored at -80 ^{o}C.

A volume of cell lysate corresponding to 10-50 µg protein was mixed with NuPAGE® LDS Sample Buffer 4X (Invitrogen) (5 µl), 1M dithiothreitol (DTT) 20X (1 µl) and dH_2O to a final volume of 20 µl. Samples were then vortexed briefly and placed at 70 ^oC for 10 min. In case of too high protein concentrations, lysate was diluted in complete Triton-X lysis buffer II. A ladder consisting of Seeblue® Pre-Stained Standard (1X) (Life Technologies) and MagicMark XP Western Protein Standard (Invitrogen) were mixed (1:1) and placed on ice. NuPAGE® 4-12% Bis-Tris Gel (Invitrogen) was washed with dH_2O and combs were gently removed. The wells were rinsed with NuPAGE® MOPS SDS Running Buffer (Life Technologies) before gel and electrophoresis chamber were assembled. The inner chamber was then filled with running buffer to exceed wells. Ladder (7 µl) was loaded in the outermost wells with samples (18 µl) in between. The outer chamber was filled with running buffer, and gel run by Powerease 500 (Invitrogen) at 200 V for 50 min.

PDVF membranes (1-2) and filter papers (2-4) were cut to sizes equal to the gel. Blotting pads were prepared by soaking them in NuPAGE® Transfer Buffer (Life Technologies). The membrane was prepared by incubation in methanol (MeOH) (30 sec), before washed in dH_2O and transferred to transfer buffer. The gel cassette was removed by using a gel knife, and the gel transferred onto a soaked filter paper. The blotting cassette was built with blotting pads, filter papers, gel and membrane as shown in **Figure 6.** Proteins will be transferred from negative to positive terminal, thus it is important to place the membrane on top of the gel. The cassette was placed in the blotting module and the core filled with transfer buffer. The outer chamber was filled with dH_2O. Blotting was run at 30 V for 60 min. The principles behind western blot and Bradford assay are described in **Appendix 1.**

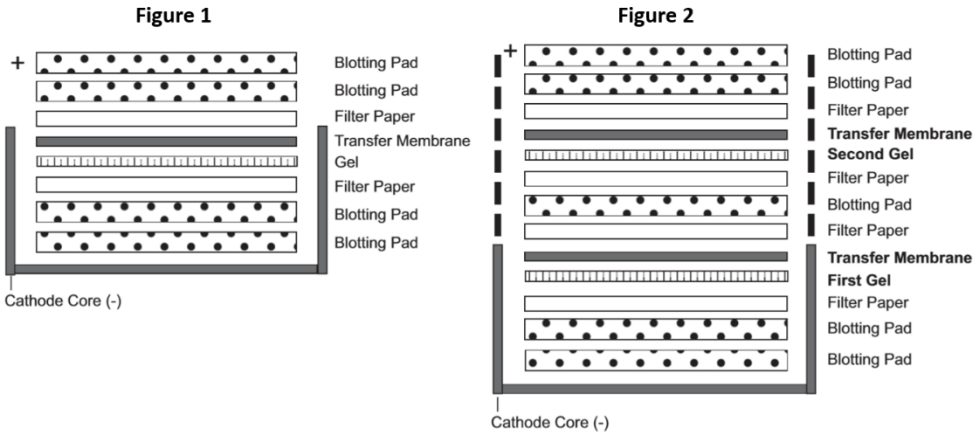

Figure 6: The building order of the blotting cassette, showing order dependent on blotting of either one (Figure 1) or two gels (Figure 2). The cassette is filled with plotting pads, filter papers, gel and PDVF transfer membrane. Figure modified from XCell II™ Blot Module user manual (Invitrogen).

xCELLigence

The RTCA xCELLigence system (ACEA Biosciences) was set up according to the manufacturer's instructions. Minimum 2 hrs. before the experiment, the RTCA SP station were placed inside an incubator with 5% CO_2 at 37 ^oC for achieving equilibrium. McCoy's 5a culture medium (100 µl) with Gentamicin (0,05%) ± FCS (10%) was added to the E-96 plate and left in the tissue culture hood for 30 min at RT for equilibration. The E-96 plate was inserted into the RTCA SP station and background impedance was measured.

Meanwhile, cells were trypsinized and counted, before resuspended in McCoy's 5a culture medium with Gentamicin (0,05%) ± FCS (10%). ON-TARGETplus LCN2 siRNA, Allstars Negative Control siRNA (Qiagen) and RNAiMAX transfection reagent were diluted and mixed according to the manufacturer's protocol. Complexes were added to cell suspensions to a final volume of 100 µl and 12,5 nM siRNA per well. The E-96 plate was removed from the RTCA SP station and added the appropriate conditions of cell suspension, resulting in a total volume of 200 µl/well. The complete set up with different experimental conditions are shown in **Figure 1, Appendix 3.** Cells were allowed to settle for 30 min in the tissue culture hood, before reinsertion into the SP station. The impedance was measured and recorded every 15 min. for 48 hrs. xCELLigence was conducted twice, with 8 technical replicates. The principles behind the procedure are described in **Appendix 1.**

Fluorescence Microscopy

Transfected cells and organoids were visualized by EVOS FL Auto 2 (Thermo Fischer Scientific), Confocal Zeiss Airyscan (Zeiss) and LEICA 3 SP8 STED 3X confocal microscope (Leica Microsystems).

Statistics

Protein expression levels obtained by western blots were normalized against internal controls and quantified by Image J. The treatment group with highest mean signal was set as reference (100%) expression level.

The values from the xCELLigence growth assay were min-max normalized, followed by statistical analyses conducted with GraphPad Prism 8, using a two-sided unpaired T-test (Welch's T-test). Results were assessed as statistically significant with $p<0.05$, designated with*.

Results

Part 1 – Organoid Culture

Optimized protocols for culture and passage of intestinal colonic organoids long-term have been developed and optimized the last decade. In our lab, intestinal colonic crypts were isolated from patient biopsies and embedded in Matrigel and culture medium for establishment.

The utilization of organoid-specific protocols describing essential growth requirements, led to the development of multicellular, 3D organoid structures. Supplementation of factors such as Wnt, Nicotinamide, SB202190, Noggin and A-83-01 facilitated the maintenance of an immature organoid phenotype, mainly consisting of ISCs. 12-14 days old, undifferentiated organoids are depicted in **Figure 7, A.** Most of these organoids appeared with a spheroid structure **(Figure 7, A),** while the characteristic crypt-villus structure seen *in vivo* and in differentiated organoids were absent. However, some of the specimens showed a slightly more budded structure **(Fig. 7, B** and **C)**, possibly caused by long culturing time and a spontaneous initiation of differentiation. Furthermore, the epithelial monolayer of the organoids formed a central lumen, with apical sides pointing inwards. The cells' basal sides pointed out towards to the extracellular environment.

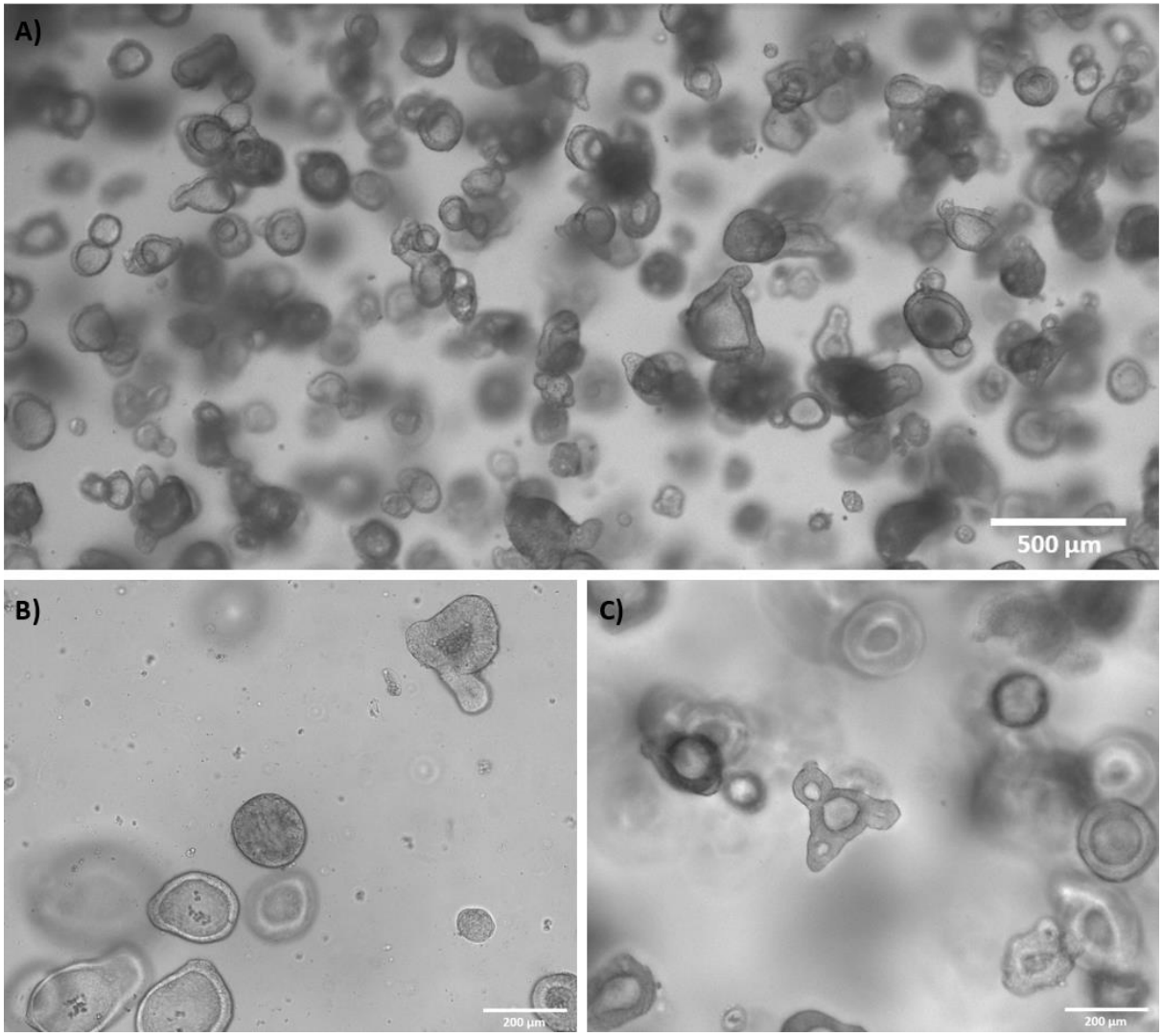

Figure 7: A) Undifferentiated patient derived colonic organoids after 12-14 days of growth. The organoids are cultured in media with high levels of Wnt and RSPOs to facilitate a spheroid stem cell phenotype. **B)** and **C)** Some of the specimens showed a more budded phenotype, resembling the crypt-villus structure observed *in vivo* or the structure of differentiated organoids.

Part 2 – Electroporation

Introductorily, the first approach to transfection was utilization of the NEON electroporation system. Here, HT-29 cells and organoids were resuspended in a conductive solution and exposed to electric current. This mediating transient pores in the cell membrane, facilitating uptake of nucleic acids.

Electroporation of HT-29 and Organoids with CRISPR/cas9 LCN2 KO Plasmids

Initially, electroporation was conducted on HT-29 cells with the CRISPR/Cas9 LCN2 KO plasmids. The experiment was conducted several times, with variations in voltage, pulse width and number of pulses (**Table 1, Appendix 4**). No GFP-positive cells were observed in either of the experiments upon visualization by EVOS FL Auto 2. Electroporation was also conducted on a single cell suspension of colonic organoids, but negative results were shown by the absence of GFP-positive cells. Hence, restriction digest assays were carried out, to verify the sequence information provided by manufacturer. Files containing plasmid sequences were assessed in Genome Compiler. All four plasmids were identified to have two restriction sites for EcoRI, giving the fragment sizes 1128 bp/6876 bp and 1103 bp/5962 bp for G1, G2 and S, and D, respectively.

Expected fragments of approximately 1100 bp were present in all digests. However, large bands did not give predicted fragments for any of the plasmids (**Figure 8, A.**). New sequence files were provided, and processing in Genome Compiler now suggested one restriction site of EcoRI for D. New digestions were conducted with EcoRI and BamHI, which were expected to give the fragments 1103 bp/5963 bp. The restriction enzymes and fragments for G1, G2 and Scramble were unchanged. Undigested, supercoiled plasmids were also loaded as a control (*). Similar results from digestion were observed here as well, with large bands diverging from predicted sizes **(Figure 8, B.).** Finally, D was digested with XbaI and BamHI, with expected 1738 bp/ 5328 bp fragments. As gel electrophoresis results show **(Figure 8, C.)**, both bands of D were consistent with predicted sizes, while large bands of G1, G2 and S were still larger than expected.

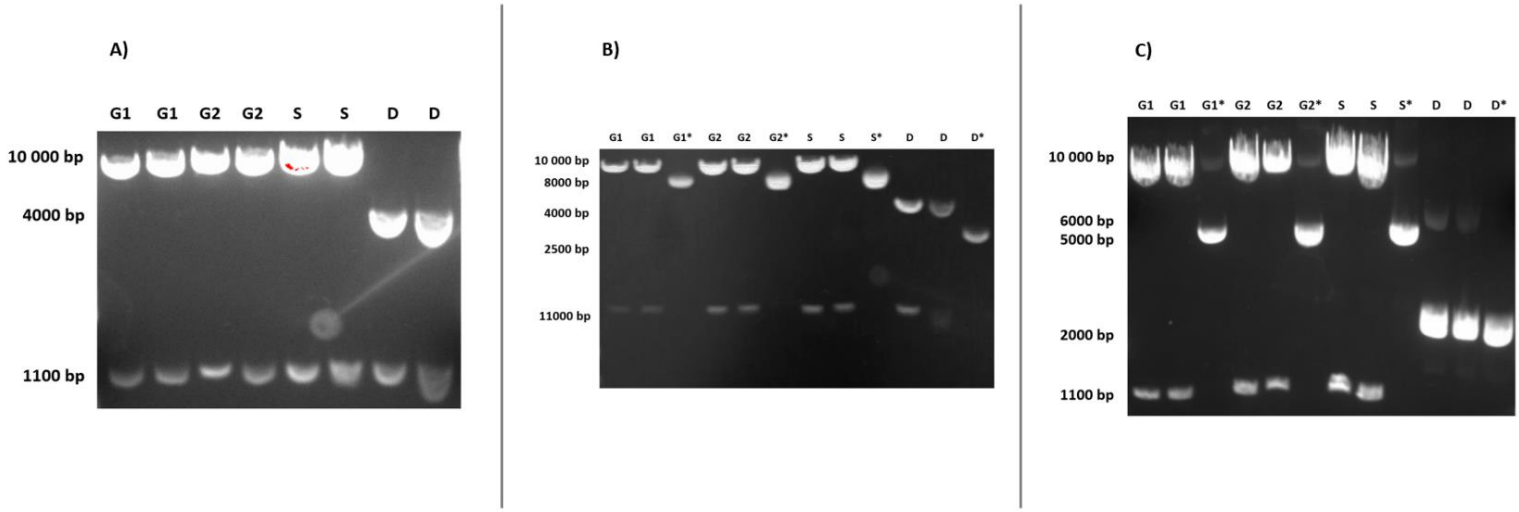

Figure 8: Restriction digest assay of CRISPR/Cas9 LCN2 KO plasmids, with digests of G1, G2, S and D. **A)** All four plasmids were digested with EcoRI restriction enzymes. **B)** G1, G2 and S were digested with EcoRI, while D was digested with EcoRI and BamHI. Undigested samples of all plasmids were also present (*). **C)** G1, G2 and S were digested with EcoRI, while D was digested with BamHI and XbaI.

Electroporation of HT-29 with pCMV-LifeAct

To resolve whether the negative results of the CRISPR KO plasmids were due to the plasmids, low efficiency of HDR or the experimental procedure itself, HT-29 cells were transfected with the GFP-positive control plasmid, pCMV-LifeAct. A fraction of the cells showed clear GFP expression when visualized by EVOS FL Auto 2 (**Figure 9**). These cells were exposed to gentle electroporation parameters. Despite this, post transfection, cells looked unhealthy, lacking normal morphology and cell proliferation.

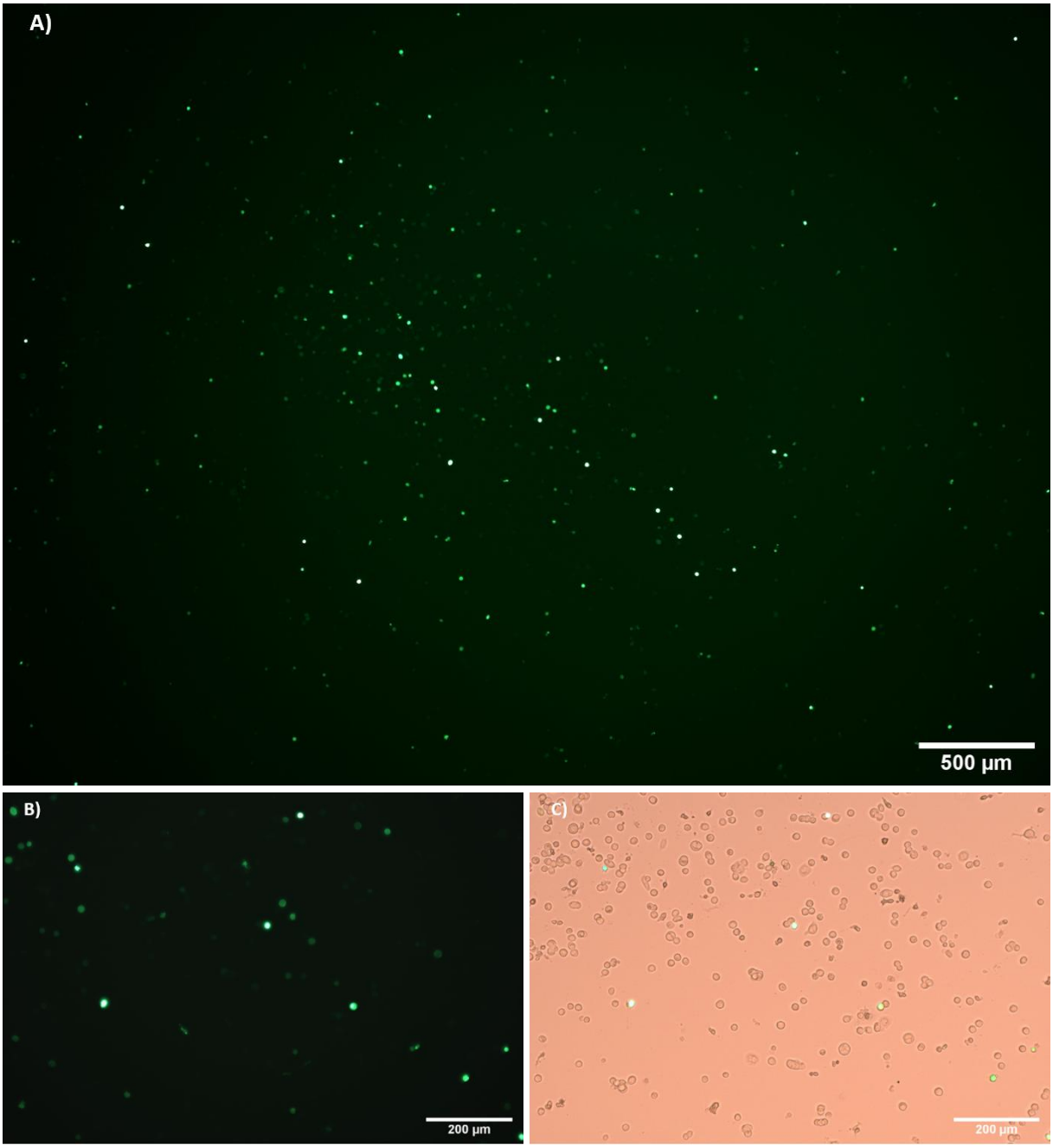

Figure 9: **A), B)** and **C)** HT-29 cells electroporated with pCMV-LifeAct positive control plasmid. Despite a fraction of GFP-positive cells, cell viability was markedly reduced by the electroporation procedure.

Part 3 – Lipofection

The unsatisfactory results from electroporation motivated the next step; exploration of lipofection, which is an efficient and more gentle delivery method. Plasmids and siRNA were incubated with a liposomal reagent for complex formation, before supplemented in the cell culture medium. The variations between the individual lipofection experiments are listed in **Table 2, Appendix 4.**

Lipofection of HT-29 with pCMV-LifeAct Plasmid

Initially, lipofection was first tested with pCMV-LifeAct positive control in HT-29 cells to verify that the protocol and the transfection reagent functioned as expected. The cells were transfected with equal amounts of plasmid (500 µg/well), but optimized for volumes of Lipofectamine 2000 (1-5 µl/well). The transfection efficiency was evidently improved compared to electroporation (**Figure 10**), and was furthermore enhanced with increased amount of Lipofectamine 2000. Higher amounts of Lipofectamine 2000 did not change cell viability.

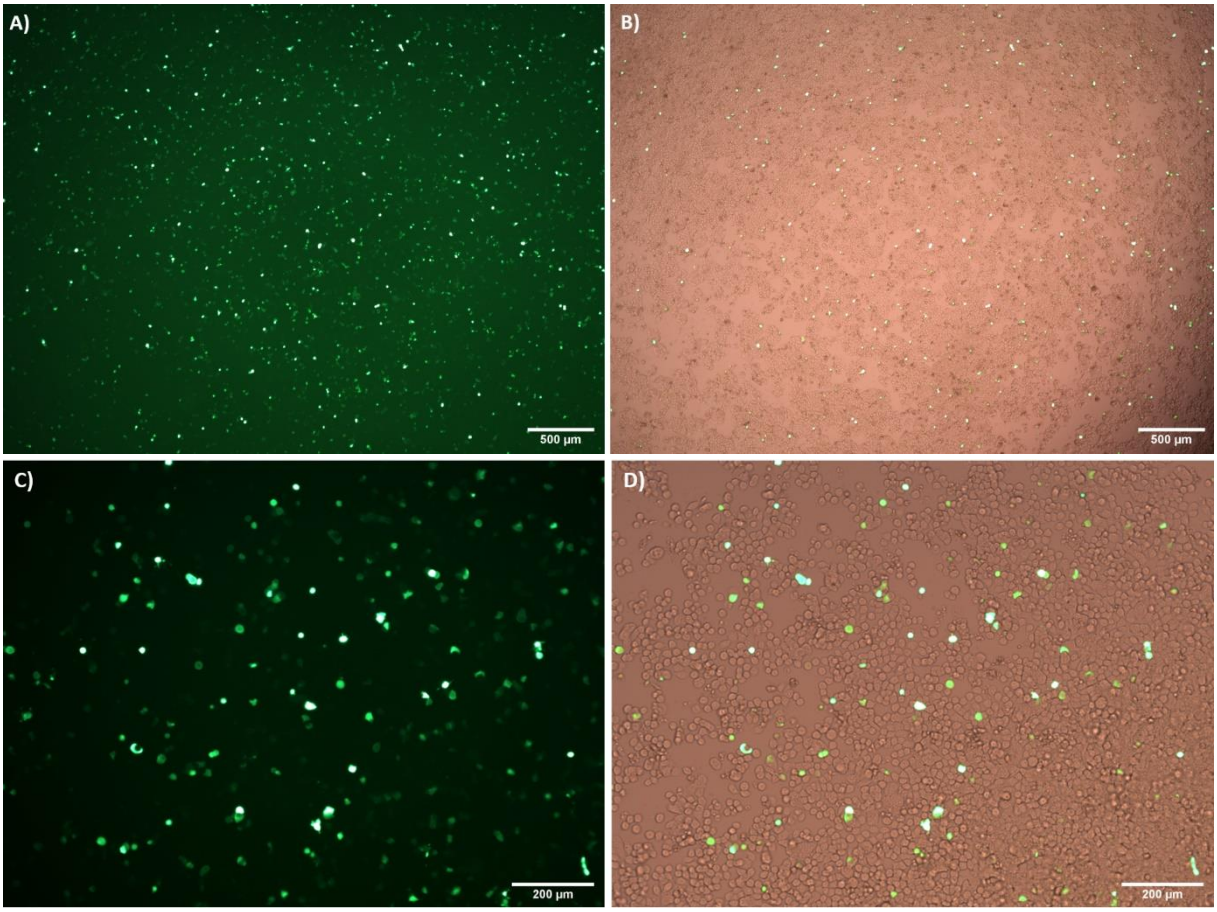

Figure 10: A)-D) HT-29 cells were transfected with transfection reagent Lipofectamine 2000 (4 µl/well) and pCMV-LifeAct (500 ng/well). The transfection efficiency was strongly improved from previous electroporation procedures and alterations of cell proliferation was not observed.

Lipofection of HT-29 with CRISPR/cas9 LCN2 KO Plasmids

After verifying the experimental procedure with pCMV-LifeAct as a positive control, HT-29 cells were transfected with CRISPR/Cas9 LCN2 KO plasmids and Lipofectamine 2000. Once again, no GFP-positive cells were observed by fluorescent microscopy. To examine whether LCN2 KO had proceeded through NHEJ rather than HDR, a western blot was run on cell pellets from two transfection experiments of HT-29 cells. Cells were transfected with the following combinations of plasmids: G1+D, G2+D and G1+D and G1 alone. None of the samples showed LCN2 protein knockdown compared to Lipofectamine control samples and the housekeeping gene (**Figure 11**). Quantitation of protein expression using Image J is shown in **Figure 2, Appendix 5.**

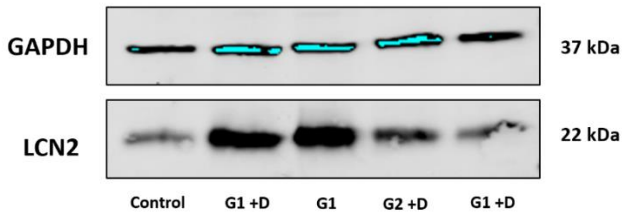

Figure 11: HT-29 cells transfected by lipofection with CRISPR/Cas9 LCN2 KO plasmids, with the following plasmid combinations: G1+D, G2+D and D alone. LCN2 expression was compared to negative control, with no indication of protein knockdown.

Lipofection of Intestinal Organoids with pCMV-LifeAct Plasmid

Based on the before mentioned experiments observing GFP-positive HT-29 cells transfected with pCMV-LifeAct and Lipofectamine 2000, the method was adapted to use in organoid cultures. In the first attempt, complexes with pCMV-LifeAct together with Opti-MEM culture medium were added to organoids, which were still embedded in Matrigel. The complexes and culture medium were prepared ± FCS during both the complex formation and in the media. In neither condition, GFP fluorescent cells were observed.

Suspecting that Matrigel might be a physical barrier obstructing the liposomal-plasmid complexes from the organoids, Matrigel was disrupted in the following experiments and incubated with transfection complexes for 5-6 hrs. Whole organoids were incubated at the same conditions as in the previous experiment (± FCS, 500 ng plasmid/well). Still, the procedure did not result in GFP-positive cells. The amount of plasmid was therefore increased from 500 ng to 2 µg/well, while complexes were prepared ± FCS and with FCS (10%) in the culture medium for both conditions. The organoids transfected with complexes made in the presence of FCS did not show cells expressing fluorescence. However, for the first time, organoids transfected without FCS during complex formation showed GFP-positive organoid cells (**Figure 12**).

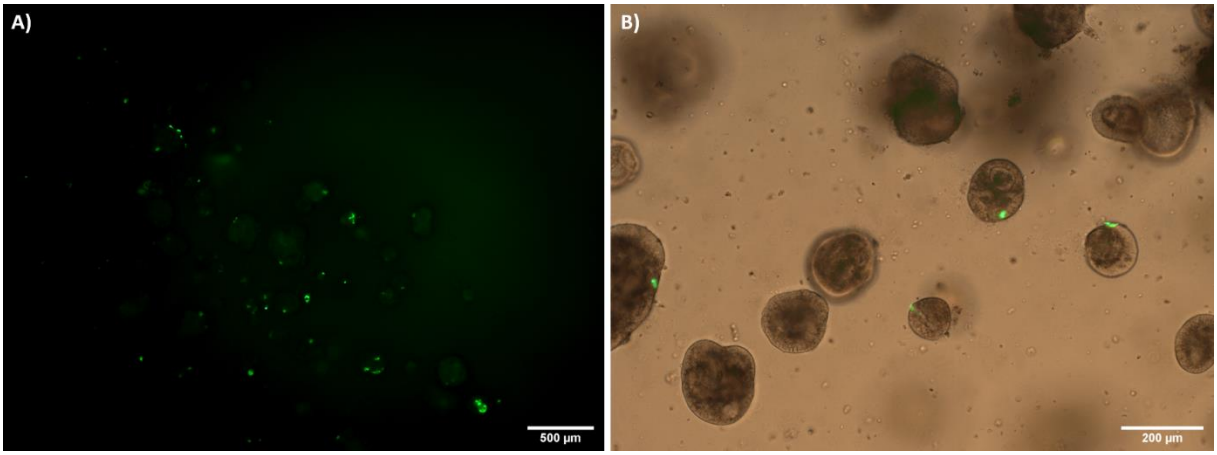

Figure 12: A) Intestinal colonic organoids transfected by Lipofectamine 2000 (4 µl/well) and pCMV-LifeAct (2µg/well). Organoids were treated with liposome-plasmid complexes prepared in the absence of FCS, but with FCS supplementation in the culture medium (10%). GFP-positive cells were observed in a fraction of the organoids. Complexes made in the presence of FCS gave no positive results. **B)** Single cells within the organoids expressed GFP.

Next, organoids were transfected completely without FCS, both during complex formation and in the culture media. GFP fluorescence was not observed, indicating that FCS aid transfection as long as it is not present during complex formation.

Undifferentiated organoids consist mainly of ISCs. Therefore, a change was made in use of transfection reagent by exchanging Lipofectamine 2000 with Lipofectamine Stem Reagent,

due to its suitability for hard-to-transfect cells. Organoids were transfected with pCMV-LifeAct (2 µg), both as whole organoids and single cell suspensions. Based on experiences from preceding experiments, complexes were formed without presence of FCS, while transfection was performed with FCS (10%) in the culture media. The experiment thus resulted in the most effective transfection so far (**Panel Figure 13**). In the wells of whole organoids, a larger fraction of GFP-positive cells was observed compared to the wells containing single cells (**Figure 14**).

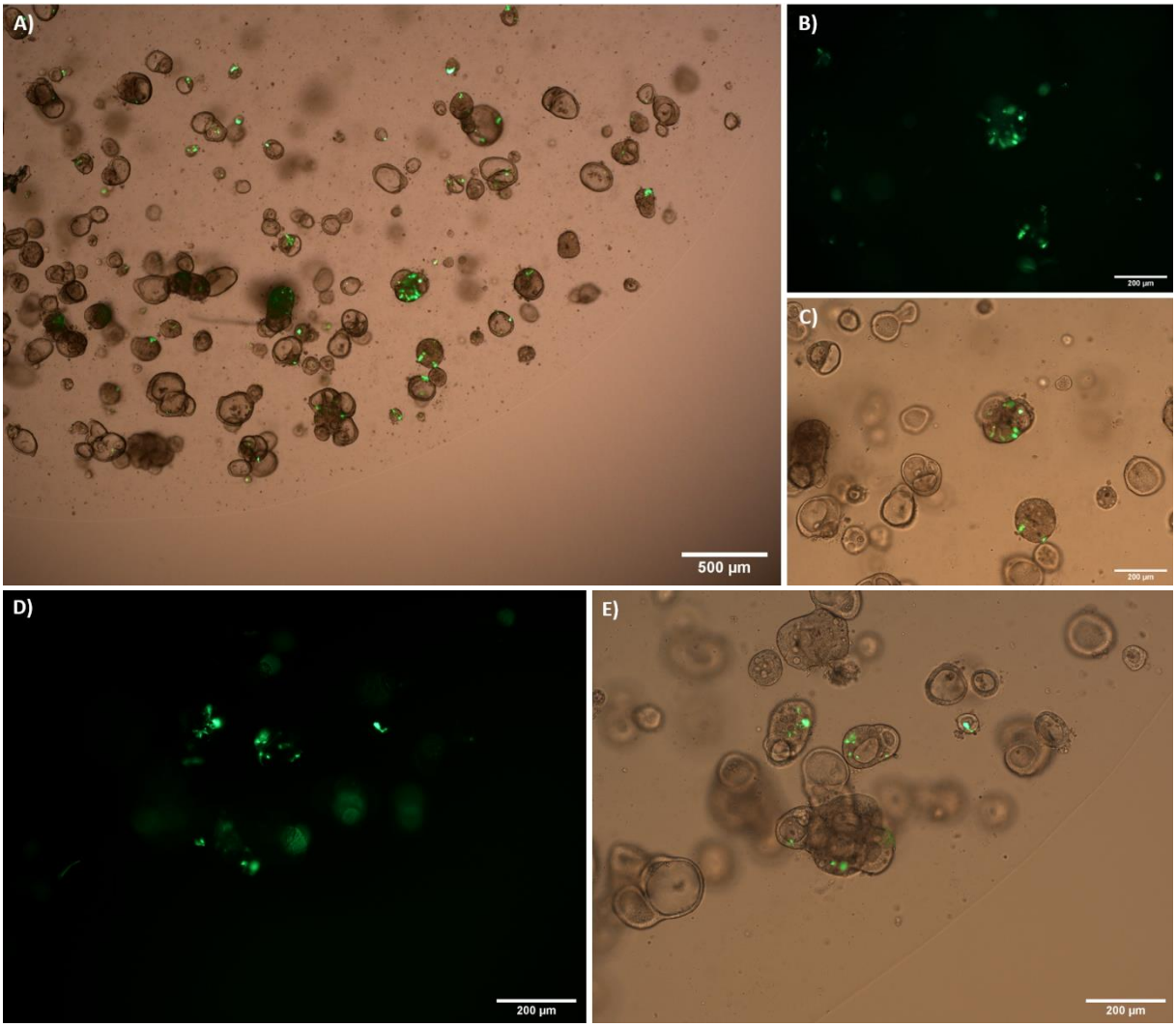

Figure 13: A)-E) Intestinal colonic organoids transfected by Lipofectamine Stem Reagent (1-2 µl/well) and pCMV-LifeAct (2µg/well). The liposomal complexes were prepared in the absence of FCS and FCS was further supplemented in the culture medium (10%). Compared to previous attempts, the transfection efficiency of organoids was strongly improved.

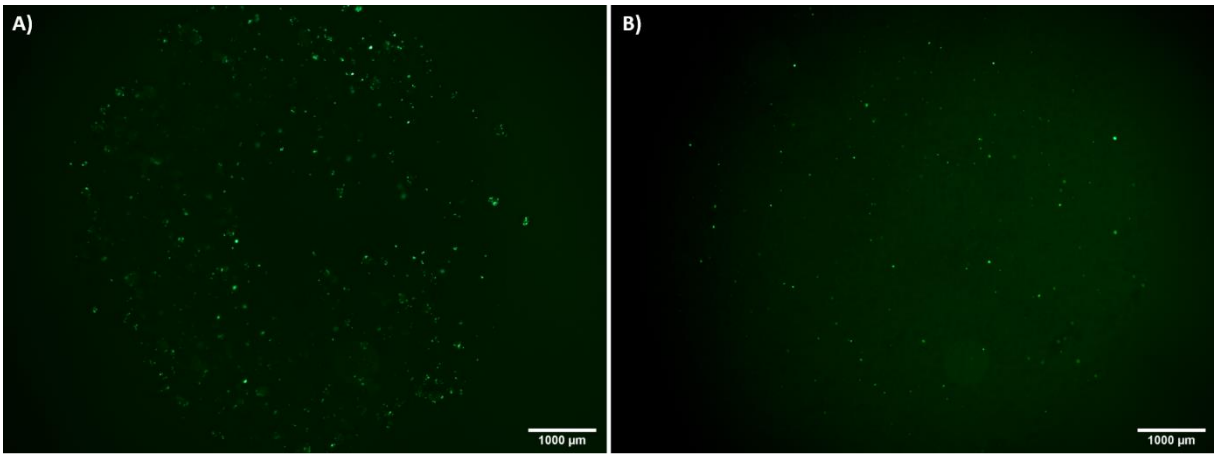

Figure 14: A) Whole organoids gave a larger fraction of GFP-positive cells, compared to transfection of single cell suspensions (**B**).

The EVOS FL Auto 2 fluorescent microscope does not have the magnification or resolution to image cellular features of the single cells within the organoids. As a proof of concept, showing that pCMV-LifeAct binds filamentous actin within the cell as intended, organoids were prepared for imaging in LEICA 3 SP8 STED 3X confocal microscope. Cross-sections of a GFP-positive cell with Hoechst 33342 (blue) nuclear staining are shown in **Figure 15.** The nucleus appears fractional, but this may be due to debris from other dead cells that have been captured in the Matrigel upon re-plating, thus creating background noise.

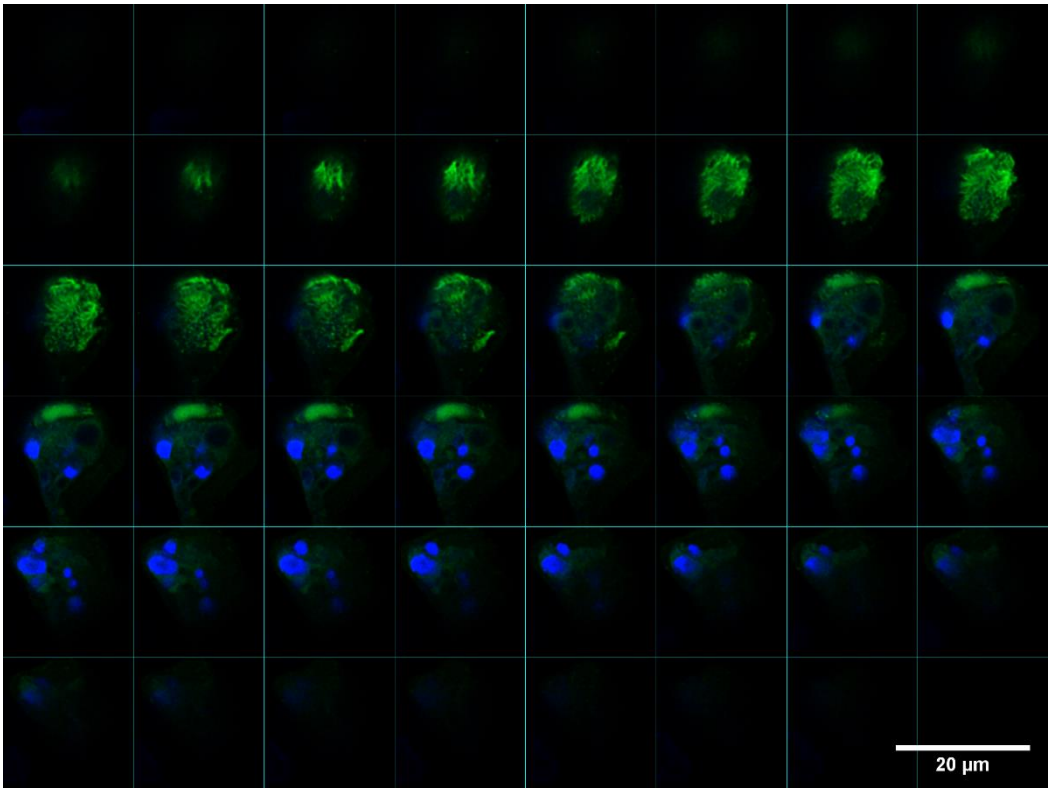

Figure 15: A cross-section of a positively transfected cell within an intestinal organoid. F-actin is visualized by GFP (green), and the nucleus (blue) is stained with Hoechst 33342. The fractional nucleus may be caused by surrounding cell debris embedded in the Matrigel.

Lipofection with Accell siRNA into Organoids

The use of Lipofectamine Stem Reagent and the obtained insight of FCS requirements finally led to GFP-positive organoids. However, pCMV-LifeAct is only used as a transient positive control plasmid, with no relevant function except verifying plasmid uptake. Furthermore, the total number of positively transfected cells were too low to exert any effects under other experimental settings. Since the generation of stable KO organoids is a time-consuming and difficult process, siRNA knockdown was explored as a method for functional assays.

Accell red fluorescent non-targeting control siRNA was transfected into organoids by Accell Delivery media at 1 µM (recommended) or 30 nM (recommended by other transfection reagent suppliers) per well. The organoids showed evident siRNA uptake (**Figure 16**). No distinct differences in uptake was observed by comparing images of organoids receiving high and low siRNA concentrations. Furthermore, the siRNAs were observed to accumulate in the organoid lumen. Protein knockdown was explored by delivery of Accell GAPDH positive control siRNA (30-, 100-, 250-, 500- and 1000 nM/ well) to the organoids. Protein knockdown was not observed by western blot analysis. GAPDH was strongly expressed in all samples, regardless of received siRNA-concentration (**Figure 17**).

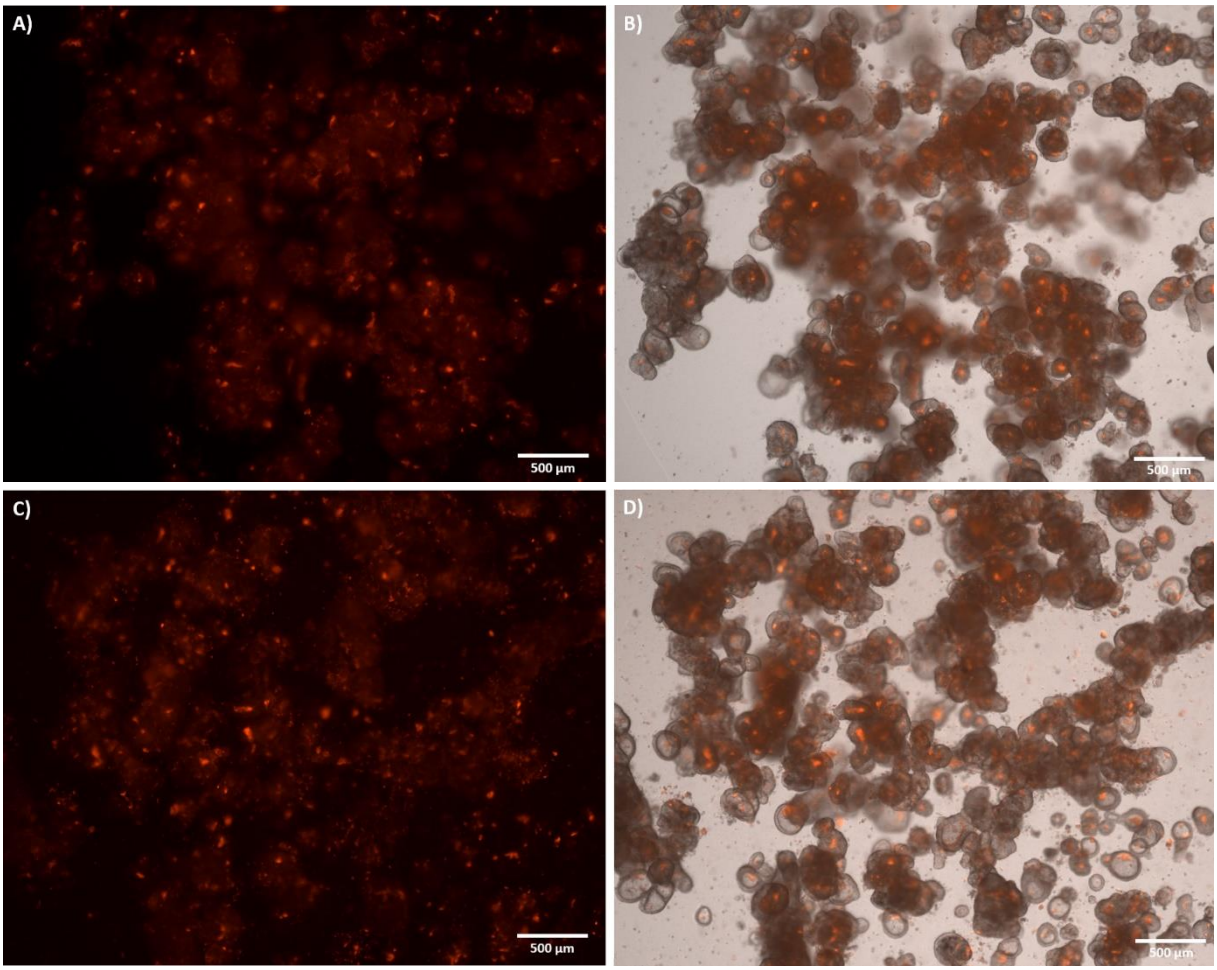

Figure 16: Intestinal colonic organoids transfected by Accell Red Non-targeting Control siRNA and Accell Delivery Media at 1 µM (**A** and **B**) and 30 nM (**C** and **D**)**.** Fluorescent signal and accumulation in the organoid lumen suggest siRNA uptake. The differences in siRNA concentrations did not seem to alter efficiency remarkably.

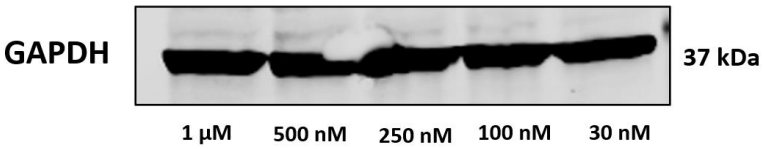

Figure 17: Western blot showing protein expression of GAPDH in organoids after transfection with Accell GAPDH siRNA positive control. GAPDH was strongly expressed at all siRNA concentrations.

Lipofection with ON-TARGETplus siRNA into HT-29

Due to high costs and unsatisfactory results using Accell siRNA, ON-TARGETplus siRNA for LCN2 and GAPDH were explored for efficiency of gene silencing. The negative results of siRNA transfection in organoids led us to return to HT-29 as a model system. siRNA transfection of HT-29 was conducted with RNAiMAX. RNAiMAX is a transfection reagent widely used for siRNA delivery. The cells were harvested at three timepoints; 48-, 72- and 96 hrs. Strong knockdown of LCN2 was seen for all three timepoints by western blot analysis (**Figure 18**), which was further supported by quantitation of protein expression in Image J (**Figure 19**). Furthermore, an unknown band at ~50 kDa was observed, indicating either unspecific binding, contamination or presence of possible LCN2- dimers (**Figure 20, A**). Suspecting FCS as a contaminant, an additional western blot was conducted with pure FCS, McCoy's 5A base medium (÷FCS) and HT-29 supernatant (10% FCS) harvested after 48- and 72 hrs. The band of 50 kDa was seen in FCS samples and samples from cell supernatant, but not in McCoy's 5a base medium (**Figure 20, B**).

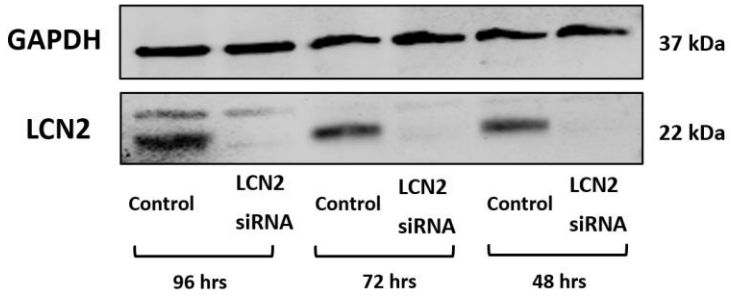

Figure 18: Protein knockdown was mediated by ON-TARGETplus LCN2 siRNA and RNAiMAX transfection reagent. Western blot analysis showed strong LCN2 knockdown (22 kDa) compared to GAPDH controls (37 kDa) for all timepoints.

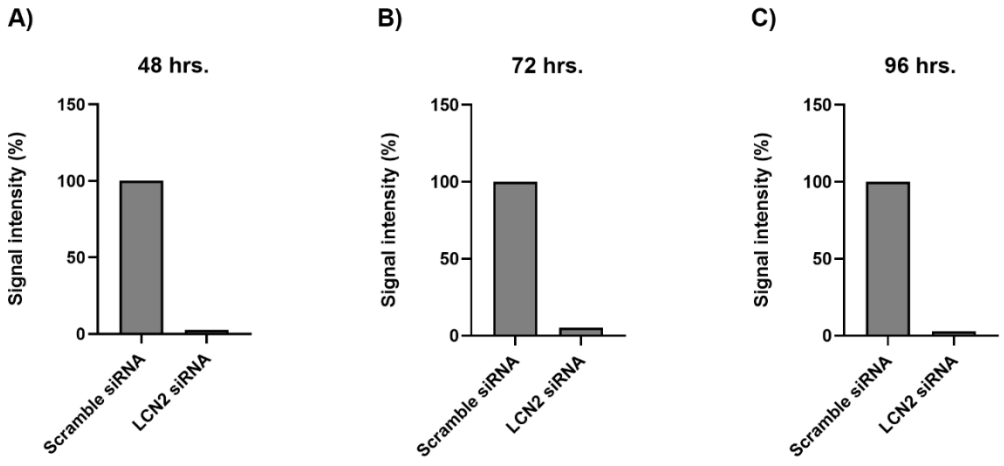

Figure 19: LCN2 protein expression from western blotting of cells transfected with LCN2 siRNA and RNAiMAX was quantified by Image J. Expression was normalized against GAPDH housekeeping gene.

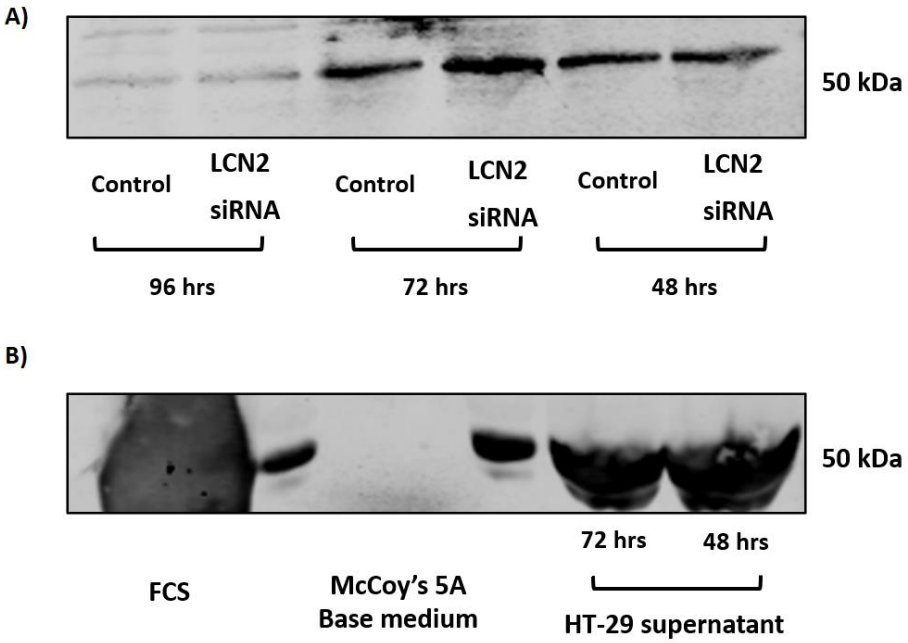

Figure 20: **A)** Unknown band at 50 kDa caused by unspecific binding, contamination or presence of LCN2-dimers were evaluated by western blot analysis. **B)** FCS and cell supernatant harvested at 48- and 72 hrs. showed all the same band. McCoy's 5a base medium did not show any positivity.

Part 4 – Viral Transduction

Initially, protocols and procedures of lentiviral transduction were conducted in HT-29 cells. Viral particles containing Cas9 and eGFP positive control, respectively, were produced in HEK293T packaging cells. Transfection of HEK293T cells was carried out with one expression plasmid and three packaging plasmids for each type of lentiviral particle produced. HT-29 cells transduced with eGFP and Cas9 lentiviral particles were selected upon puromycin resistance and passaged one time before analysis. Transduction of HT-29 cells with eGFP resulted in superior fluorescent expression compared to both electroporation and lipofection when visualized by EVOS FL Auto 2 (**Figure 21**). Strong eGFP-expression was still observed after one week of puro-selection and passage.

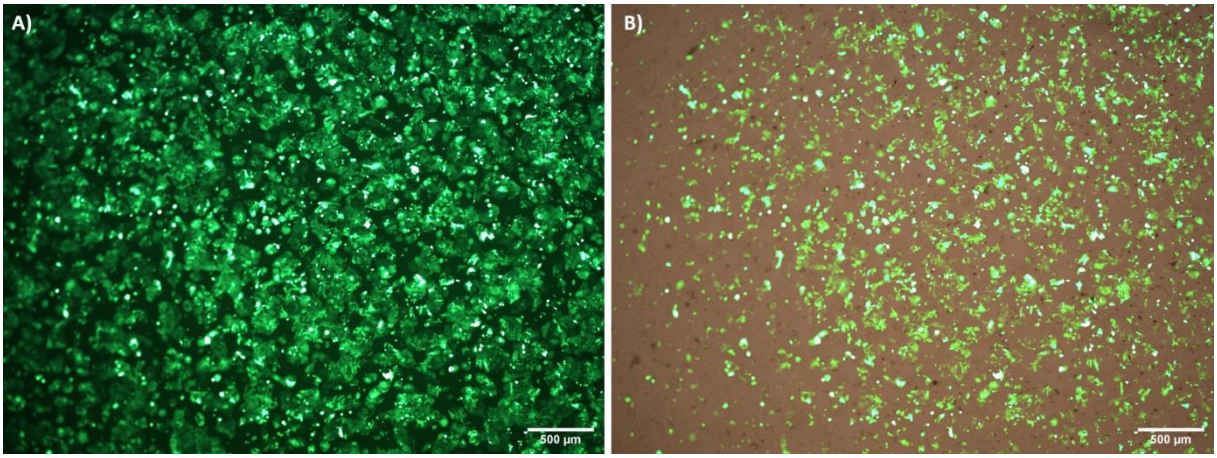

Figure 21: A) and **B)** HT-29 cells imaged after transduction by eGFP-lentiviral particles, one week of puromycin selection and cell passage. The efficiency was superior compared to both electroporation and lipofection, and without altering cell characteristics and viability.

HT-29 cells transduced with Cas9 lentiviral particles were harvested and pelleted for western blot analysis approximately one week post transduction. The western blot showed expression of Cas9 in transduced cells (**Figure 22**).

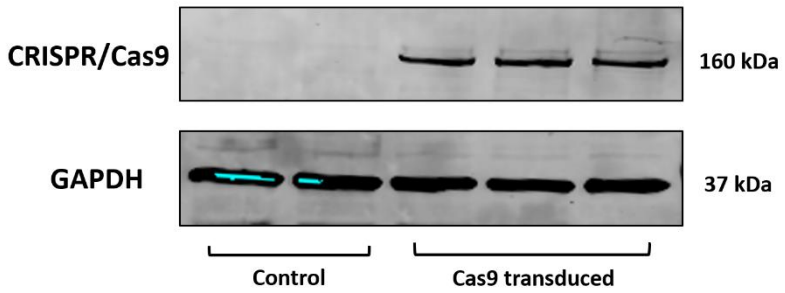

Figure 22: HT-29 cells transduced with Cas9-lentiviral particles showed clear protein expression of Cas9 (160 kDa). GAPDH used as a control (37 kDa).

Part 5 – xCELLigence: Assessing Gene Function Real Time

The RTCA xCELLigence system measures cell proliferation, migration or adhesion real time, based on reduced electron-flow, so called cellular impedance. HT-29 cells were transfected with either Allstars Negative Control siRNA (scramble) or ON-TARGETplus LCN2 siRNA (12,5 nM/well) with RNAiMAX transfection reagent. The two conditions were incubated in media ± 10% FCS. Cellular impedance was measured every 15 min. for 48 hrs. The experiment was repeated twice, with eight technical replicates for each condition (**Figure 1, Appendix 3**).

The differences between scramble- and LCN2 siRNA (10% FCS) at chosen timepoints (1-, 12-, 24-, 36-, 48 hrs.) are depicted in **Panel Figure 23** and **Figure 24**. Significant difference in cellular impedance was observed after 36- and 48 hrs. (p-value=0.0161 and 0.0002). Results were considered significant when $p<0.05$, designated with *. Higher cellular impedance reflects higher rates or proliferation, migration, or adhesion of cells treated with LCN2 siRNA compared to scramble siRNA. No significant differences were observed for cells treated ÷ FCS (**Figure 4, Appendix 5**). Verification of LCN2 knockdown was conducted by western blotting (**Figure 25**) and protein expression quantified by Image J. Quantitation of signal intensity showed an average LCN2 knockdown of 87% compared to cells treated with scramble siRNA. (**Figure 26, A**)**.** HT-29 cells were also seeded in parallel with equal siRNA concentrations as used in the xCELLigence assay (12,5 nM/well). To gain insight into whether higher impedance reflects higher rates of proliferation, these cells were counted before harvesting. However, the result was non-significant and the SD too high to be used for evaluation of proliferation **(Figure 26, B).**

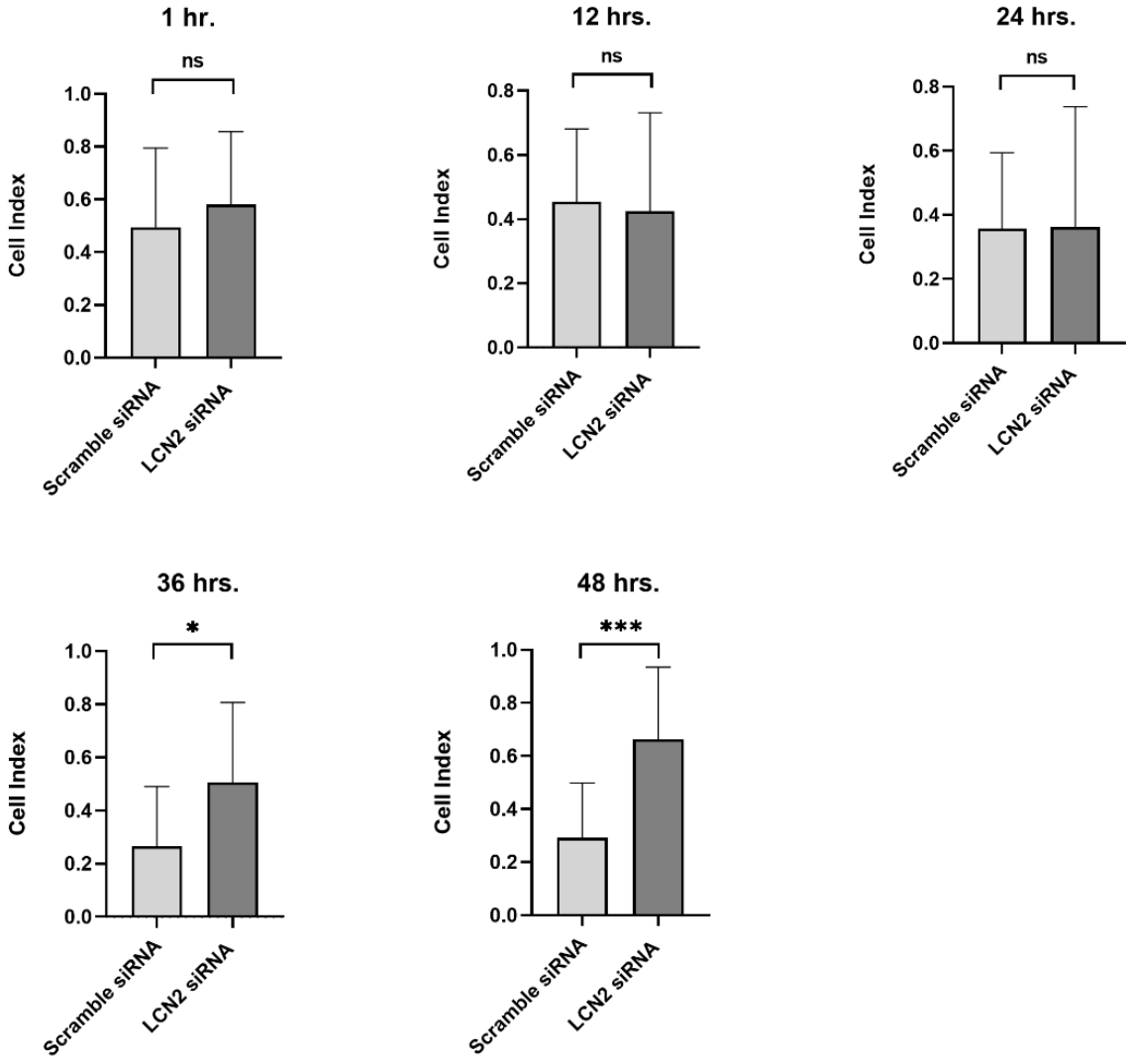

Figure 23: Cellular impedance measured at chosen timepoints (1-, 12-, 24-, 36-, 48 hrs.) showing significant differences of HT-29 cells treated with LCN2 and Scramble siRNA (12,5 nM/well) after 36- and 48 hrs. of incubation (p=0.0161 and 0.0002). Significance when p<0.05, designated with*.

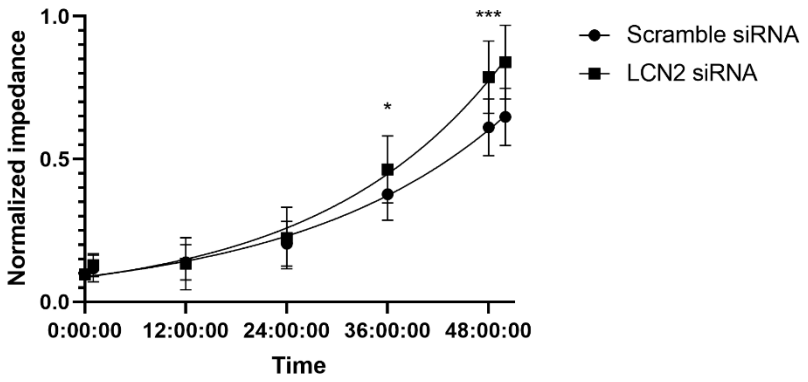

Figure 24: The growth curves of cells treated with LCN2- and scramble siRNA (12,5 nM/well), respectively. Cellular impedance was measured for 48 hrs.

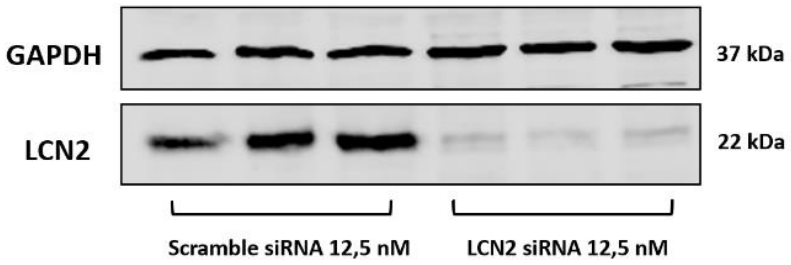

Figure 25: Verification of LCN2 knockdown mediated by ON-TARGETplus LCN2 siRNA (12,5 nM/well) and RNAiMAX, compared to scramble controls (12,5 nM) and GAPDH housekeeping gene.

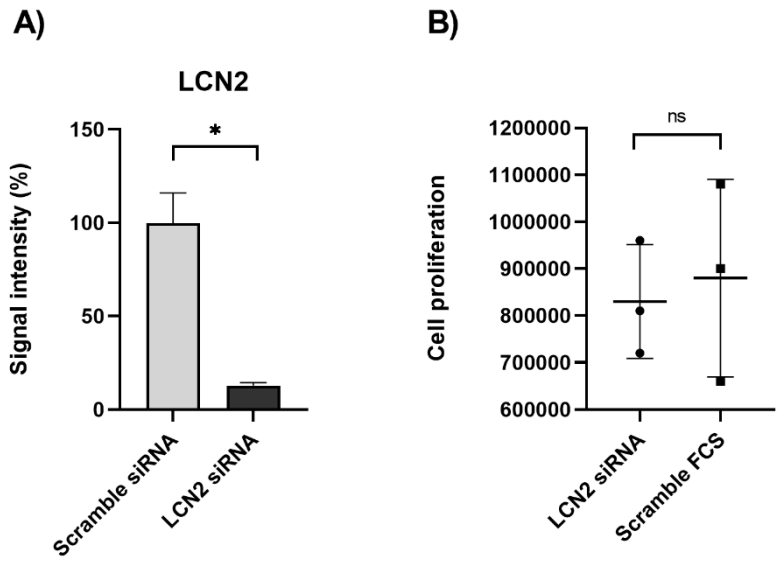

Figure 26: A) LCN2 protein expression from western blot of cells transfected with LCN2 siRNA (12,5 nM/well) and RNAiMAX was quantified by Image J. 13% expression of LCN2 was observed in LCN2 siRNA samples compared to the expression levels in scramble siRNA samples (set to 100%) ($p=0.0140$). Significance when $p<0.05$, designated with*. **B)** Differences in cell proliferation between HT-29 cells treated with LCN2- or scramble siRNA (12,5 nM/well), counted by Countess cell counter after 48 hrs. (ns).

Discussion

Viral Transduction was Demonstrated as the Most Effective Transfection Method

The main objective of this thesis was to explore various methods of gene editing to establish an easy and effective protocol that could be applied to generate stable KO organoid cultures. Electroporation, lipofection and lentiviral transduction have all been examined for their suitability in genetic engineering of sensitive organoids, as well as cancer cell lines. Variants of all these methods have been described in the literature for use in organoid cultures[108-110]. However, establishment of these method is not trivial, and standardization of protocols for gene editing of patient derived organoids is required.

Electroporation was chosen as the initial approach, due to simple set up and a straightforward protocol, bearing promise of being an effective and fast procedure for creation of genetically altered clones. However, our results from the electroporation experiments were far from satisfying.

Firstly, despite optimization of voltage, number of pulses and time of exposure to favor cell survival, the electroporation resulted in low cell viability. Furthermore, the limited number of cells that survived, struggled to recover, even days after exposure. Normally, HT-29 cells have a doubling time of 1-2 days[111]. This was not observed in the electroporated cells, which struggled to obtain confluency even after a week of culture. Bearing in mind that the goal was to optimize a protocol that could be adapted to the far more fragile organoid culture excluded electroporation as a suitable candidate, when even robust HT-29 cells demonstrated low tolerance for the procedure.

Another concern related to electroporation, was the requisite need of taking cells out of the sterile hood to insert cells into the electroporation-station, increasing the risk of infections. Further, the few cells surviving such harsh procedures are often the most robust and transformed ones, which may not represent the characteristics and cell responses of normal epithelial cells. The efficiency of transfection by electroporation was based on GFP fluorescence observed in microscope after transfection with pCMV-LifeAct control. Some GFP-positive cells were observed, but not to the extent that was claimed possible from the manufacturer.

This led us to explore lipofection as an alternative method of gene delivery. Lipofection is equally as labor-effective as electroporation, where nucleic acid-liposome complexes simply are added to cells and culture medium. Cell toxicity of liposomal transfection reagents have been reported[112]. However, we did not observe any differences in cell viability between the

alternative concentrations used, for any of the transfection reagents. Increased concentration of transfection reagent correlated with higher transfection efficiency. Results from HT-29 transfection with pCMV-LifeAct showed a clear improvement with lipofection compared to electroporation. The improved results led us to explore the effectiveness of lipofection in organoids, using pCMV-LifeAct as a positive control.

As demonstrated by the results, transfection of organoids turned out to be quite difficult compared to the treatment of HT-29 cells. Lipofection of organoids while still embedded in Matrigel was not successful. However, some improvements were observed when organoids were incubated with complexes in suspension before re-embedding in Matrigel. Transfection efficiency was also influenced by FCS concentration. Organoid cells transfected as whole organoids showed higher efficiency compared to organoid cells transfected in a single cell suspension. This difference may have been caused by the relatively long incubation period in suspension, where single cells could have experienced more stress than cells positioned together within the organoid structures. Nevertheless, despite that some fluorescent cells were detected, the efficiency of the procedure was extremely low. In positively transfected organoids, only a few cells showed GFP expression.

Lipofection with siRNAs as a transient silencing alternative to stable KO was further tested on both HT-29 cells and organoids. siRNA transfection of HT-29 cells resulted in strong knockdown using the RNAiMAX transfection reagent. Upon testing of RNAiMAX and ON-TARGETplus LCN2 siRNA, we discovered an additional unknown band of ~50 kDa in our western blot. Concerned with the probability that this band resulted from protein expression of LCN2-dimer rather than unspecific binding or contamination, an additional western blot was conducted. We tested cell supernatants harvested at different timepoints (48- 72 hrs.), as well as pure FCS and McCoy's 5a base medium without FCS supplementation. The band of 50 kDa was seen for pure FCS and cell supernatants, but not in base medium. This result support our hypothesis of FCS contamination, thus suggesting that the band originated from FCS in the cell supernatant. Since siRNA successfully silenced the expression of monomeric LCN2, it is improbable that the dimeric protein could originate from the cell culture.

siRNA knockdown in organoids was conducted with both a red fluorescent non-targeting control and a GAPDH siRNA positive control. Despite apparent uptake of fluorescently labeled siRNA, the western blot analysis showed no protein knockdown of GAPDH. The fluorescent siRNAs showed strong accumulation in the organoid lumen. However, the strong protein expression of GAPDH suggests that siRNA may have entered between the cells, rather than through actual cellular uptake. As a preliminary conclusion, lipofection stands out as a convenient and functional method for transient transfections in cell lines which are easy

to manipulate. However, organoids require either further optimization of the procedure or another delivery strategy.

Viral transduction is efficient in delivering gene products, due to viruses' natural mechanisms of action. In the generation of stable cell lines, viral transduction has become the method of choice. It is effective and gentle, thus suitable for primary-, sensitive- and hard-to-transfect cells. However, the method is labor intensive, and it should thus be considered whether stable or transient expression is needed. Other limitations that should be mentioned are the safety measures and mechanisms of viral integration. Despite improvements in the development of safer viral systems, lentiviruses are based on HIV-1 and should be handled with care[113]. Furthermore, genetic material provided by lentivirus is randomly integrated into the hosts DNA. Thus, insertion occurs at different locations in the DNA of various cells, which might interrupt essential cell functions or give changes other than intended. In addition, lentiviruses have limited capacity regarding size of insert and large inserts have been shown to give reduced viral titers compared to small inserts[114].

As with previous methods, the transduction was initially tested in HT-29 cells. There were several reasons for testing the procedure in HT-29 before commencing organoid transduction. We verified the of identity and functionality of the plasmids, the production of functional infectious viral particles, as well as confirming successful integration of genetic material into target cells. HT-29 cells were transduced with Cas9- and eGFP lentiviral particles, respectively. eGFP expression and transduction efficiency were demonstrated as superior compared to both electroporation and lipofection. Further, Cas9 transduced HT-29 cells showed evident protein expression of Cas9 when analyzed by western blot. Imaging and harvesting of cells were performed after one week grown in selective media. During this period, cells were also passaged. The continued expression suggests stable integration. Selection of clones is recommended to be conducted for approximately two weeks. Hence, increasing the period of selection of Cas9 expressing cells might result in stronger expression than was observed in our western blot. In contrast to electroporation, the cells tolerated both the transduction procedure and puromycin-selective media well. Positively altered cells did not show reduced proliferation or loss of morphological characteristics. These findings led to the conclusion that lentiviral transduction is the most effective and gentle gene delivery strategy. Furthermore, the procedure is a promising alternative for efficient KO in intestinal organoids in future experiments.

While testing the different methods, we mainly chose to use fluorescent imaging as a qualitative measure. Fluorescent images readily provide qualitative measures, and the need for quantitative analyses are not always clear. However, withdrawal of numerical features

from microscope images are important for quantitation and comparison of protein expressions between samples, localization of cellular structures, or determination of transfection efficiency, amongst others. Use of automated quantitation also reduce the possibility of bias that might influence the data analysis. Several methods may be used to quantify fluorescent signals from acquired images. Considerations around the quantification and analyses of the data before the imaging process is recommended.

Quantitation methods may be based on counts of cells or structures, size and area of fluorescent signals, or by measuring intensity of pixels[115,116]. Intensity measures can reflect levels of gene expression, while counts and area determinations rather reflect the distributions of signal. To increase chances of comparing actual biological differences rather than image conditions, constant microscope settings throughout the experiment are important[115]. The process of assigning pixels with specific labels, is called segmentation. Typically, the steps in segmentation are based on a determination of the foreground (the objects) from the background, which is obtained by choosing a threshold value. Determining the appropriate threshold value may be challenging, and specific thresholds might be applied for the various images[116]. Use of edge detection by defining the boundaries of where intensity is considerably changed, is also a feature that separates objects of interest from the background.

Several software packages may be utilized for image analysis. A widely used software is Image J; which is a free program possessing many of the features that enables quantitation of microscope images[117]. In our experiments, transfection efficiency was based on observations of differences in fluorescent signals only, and no quantitation was carried out. Ideally, a larger collection of images from all transfection experiments should have been acquired, making it possible to quantify differences in signal distribution across the different methods. Furthermore, the data could have been handled in Image J. The need for quantitation was not deemed essential while experiments where mainly negative, and too inefficient to be a viable option. However, being able to provide additional quantitative evaluations would have supported our conclusions. While signals in HT-29 can be quantified by the methods suggested above, quantitation of organoids by 2D fluorescent imaging poses a challenge. For example, calculations of size and area might not reflect the organoid volume. Organoids are spheroid 3D structures, as well as being positioned in several layers in the Matrigel. Thus, imaging solutions taking all three dimensions into account is needed for accurate signal detection. An alternative method for determining efficiency of organoid transfection or transduction could be visualization of protein expression referenced against a housekeeping gene, such as by western blotting. This type of evaluation was conducted in

Cas9-expressing HT-29 cells. Furthermore, quantitation of LCN2 expression from western blots were carried out in the experiments of LCN2 siRNA knockdown.

HDR and CRISPR/Cas9 KO plasmids constitute a challenge in generation and validation of positive KO- cells

Preconstructed CRISPR/Cas9 plasmids with sgRNA for LCN2 KO were obtained in order to bypass the demanding experimental procedures of constructing own inserts. The donor plasmid consisted of GFP-puro functional cassette and flanking homology arms, enabling HDR. The insertion of GFP should in theory facilitate both the verification and selection process after transfection. However, despite several trials of transfection using these plasmids both by electroporation and lipofection in HT-29 cells and organoids, no positive clones were observed. The unsuccessful results can have occurred due to several factors. Using the gene delivery system, both the Cas9/guide plasmid and the donor-plasmid must have been co-delivered in order to obtain GFP fluorescent cells. Further, the sgRNA must have succeeded in guiding the Cas9 to target site, with subsequent initiation of a DSB. Lastly, the donor template must have been present at the target site, as well as been inserted through the HDR pathway. Obviously, this is not a straightforward approach, and efficiency rates are low.

The negative experimental results led us to conduct restriction digest assays, based on sequence information provided from the manufacturer. Problems related to the functionality of Cas9/guide- or donor- plasmids would also abrogate further downstream integration events. For all runs of restriction digest, the smaller fragments of all plasmids had the expected sizes. However, none of the larger fragments did travel as far as expected. This may have been caused by experimental errors, such as e.g. too high agarose concentration, preventing migration. However, indications of this was not seen when comparing plasmid fragments to sizes of the ladders. New sequence information was provided from OriGene, with some changes in number of base pairs. When evaluated in Genome Compiler, this led to different anticipations of the number of restriction sites for the various enzymes. Nevertheless, new combinations of restriction enzymes were tested. In the last round of experiment the results improved, but were still unsatisfactory. Uncertainty concerning the sequence information and validation of plasmids speaks in favor of constructing own plasmids, or at least conduct verification of plasmid identity by sequencing.

Despite that no GFP-fluorescent cells were observed after transfection, Cas9 could have led to DSB in LCN2 region and repair through NHEJ. Protein expression was analyzed by western blot of CRISPR-transfected HT-29 cells but results did not show loss of LCN2, thus indicating either KO in too few cells to exert any effect, or no KO at all.

HDR has extremely low efficiency and occurs in much lower frequency than NHEJ, which constitute the major endogenous repair pathway. Homologous recombination (HR) happens mainly during late S- and G2- phase of the cell cycle, demanding actively dividing cells and timing. Several methods for optimizing HDR efficiency have been developed. One of the strategies is based on synchronization of the cell cycle and capture of target cells in S and G2-phase, increasing the probability of nucleic acid delivery and donor integration[118,119]. Since NHEJ often outcompetes HDR mechanisms, several studies describe strategies of inhibiting the NHEJ pathway[120]. Approaches used have been inhibition of key enzymes, e.g. using enzyme antagonists and RNA interference, such as siRNAs[121]. Enhancement of the HDR pathway by small molecules have also shown to improve donor integration, while *Charpentier, M. et al* showed HDR improvements by making a recombinant Cas9 fused to Ct-BP interacting protein (CtIP), which is a key protein in the initiating steps of HDR[122,123]. Other factors influencing the efficiency are the ratios between sgRNA/Cas9 plasmids and the HDR template. One study showed that a ratio of 5:1 compared to 1:1 ratio of sgRNA/Cas9 and HDR template, respectively, increased HDR.

Design of homology arms is also of great importance. Firstly, the homology regions should be as close as possible to the DSB[124]. Advise has also been to sequence the region where editing will occur in the specific target cells, since cell specific mutations or SNPs might affect the targeting efficiency drastically[125]. It has been reported that only 1 mismatch in 100 bp reduce HR six-fold[126]. By amplifying cell specific homology arms and creating own donor constructs based on sequencing information from own cells, the possible divergence from the reference genome could be abolished[125]. Our use of pre-constructed plasmids aborts the possibility of cell specific homology arms, where the inserts are based on reference sequences. However, the trade-off between high specificity and labor-intensiveness should be considered. Sequencing and fragment amplification, as well as construct design are resource and labor demanding. On the other hand, a lot of time was invested in testing and validation of pre-made plasmids, which could have been channeled into more rewarding lab activities. A strategy that could have been reasonable to try, is synchronization of cell cycles and optimization of plasmid ratios. We only assessed a 1:1 and a 2:1 ratio between sgRNA/Cas9 plasmids and donor plasmid. As the initial experiments gave no positive results and due to the uncertainties concerning the plasmids, we chose to abandon this method in order to focus our effort on other options. If the use of pre-designed guide/donor plasmids should have been continued, attempts should have focused on a more rigorous set of optimization experiments including varying plasmids ratios and concentrations.

The role of FCS in Transfection of Cell Lines and Intestinal Organoids

The presence or absence of FCS in lipid-based transfection seems to influence transfection efficiency noticeably. In lipofection of 2D cell line cultures, the presence of FCS during complex formation results in a reduced effect on plasmid uptake, as well as siRNA-mediated gene silencing[127]. FCS is thought to interfere with complex formation by blocking aggregation of DNA-liposomes and the positive charge of complexes, which facilitates cell uptake[128]. All our lipofection procedures with HT-29 cells were carried out as recommended from manufacturers, with complex formation conducted in serum reduced Opti-MEM, but otherwise normal amounts with FCS (10%) in the cell culture medium. Both in experiments with pCMV-LifeAct and knockdown experiments with siRNA, these conditions were found to function adequate.

Few have managed to obtain a simple and effective way of transfecting organoids in the same manner, and nucleic acid delivery such as siRNAs has proven difficult. The surrounding Matrigel constitute a physical barrier, preventing complexes from entering the cells. Several strategies have been developed in order to bypass this hurdle, such as mechanical disruption of Matrigel and organoids into single cell suspension before transfection, or mixing by siRNAs into the Matrigel[129,130]. A methodological study by Morgan, R. G. *et al* stated that presence of serum in the media during siRNA preparations both promotes entry and internalization in organoids within short time[127]. They tested both fluorescent labeled non-targeting siRNA, as well as siRNA targeting catenin beta 1 (*CTNNB1*) mRNA, assessing whether uptake resulted in gene knockdown or not. Complexes prepared in serum reduced Opti-MEM were shown to be retained at the Matrigel boundaries[127].

In our organoids, we tested both conditions; the presence and absence of FCS during complex formation between the transfection reagent Lipofection 2000 and pCMV-LifeAct. No fluorescent organoids were obtained, either with or without FCS. However, this experimental set up was performed only once, with one plasmid concentration. We should preferentially have conducted this experiment several times to conclude whether FCS enhances complex uptake in the organoids or not. Further, the study was optimized for siRNA delivery and not plasmids, which may have been a factor influencing the negative results. As we deemed Matrigel as the most plausible limiting factor, the continued lipofection procedures were conducted in Matrigel-free organoids. Here, we did an intermediate between organoids embedded in Matrigel and single cell suspension; Matrigel was disrupted, but organoids were kept intact. The free organoids were then transfected in suspension for 5-6 hrs. As described earlier, a number of combinations of FCS presence and absence were tested. As for 2D cell lines, our results showed the best transfection efficiency upon FCS absence during complex

formation and presence in the culture medium. The rationale for keeping whole organoids are related to the nature of the siRNAs. siRNAs are functional in a short period of time (~96 hrs.) and constitute a challenge in context of the slow growing organoids. Organoids require approximately two weeks of growth before they can be utilized in experiments. Creating single cell suspensions before siRNA transfection is therefore pointless, and strategies are needed for highly efficient siRNA transfection in grown organoids.

Differences in Promotor Requirement might Impact Transfection Efficiency

Nonspecific promotors have been widely used for gene editing purposes, due to their stable and high expression activity in most cell types and cell lines. The cytomegalovirus- (CMV) and the Elongation Factor 1 α- (Elf1α) promotor are two examples of promotors used in various construct designs[131]. The vector constructs of both the CRISPR/Cas9 LCN2 KO and LifeAct plasmid contained the CMV-promotor system.

Throughout the experiments conducted on cell lines and organoids, we struggled with adequate transfection efficiencies and expressions of GFP-positive cells. Relatively successful results were obtained in HT-29 cells, but expression in organoids were in all cases limited. Some of the causes limiting transfection efficiency and uptake have already been discussed. However, limited efficiency may be related to low expression activity of the promotor. In comparative studies conducted on mice embryonic stem cells (ESC), the promotors CMV, Elf1α, phosphoglycerate kinase-1 (PGK) and the hybrid CMV enhancer/chicken β-actin (CBA) were tested for expression activity of the enhanced green fluorescent protein (EGFP)[132,133]. The results showed most stable expression by Elf1α and CBA, followed by PGK. The CMV showed weakest expression or inactivity. Differentiation of ESC showed that CMV here as well yielded weaker signals than the other promotors[132]. Despite the earlier described high activity of CMV, these studies suggest that stem cells might have different promotor requirements. Although differences between mouse ESC and human ASC exists, CMV activity in the stem cells might be a possible explanation of why higher GFP expression levels in the organoids were not obtained. In future gene delivery experiments, it would be strategically sound to test plasmids with different promotor systems. The lentivirus plasmids do not have CMV as promotor system. Here, the Cas9 construct is placed under control of Elf1α, while the sgRNAs are under the U6 promotor. Problems related to U6 and expression levels in stem cells are by our knowledge not reported, and several studies have used the U6-promotor system in shRNA gene silencing studies, both in embryonic stem cells and organoids[134]. For now, these plasmids have only been tested in HT-29 cells with success. It remains to be elucidated whether efficiency can be increased upon transduction of organoids with new promotor systems.

Stable vs. Transient Gene Knockdown and the Benefits of Creating Specific KO- or KI- Models

The choice between a stable or transient transfection strategy in gene function experiments should be based on several considerations. Transient transfection is advantageous in experimental designs where gene knockdown and function can be evaluated within a short period of time. In these cases, siRNA transfection has been widely used, due to its simplicity, efficiency, as well as the low costs relative to other procedures. Transient transfection leads to uptake of nucleic acids into cytosol, but not integration into the genome. Thus, the exogenous genetic material is not passed on to progenitor cells. A positive feature of transient transfection is bypassing several weeks of clonal selection. On the other hand, stable transfection may offer a valuable tool in many research settings. Here, the genetic material is integrated into the host genome and expressed either constitutively or upon induction, dependent on the promotor system. Genetic changes are permanent and will follow progenitors during cell division. Clones of interest can therefore be passaged and stored long term.

The disadvantage of stable transfection is labor intensiveness; positive clones might be more difficult to obtain than transient effects, and selection processes are demanding, particularly for organoids. However, Cas9 expressing HT-29 and possible future Cas9 expressing organoids are concrete examples on why stable transfection might be worth the work. They constitute a versatile tool, enabling a shortcut to generate virtually any gene KO model. Cas9 expressing cells could be transduced with sgRNA lentivirus or transfected by transient sgRNAs for establishment of specific KO-models. In many diseases, candidate genes might have prominent roles in the pathophysiology. KO models of such candidate genes are not only important for single experiments, but can most likely be implemented in several projects. LCN2 and its role in IBD is one such example.

Gene Knockdown of LCN2 Suggests a Role in Proliferation, Migration or Cell Attachment

Based on previous research and literature, we hypothesized that the xCELLigence assay with LCN2 siRNA knockdown would lead to lower cellular impedance than for wildtype (WT) cells treated with scramble siRNA[55,56,59]. Surprisingly, our results showed the opposite. LCN2 knockdown led to increased cellular impedance compared to WT, thus indicating that loss of normal LCN2 protein expression leads to either increased proliferation, migration or cellular extension. HT-29 cells supplemented with scramble or LCN2 siRNA were seeded in parallel to the xCELLigence experiment, in order to examine differences in proliferation. Cells were seeded and counted 48 hrs. later using Countess cell counter. This experiment did not show any significant difference between WT and LCN2 siRNA cells. However, the SDs were too large to draw any conclusions. Methods specifically monitoring proliferation and cell viability would give better insight into mechanisms underlying differences observed in xCELLigence. Ideally, these features should be examined by methods such as MTT- or Luminescence ATP assays[135,136].

Despite results diverging from our expectations, several others have reported similar tendencies[62,65,137,138]. A study conducted on HT-29 and several other colorectal cell lines, demonstrated that LCN2 knockdown downregulated cell proliferation, as well as inhibiting EMT and migration[62]. An important aspect when interpreting these results are the specific characteristics of cancer cell lines. Therefore, results might not be equally as relevant for patient-derived organoids as for cancer cell lines.

One way of understanding the results might be in association with levels of cell junctional proteins and anchorage dependency, some of the features defining an epithelial phenotype. Restoration of homeostatic levels of CDH1 and ZO proteins were observed after supplementation of LCN2 after TNFα treatment in brain endothelial cells[65]. The same was seen in the Ras-transformed breast cancer cell line, 4T1, where LCN2 converted tumor cells to a more epithelial phenotype by increased expression of CDH1[138,139]. In a study involving renal injury, suppression of LCN2 resulted in increased cyst formation. Hepatocyte growth factor (HGF) was reported to stimulate LCN2 secretion, and these two in direct association were further seen to inhibit HGF-stimulated cell migration and branching[140]. HGF is an activator of c-Met, leading to further activation of MAPK and PI3- signaling pathways, both implicated in cell proliferation and migration processes. Thus, inhibition of HGF by LCN2 also reduced activity of these proliferative pathways. Further, LCN2 was seen to stimulate organization of epithelial cells into tubular structures[140].

Another network-based study examined the effect of LCN2 overexpression in esophageal squamous cell carcinoma by identifying differentially expressed genes (DEGs)[141]. Findings showed a clear upregulation of LCN2-related genes, such as low density lipoprotein-related protein 2 (*LRP2*), *MM2*, *MMP9* and *HGF*. Also alpha-2-macroglobulin (*A2M*) was found upregulated, which is a gene involved in inhibition of proteases and proinflammatory cytokines. Another DEG reported downregulated, was the *TGFB1* gene. *TGFB1* is involved in cell proliferation, differentiation and migration. This gene is often highly upregulated in various cancers and is associated with EMT, increased tissue invasion and angiogenesis[142]. Therefore, in a cancer setting (and perhaps in HT-29 cells), LCN2 seems to be important for inhibition of EMT, keeping an epithelial phenotype, partially by upregulation of cell-cell interaction proteins.

Overall, conflicting results whether LCN2 increases or decreases proliferation and migration makes its role difficult to understand. However, from our results and the studies highlighted here, it may be suggested that LCN2 is important for regulation and proper organization of new tissue during regeneration processes, rather than being a prominent component in proliferation and migration itself. These diverse processes are highly associated and might explain why LCN2 expression is repeatedly correlated with both proliferation and migration. For example, in wound edges, components with different roles need to be present. Proliferation is important for production of new cells, migration for correct positioning, and differentiation important for organization and development into specific cellular structures.

The cancer cell lines are poorly suited for studies of LCN2's effect on cellular differentiation. Utilizing growing and differentiating epithelial organoids in connection with LCN2 KO would enable us to conclude whether proliferation, differentiation, cell junction formation or a combination of these factors, is affected by loss of LCN2.

Future Perspectives

Due to time constraints, we have not yet tried to transduce the organoids with cas9- and LCN2 sgRNA lentiviral particles. However, we believe that the procedure established for cell line transduction can be translated to organoids as well. Nevertheless, there are some additional factors which needs to be considered. The organoids survive for only a short period when released from Matrigel. Therefore, the time window for virus incubation is more limited than for cancer cells. In transduction of HT-29, viral supernatants were harvested three times at different timepoints, and cells were allowed to incubate with the viral supernatant in ~48 hrs. This is not possible for organoids, and the exposure time, as well as viral titer might be a limiting factor. One option would be to reduce the number of cells to be transduced, in order to optimize the ratio between cells and virus. However, this might be

problematic due to challenges with the subsequent collection of cells and re-embedding in Matrigel. Other published protocols have overcome similar obstacles by concentrating virus by ultra-centrifugation, and by spin inoculation of organoids[143,144]. Spin inoculation involves adding a viral supernatant to the organoid cells, and then spin the whole plate at low rpm during incubation in order to increase contact between cells and virus.

Conclusion

In the current thesis, intestinal colonic organoids and HT-29 cancer cell line have been utilized for exploring gene editing- and delivery strategies. siRNA, plasmids, and lentivirus have been used as vectors and tried transfected through electroporation, lipofection and lentiviral transduction. Evaluation of efficiency across the different methods has been based on the overall distribution of fluorescent signal visualized by EVOS FL Auto 2 fluorescent microscope. Fluorescence was provided by uptake of pCMV-LifeAct transient plasmid or lentiviral particles containing an eGFP sequence. Lentiviral transduction was further evaluated by western blot, by examining Cas9 protein expression in transduced HT-29 cells.

Altogether, results suggest viral transduction as the most efficient method, despite being a laborious procedure. Lentiviral transduction with Cas9- and eGFP viral particles was only performed in HT-29 cells, and we did not have time to test *LCN2* sgRNA viral particles. However, it has prospects of being the most optimal and gentle delivery strategy for organoids, as well as mediating stable integration of nucleic acids.

Electroporation was early abandoned as a delivery strategy, due to low efficiency and reduced cell viability. On the other hand, lipofection gave satisfactory results in HT-29 cells, especially upon siRNA transfection with RNAiMAX transfection reagent. Despite GFP-positive organoids after lipofection, the efficiency was overall low. Transfection of organoids remained challenging, both by plasmid and siRNA delivery. Matrigel constituted a physical barrier and was disrupted for increasing contact between delivery vectors and target cells. Furthermore, the presence and absence of FCS influenced transfection efficiency. The promotor-system was also believed to influence the expression of GFP. The CMV-promotor has been suggested to have lower expression activity in stem cells compared to promotors such as Elf1α and U6. Overall, the best method for establishment of genetically engineered organoids remains to be elucidated, as well as optimizing a protocol for successful siRNA knockdown in grown organoids.

Our second objective was to gain deeper insight into the functional roles of LCN2. As previous studies show, LCN2 is associated with regeneration processes, proliferation, migration, and cell junctions. xCELLigence, assessing cell proliferation and adhesion, was conducted to investigate whether loss of LCN2 showed differences in growth characteristics of HT-29 cells. Cells treated with LCN2 siRNA showed significant increased impedance compared to WT, thus indicating increased cell migration, adhesion, or proliferation. Based on our results and the current literature, LCN2 may be more important for differentiation, organization, and the maintenance of cell junctions, rather than a prominent stimulator of proliferation and migration itself.

Despite these results, the role of LCN2 is far from clarified. Establishment of *LCN2* KO organoids would be extremely relevant for studying the impacts on cell differentiation and growth. Furthermore, patient derived intestinal organoids have the benefits of omitting the transformed cancer characteristics of HT-29 and resembles the actual epithelium of IBD patients.

References

1 Kaser, A., Zeissig, S. & Blumberg, R. S. Inflammatory Bowel Disease. *Annual Review of Immunology* **28**, 573-621, doi:10.1146/annurev-immunol-030409-101225 (2010).

2 Fakhoury, M., Negrulj, R., Mooranian, A. & Al-Salami, H. Inflammatory bowel disease: clinical aspects and treatments. *J Inflamm Res* **7**, 113-120, doi:10.2147/JIR.S65979 (2014).

3 Liu, T. C. & Stappenbeck, T. S. Genetics and Pathogenesis of Inflammatory Bowel Disease. *Annual review of pathology* **11**, 127-148, doi:10.1146/annurev-pathol-012615-044152 (2016).

4 Khor, B., Gardet, A. & Xavier, R. J. Genetics and pathogenesis of inflammatory bowel disease. *Nature* **474**, 307-317, doi:10.1038/nature10209 (2011).

5 Levine, J. S. & Burakoff, R. Extraintestinal manifestations of inflammatory bowel disease. *Gastroenterol Hepatol (N Y)* **7**, 235-241 (2011).

6 Alatab, S. *et al.* The global, regional, and national burden of inflammatory bowel disease in 195 countries and territories, 1990–2017: a systematic analysis for the Global Burden of Disease Study 2017. *The Lancet Gastroenterology & Hepatology* **5**, 17-30, doi:https://doi.org/10.1016/S2468-1253(19)30333-4 (2020).

7 Ng, S. C. *et al.* Worldwide incidence and prevalence of inflammatory bowel disease in the 21st century: a systematic review of population-based studies. *The Lancet* **390**, 2769-2778, doi:https://doi.org/10.1016/S0140-6736(17)32448-0 (2017).

8 Burisch, J., Jess, T., Martinato, M. & Lakatos, P. L. The burden of inflammatory bowel disease in Europe. *Journal of Crohn's and Colitis* **7**, 322-337, doi:https://doi.org/10.1016/j.crohns.2013.01.010 (2013).

9 Loftus, E. V., Jr. Update on the Incidence and Prevalence of Inflammatory Bowel Disease in the United States. *Gastroenterol Hepatol (N Y)* **12**, 704-707 (2016).

10 Williams, C., Panaccione, R., Ghosh, S. & Rioux, K. Optimizing clinical use of mesalazine (5-aminosalicylic acid) in inflammatory bowel disease. *Therap Adv Gastroenterol* **4**, 237-248, doi:10.1177/1756283X11405250 (2011).

11 Waljee, A. K. *et al.* Corticosteroid Use and Complications in a US Inflammatory Bowel Disease Cohort. *PLoS One* **11**, e0158017-e0158017, doi:10.1371/journal.pone.0158017 (2016).

12 Pagnini, C., Pizarro, T. T. & Cominelli, F. Novel Pharmacological Therapy in Inflammatory Bowel Diseases: Beyond Anti-Tumor Necrosis Factor. *Frontiers in Pharmacology* **10**, doi:10.3389/fphar.2019.00671 (2019).

13 Levy, A. N. & Allegretti, J. R. Insights into the role of fecal microbiota transplantation for the treatment of inflammatory bowel disease. *Therap*

Adv Gastroenterol **12**, 1756284819836893-1756284819836893, doi:10.1177/1756284819836893 (2019).
14 Colman, R. J. & Rubin, D. T. Fecal microbiota transplantation as therapy for inflammatory bowel disease: A systematic review and meta-analysis. *Journal of Crohn's and Colitis* **8**, 1569-1581, doi:10.1016/j.crohns.2014.08.006 (2014).
15 Okamoto, R. *et al.* Organoid-based regenerative medicine for inflammatory bowel disease. *Regen Ther* **13**, 1-6, doi:10.1016/j.reth.2019.11.004 (2020).
16 Giannella, R. A., Broitman, S. A. & Zamcheck, N. Gastric acid barrier to ingested microorganisms in man: studies in vivo and in vitro. *Gut* **13**, 251-256, doi:10.1136/gut.13.4.251 (1972).
17 Campbell, N. A. *et al. Biology : a global approach*. 10th ed. edn, (Pearson, 2015).
18 DeSesso, J. M. & Jacobson, C. F. Anatomical and physiological parameters affecting gastrointestinal absorption in humans and rats. *Food and Chemical Toxicology* **39**, 209-228, doi:https://doi.org/10.1016/S0278-6915(00)00136-8 (2001).
19 Varol, C., Zigmond, E. & Jung, S. Securing the immune tightrope: mononuclear phagocytes in the intestinal lamina propria. *Nature Reviews Immunology* **10**, 415-426, doi:10.1038/nri2778 (2010).
20 Hillman, E. T., Lu, H., Yao, T. & Nakatsu, C. H. Microbial Ecology along the Gastrointestinal Tract. *Microbes Environ* **32**, 300-313, doi:10.1264/jsme2.ME17017 (2017).
21 Okumura, R. & Takeda, K. Roles of intestinal epithelial cells in the maintenance of gut homeostasis. *Exp Mol Med* **49**, e338-e338, doi:10.1038/emm.2017.20 (2017).
22 Khan, I. *et al.* Alteration of Gut Microbiota in Inflammatory Bowel Disease (IBD): Cause or Consequence? IBD Treatment Targeting the Gut Microbiome. *Pathogens* **8**, 126, doi:10.3390/pathogens8030126 (2019).
23 Odenwald, M. A. & Turner, J. R. in *Crohn's Disease and Ulcerative Colitis: From Epidemiology and Immunobiology to a Rational Diagnostic and Therapeutic Approach* (ed Daniel C. Baumgart) 57-66 (Springer International Publishing, 2017).
24 Peterson, L. W. & Artis, D. Intestinal epithelial cells: regulators of barrier function and immune homeostasis. *Nature Reviews Immunology* **14**, 141-153, doi:10.1038/nri3608 (2014).
25 Radtke, F. & Clevers, H. Self-renewal and cancer of the gut: two sides of a coin. *Science (New York, N.Y.)* **307**, 1904-1909, doi:10.1126/science.1104815 (2005).
26 Gerbe, F., Legraverend, C. & Jay, P. The intestinal epithelium tuft cells: specification and function. *Cellular and Molecular Life Sciences* **69**, 2907-2917, doi:10.1007/s00018-012-0984-7 (2012).
27 Neutra, M. R. Current concepts in mucosal immunity. V Role of M cells in transepithelial transport of antigens and pathogens to the mucosal

immune system. *The American journal of physiology* **274**, G785-791, doi:10.1152/ajpgi.1998.274.5.G785 (1998).
28 Martini, E., Krug, S. M., Siegmund, B., Neurath, M. F. & Becker, C. Mend Your Fences: The Epithelial Barrier and its Relationship With Mucosal Immunity in Inflammatory Bowel Disease. *Cellular and Molecular Gastroenterology and Hepatology* **4**, 33-46, doi:https://doi.org/10.1016/j.jcmgh.2017.03.007 (2017).
29 Thorsvik, S. *et al.* Expression of neutrophil gelatinase-associated lipocalin (NGAL) in the gut in Crohn's disease. *Cell and Tissue Research* **374**, 339-348, doi:10.1007/s00441-018-2860-8 (2018).
30 Bevins, C. L. in *Crohn's Disease and Ulcerative Colitis: From Epidemiology and Immunobiology to a Rational Diagnostic and Therapeutic Approach* (ed Daniel C. Baumgart) 75-86 (Springer International Publishing, 2017).
31 Altay, G. *et al.* Self-organized intestinal epithelial monolayers in crypt and villus-like domains show effective barrier function. *Scientific Reports* **9**, 10140, doi:10.1038/s41598-019-46497-x (2019).
32 Gassler, N. Paneth cells in intestinal physiology and pathophysiology. *World J Gastrointest Pathophysiol* **8**, 150-160, doi:10.4291/wjgp.v8.i4.150 (2017).
33 Brittan, M. & Wright, N. A. in *Principles of Tissue Engineering (Third Edition)* (eds Robert Lanza, Robert Langer, & Joseph Vacanti) 665-679 (Academic Press, 2007).
34 Turner, J. R. Intestinal mucosal barrier function in health and disease. *Nature Reviews Immunology* **9**, 799-809, doi:10.1038/nri2653 (2009).
35 MacDonald, T. T. & Monteleone, G. Immunity, Inflammation, and Allergy in the Gut. *Science (New York, N.Y.)* **307**, 1920, doi:10.1126/science.1106442 (2005).
36 Zhang, S.-x. *An Atlas of Histology*. 187-188 (Springer, 1999).
37 Geremia, A., Biancheri, P., Allan, P., Corazza, G. R. & Di Sabatino, A. Innate and adaptive immunity in inflammatory bowel disease. *Autoimmunity Reviews* **13**, 3-10, doi:https://doi.org/10.1016/j.autrev.2013.06.004 (2014).
38 Wen, Z. & Fiocchi, C. Inflammatory bowel disease: autoimmune or immune-mediated pathogenesis? *Clinical & developmental immunology* **11**, 195-204, doi:10.1080/17402520400004201 (2004).
39 Matricon, J., Barnich, N. & Ardid, D. Immunopathogenesis of inflammatory bowel disease. *Self Nonself* **1**, 299-309, doi:10.4161/self.1.4.13560 (2010).
40 Maloy, K. J. & Powrie, F. Intestinal homeostasis and its breakdown in inflammatory bowel disease. *Nature* **474**, 298-306, doi:10.1038/nature10208 (2011).
41 de Lange, K. M. *et al.* Genome-wide association study implicates immune activation of multiple integrin genes in inflammatory bowel disease. *Nature Genetics* **49**, 256-261, doi:10.1038/ng.3760 (2017).

42 Uniken Venema, W. T., Voskuil, M. D., Dijkstra, G., Weersma, R. K. & Festen, E. A. The genetic background of inflammatory bowel disease: from correlation to causality. *The Journal of pathology* **241**, 146-158, doi:10.1002/path.4817 (2017).
43 Ananthakrishnan, A. N. Epidemiology and risk factors for IBD. *Nature Reviews Gastroenterology & Hepatology* **12**, 205-217, doi:10.1038/nrgastro.2015.34 (2015).
44 Liu, T.-C. & Stappenbeck, T. S. Genetics and Pathogenesis of Inflammatory Bowel Disease. *Annual review of pathology* **11**, 127-148, doi:10.1146/annurev-pathol-012615-044152 (2016).
45 Zhao, M. & Burisch, J. Impact of Genes and the Environment on the Pathogenesis and Disease Course of Inflammatory Bowel Disease. *Digestive diseases and sciences* **64**, 1759-1769, doi:10.1007/s10620-019-05648-w (2019).
46 Kriss, M., Hazleton, K. Z., Nusbacher, N. M., Martin, C. G. & Lozupone, C. A. Low diversity gut microbiota dysbiosis: drivers, functional implications and recovery. *Current Opinion in Microbiology* **44**, 34-40, doi:https://doi.org/10.1016/j.mib.2018.07.003 (2018).
47 Tamboli, C. P., Neut, C., Desreumaux, P. & Colombel, J. F. Dysbiosis in inflammatory bowel disease. *Gut* **53**, 1-4, doi:10.1136/gut.53.1.1 (2004).
48 Miyoshi, J. & Chang, E. B. The gut microbiota and inflammatory bowel diseases. *Transl Res* **179**, 38-48, doi:10.1016/j.trsl.2016.06.002 (2017).
49 Abegunde, A. T., Muhammad, B. H., Bhatti, O. & Ali, T. Environmental risk factors for inflammatory bowel diseases: Evidence based literature review. *World J Gastroenterol* **22**, 6296-6317, doi:10.3748/wjg.v22.i27.6296 (2016).
50 Koloski, N.-A., Bret, L. & Radford-Smith, G. Hygiene hypothesis in inflammatory bowel disease: a critical review of the literature. *World J Gastroenterol* **14**, 165-173, doi:10.3748/wjg.14.165 (2008).
51 Moschen, A. R., Adolph, T. E., Gerner, R. R., Wieser, V. & Tilg, H. Lipocalin-2: A Master Mediator of Intestinal and Metabolic Inflammation. *Trends in Endocrinology & Metabolism* **28**, 388-397, doi:https://doi.org/10.1016/j.tem.2017.01.003 (2017).
52 Chakraborty, S., Kaur, S., Guha, S. & Batra, S. K. The multifaceted roles of neutrophil gelatinase associated lipocalin (NGAL) in inflammation and cancer. *Biochim Biophys Acta* **1826**, 129-169, doi:10.1016/j.bbcan.2012.03.008 (2012).
53 Flo, T. H. *et al.* Lipocalin 2 mediates an innate immune response to bacterial infection by sequestrating iron. *Nature* **432**, 917-921, doi:10.1038/nature03104 (2004).
54 Toyonaga, T. *et al.* Lipocalin 2 prevents intestinal inflammation by enhancing phagocytic bacterial clearance in macrophages. *Scientific Reports* **6**, 35014, doi:10.1038/srep35014 (2016).
55 Thorsvik, S. *et al.* Ulcer-associated cell lineage expresses genes involved in regeneration and is hallmarked by high neutrophil gelatinase-

associated lipocalin (NGAL) levels. *The Journal of pathology* **248**, 316-325, doi:10.1002/path.5258 (2019).
56 Miao, Q. *et al.* Tcf3 promotes cell migration and wound repair through regulation of lipocalin 2. *Nature communications* **5**, 4088, doi:10.1038/ncomms5088 (2014).
57 Kehrer, J. P. Lipocalin-2: pro- or anti-apoptotic? *Cell Biology and Toxicology* **26**, 83-89, doi:10.1007/s10565-009-9119-9 (2010).
58 Playford, R. J. *et al.* Effects of Mouse and Human Lipocalin Homologues 24p3/lcn2 and Neutrophil Gelatinase–Associated Lipocalin on Gastrointestinal Mucosal Integrity and Repair. *Gastroenterology* **131**, 809-817, doi:https://doi.org/10.1053/j.gastro.2006.05.051 (2006).
59 Yang, J. *et al.* Lipocalin 2 promotes breast cancer progression. *Proceedings of the National Academy of Sciences* **106**, 3913, doi:10.1073/pnas.0810617106 (2009).
60 Lu, Y. *et al.* CXCL1-LCN2 paracrine axis promotes progression of prostate cancer via the Src activation and epithelial-mesenchymal transition. *Cell Communication and Signaling* **17**, 118, doi:10.1186/s12964-019-0434-3 (2019).
61 Chiang, K.-C. *et al.* Lipocalin 2 (LCN2) is a promising target for cholangiocarcinoma treatment and bile LCN2 level is a potential cholangiocarcinoma diagnostic marker. *Scientific Reports* **6**, 36138, doi:10.1038/srep36138 (2016).
62 Kim, S.-L. *et al.* Lipocalin 2 negatively regulates cell proliferation and epithelial to mesenchymal transition through changing metabolic gene expression in colorectal cancer. *Cancer Sci* **108**, 2176-2186, doi:10.1111/cas.13389 (2017).
63 Moschen, Alexander R. *et al.* Lipocalin 2 Protects from Inflammation and Tumorigenesis Associated with Gut Microbiota Alterations. *Cell Host & Microbe* **19**, 455-469, doi:https://doi.org/10.1016/j.chom.2016.03.007 (2016).
64 Feng, M. *et al.* Lipocalin2 suppresses metastasis of colorectal cancer by attenuating NF-κB-dependent activation of snail and epithelial mesenchymal transition. *Molecular Cancer* **15**, 77, doi:10.1186/s12943-016-0564-9 (2016).
65 Du, Y., Li, W., Lin, L., Lo, E. H. & Xing, C. Effects of lipocalin-2 on brain endothelial adhesion and permeability. *PLoS One* **14**, e0218965-e0218965, doi:10.1371/journal.pone.0218965 (2019).
66 Shao, S. *et al.* Increased Lipocalin-2 Contributes to the Pathogenesis of Psoriasis by Modulating Neutrophil Chemotaxis and Cytokine Secretion. *Journal of Investigative Dermatology* **136**, 1418-1428, doi:https://doi.org/10.1016/j.jid.2016.03.002 (2016).
67 Hau, C. S. *et al.* Lipocalin-2 exacerbates psoriasiform skin inflammation by augmenting T-helper 17 response. *The Journal of dermatology* **43**, 785-794, doi:10.1111/1346-8138.13227 (2016).

68 Zhao, P., Elks, C. M. & Stephens, J. M. The induction of lipocalin-2 protein expression in vivo and in vitro. *The Journal of biological chemistry* **289**, 5960-5969, doi:10.1074/jbc.M113.532234 (2014).
69 Thorsvik, S. *et al.* Fecal neutrophil gelatinase-associated lipocalin as a biomarker for inflammatory bowel disease. *Journal of gastroenterology and hepatology* **32**, 128-135, doi:10.1111/jgh.13598 (2017).
70 Østvik, A. E. *et al.* Expression of Toll-like receptor-3 is enhanced in active inflammatory bowel disease and mediates the excessive release of lipocalin 2. *Clinical & Experimental Immunology* **173**, 502-511, doi:10.1111/cei.12136 (2013).
71 Kang, S. S. *et al.* Lipocalin-2 protects the brain during inflammatory conditions. *Molecular Psychiatry* **23**, 344-350, doi:10.1038/mp.2016.243 (2018).
72 Nguyen, T. L., Vieira-Silva, S., Liston, A. & Raes, J. How informative is the mouse for human gut microbiota research? *Disease models & mechanisms* **8**, 1-16, doi:10.1242/dmm.017400 (2015).
73 Sambuy, Y. *et al.* The Caco-2 cell line as a model of the intestinal barrier: influence of cell and culture-related factors on Caco-2 cell functional characteristics. *Cell Biology and Toxicology* **21**, 1-26, doi:10.1007/s10565-005-0085-6 (2005).
74 Lesuffleur, T. *et al.* Differential expression of the human mucin genes MUC1 to MUC5 in relation to growth and differentiation of different mucus-secreting HT-29 cell subpopulations. *Journal of cell science* **106 (Pt 3)**, 771-783 (1993).
75 Dotti, I. & Salas, A. Potential Use of Human Stem Cell-Derived Intestinal Organoids to Study Inflammatory Bowel Diseases. *Inflammatory bowel diseases* **24**, 2501-2509, doi:10.1093/ibd/izy275 (2018).
76 Dutta, D., Heo, I. & Clevers, H. Disease Modeling in Stem Cell-Derived 3D Organoid Systems. *Trends in molecular medicine* **23**, 393-410, doi:10.1016/j.molmed.2017.02.007 (2017).
77 Holmberg, F. E. *et al.* Culturing human intestinal stem cells for regenerative applications in the treatment of inflammatory bowel disease. *EMBO molecular medicine* **9**, 558-570, doi:10.15252/emmm.201607260 (2017).
78 Jung, P. *et al.* Isolation and in vitro expansion of human colonic stem cells. *Nature Medicine* **17**, 1225-1227, doi:10.1038/nm.2470 (2011).
79 Middendorp, S. *et al.* Adult stem cells in the small intestine are intrinsically programmed with their location-specific function. *Stem cells (Dayton, Ohio)* **32**, 1083-1091, doi:10.1002/stem.1655 (2014).
80 Liang, G. & Zhang, Y. Genetic and epigenetic variations in iPSCs: potential causes and implications for application. *Cell stem cell* **13**, 149-159, doi:10.1016/j.stem.2013.07.001 (2013).
81 Sato, T. *et al.* Single Lgr5 stem cells build crypt-villus structures in vitro without a mesenchymal niche. *Nature* **459**, 262-265, doi:10.1038/nature07935 (2009).

82 Sato, T. *et al.* Long-term Expansion of Epithelial Organoids From Human Colon, Adenoma, Adenocarcinoma, and Barrett's Epithelium. *Gastroenterology* **141**, 1762-1772, doi:https://doi.org/10.1053/j.gastro.2011.07.050 (2011).
83 Múnera, J. O. & Wells, J. M. in *Crohn's Disease and Ulcerative Colitis: From Epidemiology and Immunobiology to a Rational Diagnostic and Therapeutic Approach* (ed Daniel C. Baumgart) 167-172 (Springer International Publishing, 2017).
84 Østvik, A. E. *et al.* Intestinal Epithelial Cells Express Immunomodulatory ISG15 During Active Ulcerative Colitis and Crohn's Disease. *Journal of Crohn's and Colitis*, doi:10.1093/ecco-jcc/jjaa022 (2020).
85 Schildkraut, I. in *Encyclopedia of Genetics* (eds Sydney Brenner & Jefferey H. Miller) 834 (Academic Press, 2001).
86 Gaj, T., Sirk, S. J., Shui, S.-L. & Liu, J. Genome-Editing Technologies: Principles and Applications. *Cold Spring Harb Perspect Biol* **8**, a023754, doi:10.1101/cshperspect.a023754 (2016).
87 Rath, D., Amlinger, L., Rath, A. & Lundgren, M. The CRISPR-Cas immune system: Biology, mechanisms and applications. *Biochimie* **117**, 119-128, doi:https://doi.org/10.1016/j.biochi.2015.03.025 (2015).
88 Doudna, J. A. & Charpentier, E. The new frontier of genome engineering with CRISPR-Cas9. *Science (New York, N.Y.)* **346**, 1258096, doi:10.1126/science.1258096 (2014).
89 Tsai, S. Q. & Joung, J. K. Defining and improving the genome-wide specificities of CRISPR–Cas9 nucleases. *Nature Reviews Genetics* **17**, 300-312, doi:10.1038/nrg.2016.28 (2016).
90 Tian, X. *et al.* CRISPR/Cas9 – An evolving biological tool kit for cancer biology and oncology. *npj Precision Oncology* **3**, 8, doi:10.1038/s41698-019-0080-7 (2019).
91 Kleinstiver, B. P. *et al.* Engineered CRISPR-Cas9 nucleases with altered PAM specificities. *Nature* **523**, 481-485, doi:10.1038/nature14592 (2015).
92 Barrangou, R. & Doudna, J. A. Applications of CRISPR technologies in research and beyond. *Nature Biotechnology* **34**, 933-941, doi:10.1038/nbt.3659 (2016).
93 Nie, J. & Hashino, E. Organoid technologies meet genome engineering. *EMBO reports* **18**, 367-376, doi:10.15252/embr.201643732 (2017).
94 Clark, D. P. *Molecular biology*. 2nd ed. / David P. Clark, Nanette J. Pazdernik.. edn, (Amsterdam

London : Academic, 2013).
95 Bennett, P. M. Plasmid encoded antibiotic resistance: acquisition and transfer of antibiotic resistance genes in bacteria. *British Journal of Pharmacology* **153**, S347-S357, doi:10.1038/sj.bjp.0707607 (2008).
96 Walker, J. M., Casali, N. & Preston, A. *E. coli Plasmid Vectors: Methods and Applications*. Vol. 235 (Totowa, NJ: Humana Press, 2003).
97 Hannon, G. J. RNA interference. *Nature* **418**, 244-251, doi:10.1038/418244a (2002).

98 Whitehead, K. A., Langer, R. & Anderson, D. G. Knocking down barriers: advances in siRNA delivery. *Nature Reviews Drug Discovery* **8**, 129-138, doi:10.1038/nrd2742 (2009).
99 Lee, W.-C., Berry, R., Hohenstein, P. & Davies, J. siRNA as a tool for investigating organogenesis: The pitfalls and the promises. *Organogenesis* **4**, 176-181, doi:10.4161/org.4.3.6642 (2008).
100 Kim, T. K. & Eberwine, J. H. Mammalian cell transfection: the present and the future. *Anal Bioanal Chem* **397**, 3173-3178, doi:10.1007/s00216-010-3821-6 (2010).
101 Potter, H. Transfection by electroporation. *Curr Protoc Mol Biol* **Chapter 9**, Unit-9.3, doi:10.1002/0471142727.mb0903s62 (2003).
102 Carter, M. & Shieh, J. in *Guide to Research Techniques in Neuroscience (Second Edition)* (eds Matt Carter & Jennifer Shieh) 239-252 (Academic Press, 2015).
103 Stahl, D. A. *et al. Brock biology of microorganisms*. 14th ed., Global ed. edn, (Pearson, 2015).
104 Naldini, L. *et al.* In Vivo Gene Delivery and Stable Transduction of Nondividing Cells by a Lentiviral Vector. *Science (New York, N.Y.)* **272**, 263, doi:10.1126/science.272.5259.263 (1996).
105 Merten, O.-W., Hebben, M. & Bovolenta, C. Production of lentiviral vectors. *Mol Ther Methods Clin Dev* **3**, 16017-16017, doi:10.1038/mtm.2016.17 (2016).
106 Craigie, R. The molecular biology of HIV integrase. *Future Virol* **7**, 679-686, doi:10.2217/FVL.12.56 (2012).
107 Mahe, M. M., Sundaram, N., Watson, C. L., Shroyer, N. F. & Helmrath, M. A. Establishment of human epithelial enteroids and colonoids from whole tissue and biopsy. *J Vis Exp*, 52483, doi:10.3791/52483 (2015).
108 Schwank, G. *et al.* Functional repair of CFTR by CRISPR/Cas9 in intestinal stem cell organoids of cystic fibrosis patients. *Cell stem cell* **13**, 653-658, doi:10.1016/j.stem.2013.11.002 (2013).
109 Maru, Y., Orihashi, K. & Hippo, Y. Lentivirus-Based Stable Gene Delivery into Intestinal Organoids. *Methods in molecular biology (Clifton, N.J.)* **1422**, 13-21, doi:10.1007/978-1-4939-3603-8_2 (2016).
110 Fujii, M., Matano, M., Nanki, K. & Sato, T. Efficient genetic engineering of human intestinal organoids using electroporation. *Nature protocols* **10**, 1474-1485, doi:10.1038/nprot.2015.088 (2015).
111 Forgue-Lafitte, M. E., Coudray, A. M., Bréant, B. & Mester, J. Proliferation of the human colon carcinoma cell line HT29: autocrine growth and deregulated expression of the c-myc oncogene. *Cancer research* **49**, 6566-6571 (1989).
112 Felgner, P. L. *et al.* Lipofection: a highly efficient, lipid-mediated DNA-transfection procedure. *Proceedings of the National Academy of Sciences* **84**, 7413, doi:10.1073/pnas.84.21.7413 (1987).
113 Schambach, A., Zychlinski, D., Ehrnstroem, B. & Baum, C. Biosafety features of lentiviral vectors. *Hum Gene Ther* **24**, 132-142, doi:10.1089/hum.2012.229 (2013).

114 Kumar, M., Keller, B., Makalou, N. & Sutton, R. E. Systematic Determination of the Packaging Limit of Lentiviral Vectors. *Hum Gene Ther* **12**, 1893-1905, doi:10.1089/104303401753153947 (2001).
115 Hamilton, N. Quantification and its Applications in Fluorescent Microscopy Imaging. *Traffic* **10**, 951-961, doi:10.1111/j.1600-0854.2009.00938.x (2009).
116 Ljosa, V. & Carpenter, A. E. Introduction to the Quantitative Analysis of Two-Dimensional Fluorescence Microscopy Images for Cell-Based Screening. *PLOS Computational Biology* **5**, e1000603, doi:10.1371/journal.pcbi.1000603 (2009).
117 Abramoff, M. D., Magalhães, P. J. & Ram, S. J. Image processing with ImageJ. (2004).
118 Lin, S., Staahl, B. T., Alla, R. K. & Doudna, J. A. Enhanced homology-directed human genome engineering by controlled timing of CRISPR/Cas9 delivery. *eLife* **3**, e04766, doi:10.7554/eLife.04766 (2014).
119 Yang, D. *et al.* Enrichment of G2/M cell cycle phase in human pluripotent stem cells enhances HDR-mediated gene repair with customizable endonucleases. *Sci Rep* **6**, 21264, doi:10.1038/srep21264 (2016).
120 Maruyama, T. *et al.* Increasing the efficiency of precise genome editing with CRISPR-Cas9 by inhibition of nonhomologous end joining. *Nat Biotechnol* **33**, 538-542, doi:10.1038/nbt.3190 (2015).
121 Li, G. *et al.* Suppressing Ku70/Ku80 expression elevates homology-directed repair efficiency in primary fibroblasts. *The international journal of biochemistry & cell biology* **99**, 154-160, doi:10.1016/j.biocel.2018.04.011 (2018).
122 Charpentier, M. *et al.* CtIP fusion to Cas9 enhances transgene integration by homology-dependent repair. *Nature communications* **9**, 1133, doi:10.1038/s41467-018-03475-7 (2018).
123 Pinder, J., Salsman, J. & Dellaire, G. Nuclear domain 'knock-in' screen for the evaluation and identification of small molecule enhancers of CRISPR-based genome editing. *Nucleic Acids Research* **43**, 9379-9392, doi:10.1093/nar/gkv993 (2015).
124 Elliott, B., Richardson, C., Winderbaum, J., Nickoloff, J. A. & Jasin, M. Gene Conversion Tracts from Double-Strand Break Repair in Mammalian Cells. *Molecular and Cellular Biology* **18**, 93, doi:10.1128/MCB.18.1.93 (1998).
125 Salsman, J. & Dellaire, G. Precision genome editing in the CRISPR era. *Biochemistry and Cell Biology* **95**, 187-201, doi:10.1139/bcb-2016-0137 (2016).
126 Liu, M. *et al.* Methodologies for Improving HDR Efficiency. *Front Genet* **9**, 691-691, doi:10.3389/fgene.2018.00691 (2019).
127 Morgan, R. G. *et al.* Optimized delivery of siRNA into 3D tumor spheroid cultures in situ. *Scientific Reports* **8**, 7952, doi:10.1038/s41598-018-26253-3 (2018).

128 Zuhorn, I. S., Visser, W. H., Bakowsky, U., Engberts, J. B. F. N. & Hoekstra, D. Interference of serum with lipoplex–cell interaction: modulation of intracellular processing. *Biochimica et Biophysica Acta (BBA) - Biomembranes* **1560**, 25-36, doi:https://doi.org/10.1016/S0005-2736(01)00448-5 (2002).
129 Zhang, Q. *et al.* Commensal bacteria direct selective cargo sorting to promote symbiosis. *Nature Immunology* **16**, 918-926, doi:10.1038/ni.3233 (2015).
130 Zoldan, J. *et al.* Directing human embryonic stem cell differentiation by non-viral delivery of siRNA in 3D culture. *Biomaterials* **32**, 7793-7800, doi:10.1016/j.biomaterials.2011.06.057 (2011).
131 Zheng, C. & Baum, B. J. Evaluation of promoters for use in tissue-specific gene delivery. *Methods in molecular biology (Clifton, N.J.)* **434**, 205-219, doi:10.1007/978-1-60327-248-3_13 (2008).
132 Chung, S. *et al.* Analysis of different promoter systems for efficient transgene expression in mouse embryonic stem cell lines. *Stem cells (Dayton, Ohio)* **20**, 139-145, doi:10.1634/stemcells.20-2-139 (2002).
133 Wang, R., Liang, J., Jiang, H., Qin, L.-J. & Yang, H.-T. Promoter-Dependent EGFP Expression during Embryonic Stem Cell Propagation and Differentiation. *Stem Cells and Development* **17**, 279-290, doi:10.1089/scd.2007.0084 (2008).
134 Tang, F.-C. *et al.* Stable Suppression of Gene Expression in Murine Embryonic Stem Cells by RNAi Directed from DNA Vector-Based Short Hairpin RNA. *Stem cells (Dayton, Ohio)* **22**, 93-99, doi:10.1634/stemcells.22-1-93 (2004).
135 van Meerloo, J., Kaspers, G. J. & Cloos, J. Cell sensitivity assays: the MTT assay. *Methods in molecular biology (Clifton, N.J.)* **731**, 237-245, doi:10.1007/978-1-61779-080-5_20 (2011).
136 Lemasters, J. J. & Hackenbrock, C. R. in *Methods in Enzymology* Vol. 57 36-50 (Academic Press, 1978).
137 Feng, M. *et al.* Lipocalin2 suppresses metastasis of colorectal cancer by attenuating NF-κB-dependent activation of snail and epithelial mesenchymal transition. *Mol Cancer* **15**, 77, doi:10.1186/s12943-016-0564-9 (2016).
138 Hanai, J. *et al.* Lipocalin 2 diminishes invasiveness and metastasis of Ras-transformed cells. *The Journal of biological chemistry* **280**, 13641-13647, doi:10.1074/jbc.M413047200 (2005).
139 Venkatesha, S., Hanai, J.-i., Seth, P., Karumanchi, S. A. & Sukhatme, V. P. Lipocalin 2 Antagonizes the Proangiogenic Action of Ras in Transformed Cells. *Molecular Cancer Research* **4**, 821, doi:10.1158/1541-7786.MCR-06-0110 (2006).
140 Gwira, J. A. *et al.* Expression of neutrophil gelatinase-associated lipocalin regulates epithelial morphogenesis in vitro. *The Journal of biological chemistry* **280**, 7875-7882, doi:10.1074/jbc.M413192200 (2005).

141 Wu, B. *et al.* Network based analyses of gene expression profile of LCN2 overexpression in esophageal squamous cell carcinoma. *Scientific Reports* **4**, 5403, doi:10.1038/srep05403 (2014).
142 Hargadon, K. M. Dysregulation of TGFβ1 Activity in Cancer and Its Influence on the Quality of Anti-Tumor Immunity. *J Clin Med* **5**, 76, doi:10.3390/jcm5090076 (2016).
143 Au - Van Lidth de Jeude, J. F., Au - Vermeulen, J. L. M., Au - Montenegro-Miranda, P. S., Au - Van den Brink, G. R. & Au - Heijmans, J. A Protocol for Lentiviral Transduction and Downstream Analysis of Intestinal Organoids. *JoVE*, e52531, doi:doi:10.3791/52531 (2015).
144 Andersson-Rolf, A., Fink, J., Mustata, R. C. & Koo, B.-K. A video protocol of retroviral infection in primary intestinal organoid culture. *J Vis Exp*, e51765-e51765, doi:10.3791/51765 (2014).
145 Strain, A. J. The uptake and fate of exogenous cellular DNA in mammalian cells. *Developments in biologicals* **123**, 23-28; discussion 55-73 (2006).
146 Mahmood, T. & Yang, P. C. Western blot: technique, theory, and trouble shooting. *North American journal of medical sciences* **4**, 429-434, doi:10.4103/1947-2714.100998 (2012).
147 Bradford, M. M. A rapid and sensitive method for the quantitation of microgram quantities of protein utilizing the principle of protein-dye binding. *Analytical Biochemistry* **72**, 248-254, doi:https://doi.org/10.1016/0003-2697(76)90527-3 (1976).
148 Penna, A. & Cahalan, M. Western Blotting using the Invitrogen NuPage Novex Bis Tris minigels. *J Vis Exp*, 264, doi:10.3791/264 (2007).
149 MacPhee, D. J. Methodological considerations for improving Western blot analysis. *Journal of Pharmacological and Toxicological Methods* **61**, 171-177, doi:https://doi.org/10.1016/j.vascn.2009.12.001 (2010).
150 ACEA Bioscience. *xCELLigence RTCA SP Real Time Cell Analyzer - Single Plate*, <https://www.aceabio.com/products/rtca-sp/> (2020).
151 OriGene. *LCN2 Human Gene Knockout Kit (CRISPR)*, <https://www.origene.com/catalog/gene-expression/knockout-kits-crispr/kn207685/lcn2-human-gene-knockout-kit-crispr> (2020).
152 ibidi. *pCMV/pCAG-LifeAct Plasmids*, <https://ibidi.com/lifeact-actin-visualization/83-pcmv-lifeact.html> (2020).

Appendices

Appendix 1 – The Principles Behind Experimental Procedures

The Principles Behind Bacterial Cloning and Plasmid Isolation

Transformation is the process of horizontal gene transfer where competent bacteria take up naked foreign DNA, without the need of a living donor[94]. When competent bacteria are exposed to a shock, as for example heat, it creates pores in the cell membrane that makes DNA uptake possible. Bacteria can be made competent in the lab by chemicals or electric pulse[94]. After exogenous DNA uptake, the DNA can either persist as extrachromosomal features, such as plasmids, or be integrated in the chromosome[145].

After heat shock procedure and plasmid amplification in bacteria, the plasmids can be isolated. This procedure consists of several steps, where the first step is bacterial lysis. The solution of bacterial cells is added an alkaline lysis buffer, which breaks down the bacterial cell wall, resulting in release of bacterial content into the solution. Proteins, chromosomal DNA, as well as plasmid DNA are denatured at this step[96]. However, by adding a neutralizing solution, the plasmid DNA will reanneal and can stay solubilized. The bacterial solution is then filtered or centrifuged in order to separate supernatant containing plasmid DNA from cell debris, proteins and chromosomal DNA. The plasmid DNA is recovered by adding binding buffer to the supernatant, before the solution is loaded into a spin column and centrifuged. The spin column contains a silica gel that will bind nucleic acids depending on pH and salt concentration. DNA will preferentially bind to the silica gel at high concentrations of salts, while impurities are removed with the flow through. Salts are removed from the column by using an ethanol wash, before subsequent elution of DNA by buffers of low ionic strength such as water or TE-buffer[96].

The Principles Behind Restriction Digest Assay and Gel Electrophoresis

Restriction digest assay have several downstream applications such as PCR, restriction cloning or plasmid identification. The technique exploits the features of restriction enzymes and their binding sites in nucleic acids, such as plasmids. Restriction enzymes cut double stranded DNA at specific places based on the presence of certain short base sequences[94]. By knowing the sequence and how the plasmid of interest is constructed, identity of a plasmid can be verified by comparing predicted fragment lengths with results from digest assays. The plasmid should preferentially not contain more than one or two binding sites for a specific restriction enzyme. By choosing such a restriction enzyme, or pair of restriction enzymes, the length of each fragment can be predicted. The fragments can then be separated by gel electrophoresis and visualized[94].

The Principles Behind Western Blot

Western blotting, or immunoblotting, is a qualitative and semi-quantitative method for identifying proteins of interest by their molecular weight. The proteins are first separated by size on a polyacrylamide gel electrophoresis and can further be visualized and analyzed by antibody staining[146]. Cells are first lysed in specific lysis buffers in order to extract proteins. Protein concentrations can be assessed by Bradford Assay, a colorimetric photo-spectrometry method based on the complex formation between basic amino acid residues and Coomassie Blue staining. The presence of proteins will lead to a color change from brown to blue, and protein concentrations can be determined by comparison to a previous made standard curve of known protein concentrations[147].

In contrast to nucleic acids, proteins do not have a uniform charge, constituting a challenge in relation to gel electrophoresis. Protein lysates are therefore added LDS which assists protein denaturation as well as creating a net negative charge, and DTT, a detergent disrupting disulfide bridges within the proteins. The polyacrylamide gel consists of a polymer with crosslinks, creating pore-structures. They can exist as both fixed or graded gels, meaning equal or graded sizes of the pores[148]. Proteins with low molecular weight will travel further than large proteins, due to lower resistance. Target proteins can then be identified by comparison to a ladder of known protein sizes. Housekeeping genes are also often used for normalization. After polyacrylamide gel electrophoresis, the proteins are transferred by blotting to a membrane, which can be further stained with protein-specific antibodies. Primary antibodies captures target proteins, while secondary antibodies with a reporter system again captures the primary antibodies[146]. Reporter-systems widely used are the HRP-conjugation or the presence of a fluorescent tag[149]. Quantitative measurements of western blot are based upon intensity of the protein bands.

The Principles Behind xCELLligence

The xCELLigence system (ACEA Biosciences Inc.) exploits the flow of electrons from a negative to positive terminal. The cell culture plates used are covered by gold electrodes. Without cells present, the electrons can pass freely from one terminal to the other, resulting in low resistance, also called impedance. However, if cells are added and allowed to proliferate and spread over the well surface, the electron flow will be limited. Thus, experiments aiming to find candidate genes involved in cell proliferation, migration or attachment, can be assessed by xCELLigence, as well as the impact of different drugs or other substances on cell viability and growth[150].

The xCELLigence system consists of the RTCA Analyzer, RTCA SP station and RTCA control unit with RTCA software installed. The Analyzer measure electronic resistance by sensor electrodes. The analyzer is coupled to the control unit with installed software. The SP station is placed inside an incubator and connects the E-plates to the analyzer. The E-plate 96 is a 96-well plate, covered with gold electrodes in the bottom[150].

Appendix 2 – Gene Delivery Vectors and Target Sequences

CRISPR/Cas9 LCN2 Human Gene Knockout kit: Constructs and Target Sequences

The CRISPR/Cas9 LCN2 human gene KO kit (Origene) consisted of four plasmids; the pCas-Guide CRISPR vector 1 and 2, Scramble CRISPR vector and GFP-puro donor plasmid. The two pCas-Guide CRISPR vectors contained sgRNA sequences targeting two different regions of *LCN2.* The pCas-Scramble CRISPR vector was provided as a negative control, with a random target sequence[151]. Targeting sequences are listed in **Table 1,** and construct design showed in **Figure 1.** The GFP-puro donor plasmid contained a functional cassette consisting of a GFP- and puromycin gene sequence for selection of stably transfected clones. The cassette was flanked by homology arms and loxP-system, facilitating HDR and gene insertion. The mechanism of action for DNA integration by the CRISPR/Cas9 KO kit and the functional components of the donor plasmid are shown in **Figure 2.**

Table 1: The sgRNA target sequences of pCas-Guide CRISPR vector 1 and 2, facilitating guidance upon two different regions of *LCN2.* The pScramble CRISPR vector contains a sgRNA with random sequence, provided as a negative control.

Plasmid	Target sequence
pCas-Guide CRISPR vector 1	GGCATGCAGAGCCCCCAACA
pCas-Guide CRISPR vector 2	TGCAGAGGGACCTTGCTCAG
pScramble CRISPR vector	GCACTACCAGAGCTAACTCA

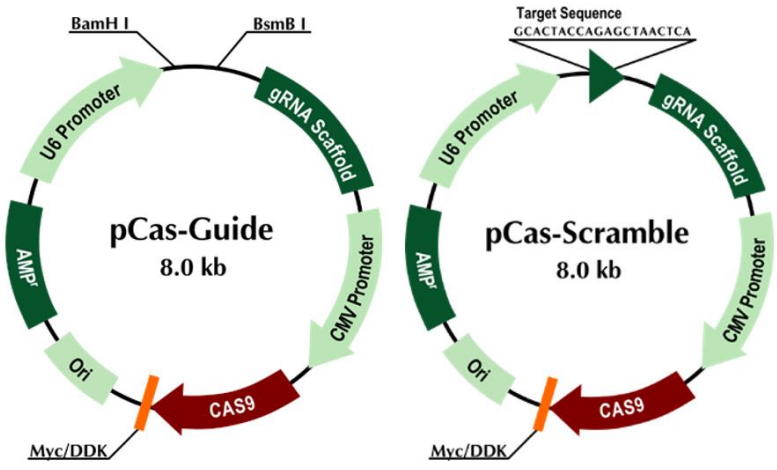

Figure 1: The construct design of pCas-Guide and pCas-Scramble plasmids. The various plasmids had different targeting sequences, but was otherwise identically organized. Figure taken from OriGene[151].

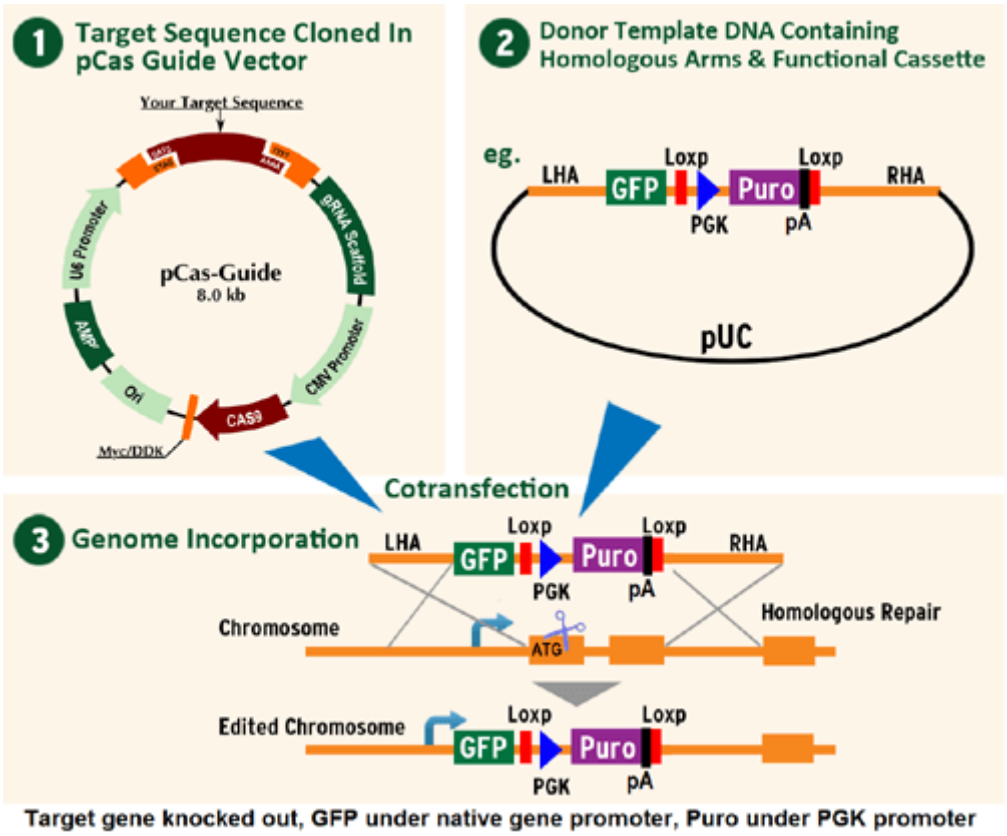

Figure 2: The mechanisms of action for integration of the donor functional cassette (1-3). The functional cassette consists of GFP fluorescence and puromycin resistance. As depicted, the loxP system is present, and the GFP-Puro cassette flanked by left and right homology arms(2). Figure taken from OriGene[151].

pCMV-LifeAct: Construct Design and Function

pCMV-LifeAct (ibidi) is used for visualization of F-actin within the target cells. The LifeAct gene contains a green fluorescent protein (GFP) tag with a binding site for F-actin. This construct has low-interfering potential with the cytoskeletal dynamics. Furthermore, LifeAct-GFP is placed under control of the CMV-promotor. The plasmid contains Neomycin resistance gene, for selection of eukaryotic cells[152]. The plasmid construct is depicted in **Figure 3.**

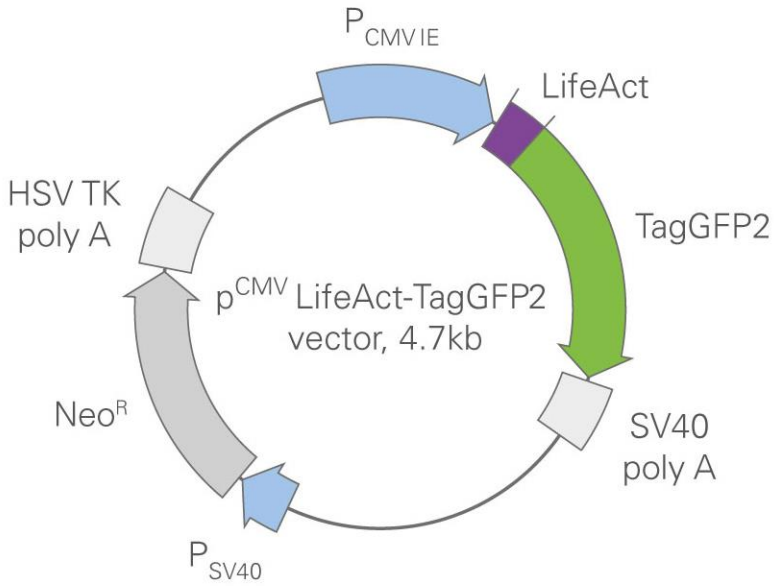

Figure 3: pCMV-LifeAct plasmid with GFP tag, placed under control of the CMV-promotor. The plasmid also contains a gene for Neomycin resistance for selection of eukaryotic cells. Figure taken from ibidi[152].

Lentivirus: Constructs and Target sequences

The lentiviral transduction system provided from GeneCopoeia™ consisted of three sgRNA lentiviral expression clones targeting *LCN2,* Cas9 nuclease lentiviral expression clone and a Lenti-Pac HIV expression packaging kit. The packaging kit contained an eGFP positive control plasmid, as well as the HIV packaging mix consisting of three plasmids with viral structural components. The various plasmids contained amp resistance gene for bacterial amplification and subsequent plasmid isolation. Furthermore, the expression plasmids had puromycin as stable selection marker and deletions in the 3'LTR, important for virus replication incompetence. The three sgRNA expression clones contained individual target sequences of *LCN2,* as listed in **Table 2.** All sgRNA contained a mCherry fluorescent tag and was further placed under control of the U6 promotor (**Figure 4**).

Table 2: The sgRNA target sequences of the three various sgRNA expression clones (a-c), facilitating guidance upon three different regions of *LCN2.*

Lentivirus sgRNA plasmid construct	Target site
sgRNA a	GGCCCCTTACTTGGTTGTCC
sgRNA b	GGGCATGCAGAGCCCCCAAC
sgRNA c	TCATGCCCCTAGGTCTCCTG

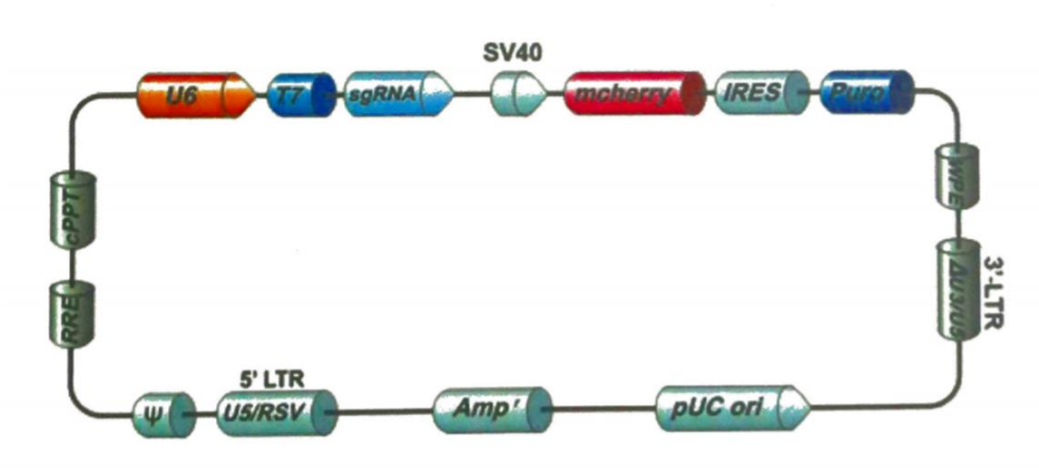

Figure 4: The construct design of sgRNA expression clones. The plasmids had different sgRNA target regions but was otherwise identical in plasmid organization, with U6 promotor, mCherry fluorescent tag, amp and puromycin resistance gene. Figure obtained from GeneCopoeia.

The Cas9 nuclease expression clone was placed under control of the Elf1α promotor and with puromycin selection gene (**Figure 5**).

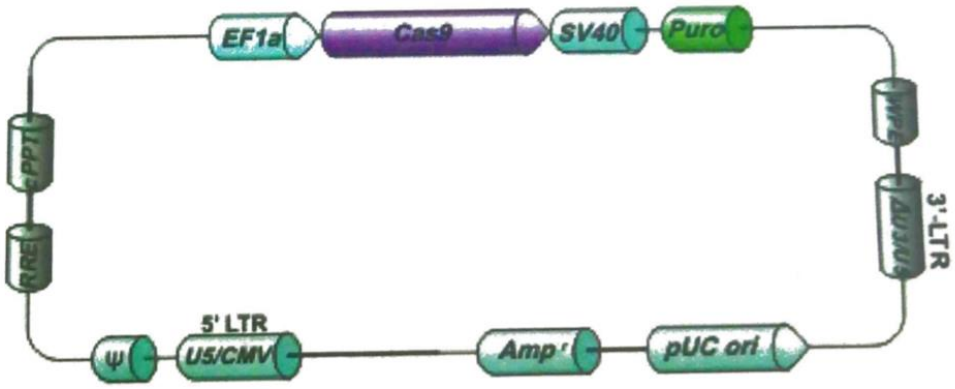

Figure 5: The construct design of the Cas9 expression clone. Cas9 was placed under the control of the Ef1a promotor, with amp and puromycin resistance gene. Figure obtained from GeneCopoeia.

Appendix 3 – Tables and Figures Material and Methods

Antibiotic Titration: Dilutions and Setup

Table 1: Serial dilution of 10 µg/mL puromycin stock prepared for antibiotic titration of HT-29 cells.

Dilution concentration (µg/mL)	Volume stock (10 µg/mL) (mL)	Volume medium (mL)
10	2	0
8	1,6	0,4
4	0,8	1,2
2	0,4	1,6
1	0,2	1,8
0,5	0,1	1,9
0	0	2

Table 2: Set up of puromycin titration experiment for HT-29. Each concentration was tested in triplicate on a 24-well culture plate.

0 µg/mL	0,5 µg/mL	1 µg/mL	2 µg/mL	4 µg/mL	8 µg/mL
0 µg/mL	0,5 µg/mL	1 µg/mL	2 µg/mL	4 µg/mL	8 µg/mL
0 µg/mL	0,5 µg/mL	1 µg/mL	2 µg/mL	4 µg/mL	8 µg/mL
			10 µg/mL	10 µg/mL	10 µg/mL

xCELLigence: Experimental Set Up

xCELLigence was run twice with identical experimental set up. HT-29 cells were seeded (5000 cells/well) in a E-96 plate and treated with either Allstars Negative Control siRNA or ON-TARGETplus LCN2 siRNA ± 10% FCS in the culture medium. Due to partially unknown constituents of FCS which could have had impact the experimental outcome, cells were also treated in absence of FCS. However, cells under these conditions did not grow satisfactory compared to cells incubated in the presence of FCS. 8 technical replicates for each condition was run and E-96 experimental set up is shown in **Figure 1**.

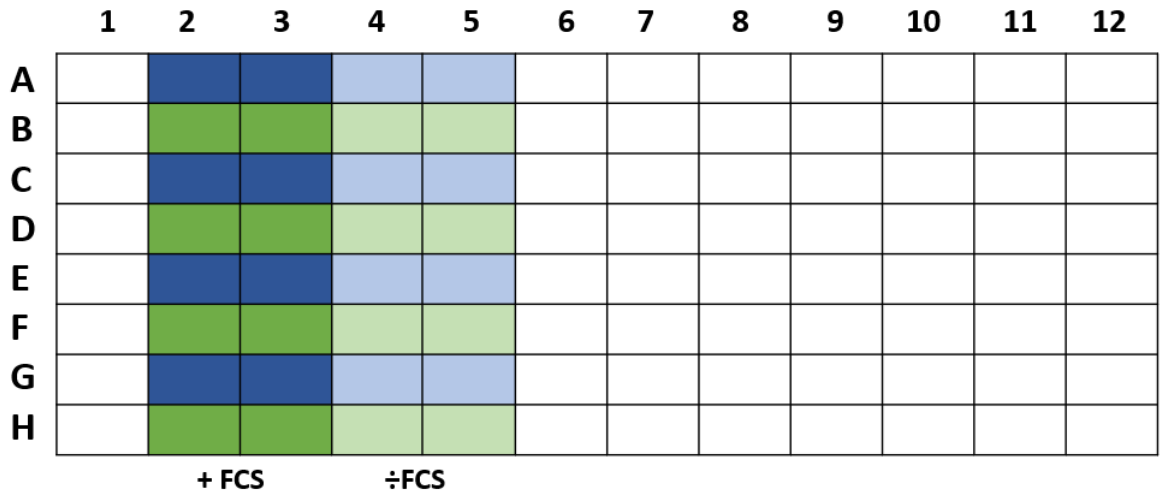

Figure 1: Experimental set up of xCELLigence experiment on the E-96 plate. HT-29 cells were treated with scramble siRNA (blue) or LCN2 siRNA (green) in the presence of 10 % FCS in the culture medium (column 2-3) or in the absence of FCS (column 4-5).

Appendix 4 – Transfection and Variation in Experimental Parameters

Electroporation

Table 1: The experimental set up of individual electroporation procedures, with variations in type of delivery vector, concentrations, electric voltage, pulse and pulse number, incubation in R-buffer. The experimental outcome of each procedure is also listed.

Cell type	Vector/ siRNA	Amounts/ well	Pulse voltage	Pulse width (milliseconds)	Pulse number	Short time in R-buffer?	Transfection successful?
HT-29	pCMV-LifeAct	1 µg/ plasmid, 2 µg in total	1650 V	10 ms	3	-	Few GFP-positive cells, only background?
HT-29	CRISPR/cas9 LCN2 KO (guide and donor plasmid)	1 µg/ plasmid, 2 µg in total	1650 V	10 ms	3	-	Non positive
HT-29	CRISPR/cas9 LCN2 KO	1 µg/ plasmid, 2 µg in total	1300 V 1300 V 1300 V 1450 V 1550 V 1650 V	20 ms 20 ms 15 ms 20 ms 10 ms 10 ms	2 3 2 3 3 3	-	Non positive
Organoids	CRISPR/cas9 LCN2 KO	1 µg/ plasmid, 2 µg in total	1650 V 1400 V	20 ms 10 ms	3 3	-	Non positive
HT-29	CRISPR/cas9 LCN2 KO	1 µg/ plasmid, 2 µg in total	1300 V 1300 V 1300 V 1450 V 1550 V 1650 V	20 ms 20 ms 15 ms 20 ms 10 ms 10 ms	2 3 2 3 3 3	-	Non positive
HT-29	CRISPR/cas9 LCN2 KO	1 µg/ plasmid, 2 µg in total	1300V	20 ms	2	Yes, >2-3 min	Non positive
HT-29	pCMV-LifeAct	2 µg	1300 V	20 ms	2	Yes, >2-3 min	GFP-positive cells, limited efficiency

Lipofection

Table 2: The experimental set up of individual lipofection procedures, with variations in type of delivery vector and transfection reagents, and the following variations in concentration. Furthermore, presence or absence of FCS during complex formation and in the culture medium, and incubation time are listed. The experimental outcome of each procedure is listed to right.

Cell type	Vector/ siRNA	Amounts/ well	Type of transfection reagent	Amounts/ well	FCS present during complex formation	FCS present in culture medium	Incubation time with transfection complexes	Transfection successful?
HT-29	pCMV-LifeAct	0.5 µg	Lipofectamine 2000	2-5 µl	÷	10%	24-48 hrs.	GFP-positive cells, increased efficiency with increased amount lipofectamine 2000
HT-29	CRISPR/cas9 KO	0.5 µg	Lipofectamine 2000	4-5 µl	÷	10%	24-48 hrs.	No positive cells
HT-29	pCMV-LifeAct CRISPR/cas9 KO	0.5 µg	Lipofectamine 2000	4 µl	÷	10%	24-48 hrs.	No positive cells transfected with CRISPR KO, GFP-positive cells transfected with pCMV-LifeAct
Organoids embedded in Matrigel	pCMV-LifeAct	0.5 µg	Lipofectamine 2000	2 or 5 µl	±	± 10%	24 hrs.	No positive organoid cells
Whole organoids ÷ Matrigel	pCMV-LifeAct	0.5-1 µg	Lipofectamine 2000	2 or 5 µl	+	10%	5-6 hrs.	No GFP-positive organoid cells.
Whole organoids ÷ Matrigel	pCMV-LifeAct	2 µg	Lipofectamine 2000	2 or 5 µl	±	10%	5-6 hrs.	GFP-positive organoid cells observed in wells added complexes ÷FCS.
Whole organoids ÷ Matrigel	Accell siRNA red non-targeting control	30 nM & 1 µM	Accell Delivery medium	Total of 500 µl medium	-	-	5-6 hrs.	Successful at high and low concentrations. Accumulation in organoid lumen?
Whole organoids ÷ Matrigel	Accell GAPD positive control	30-, 100-, 250-, 500-1000 µM	Accell Delivery medium	Total of 500 µl medium	-	-	5-6 hrs.	No protein knockdown observed by western blotting.
Whole organoids ÷ Matrigel	pCMV-LifeAct	2 µg	Lipofectamine 2000	5 µl	÷	÷	5-6 hrs.	Some positive GFP-cells, but less than organoids previously transfected with FCS in media.
Whole and single cell organoids ÷ Matrigel	pCMV-LifeAct	2 µg	Lipofectamine stem reagent	1-2 µl	÷	10%	6-7 hrs.	Most effective transfection of organoids. More GFP-positive cells in whole organoids than single cell suspension.
HT-29	ON-TARGETplus siRNA LCN2	12,5 nM	RNAiMAX	9 µl (3 µl per 1 µl siRNA)	÷	10%	24- 96 hrs.	Complete knockdown of LCN2 protein, observed by western blotting.

Appendix 5 – Results: Supplementary figures

Restriction Digest Assay

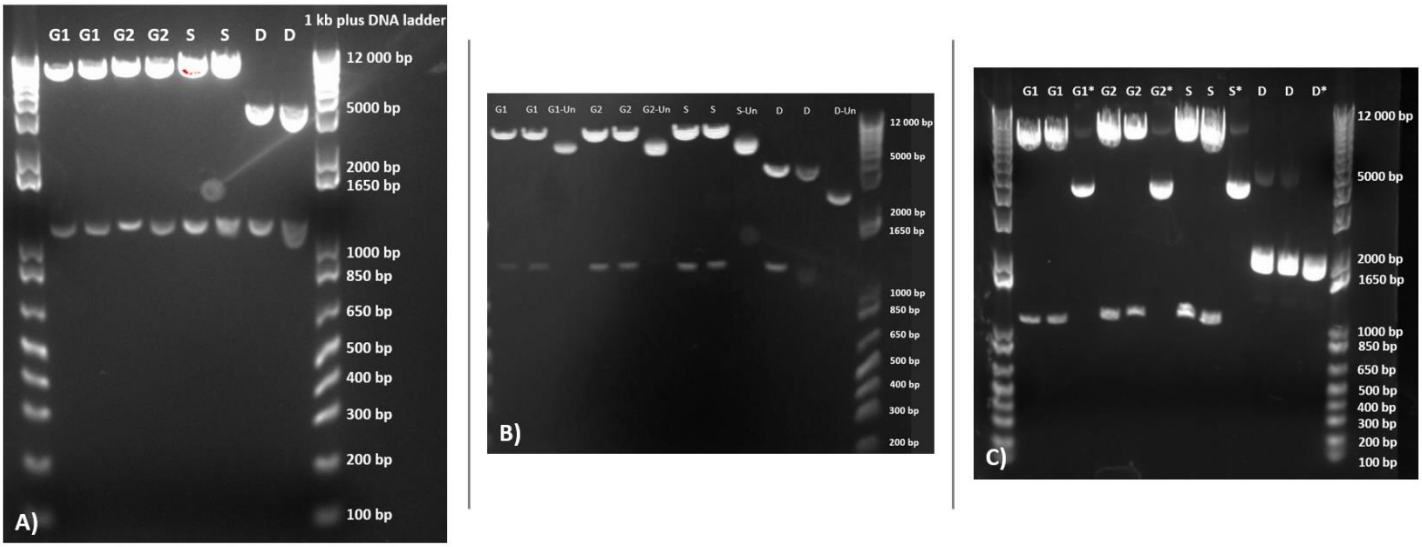

Figure 1: Restriction digest assays conducted on plasmids from the CRISPR/Cas9 LCN2 Human Gene Knockout kit, depicted with READY-LOAD™ 1Kb Plus DNA Ladder. **A)** G1, G2, S and D were digested with EcoRI restriction enzyme **B)** G1, G2 and S were digested with EcoRI, while D was digested with EcoRI and BamHI restriction enzyme. **C)** G1, G2 and S were digested with EcoRI, while D was digested with XbaI and BamHI.

Quantitation of Protein Expression – CRISPR/Cas9 LCN2 KO

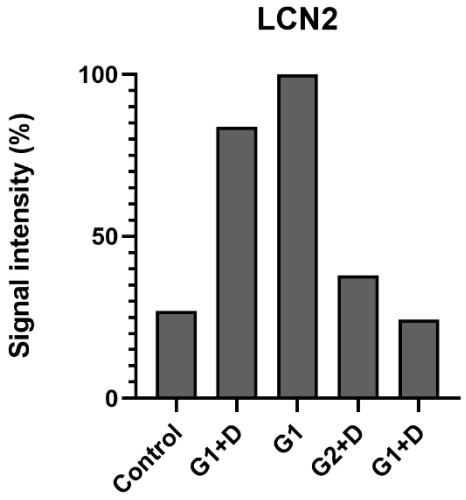

Figure 2: Quantitation of LCN2 protein expression in the samples Control, (G1+D), G1, (G2 +D) and (G1+D). The LCN2 expression was normalized against GAPDH housekeeping gene.

Western Blots

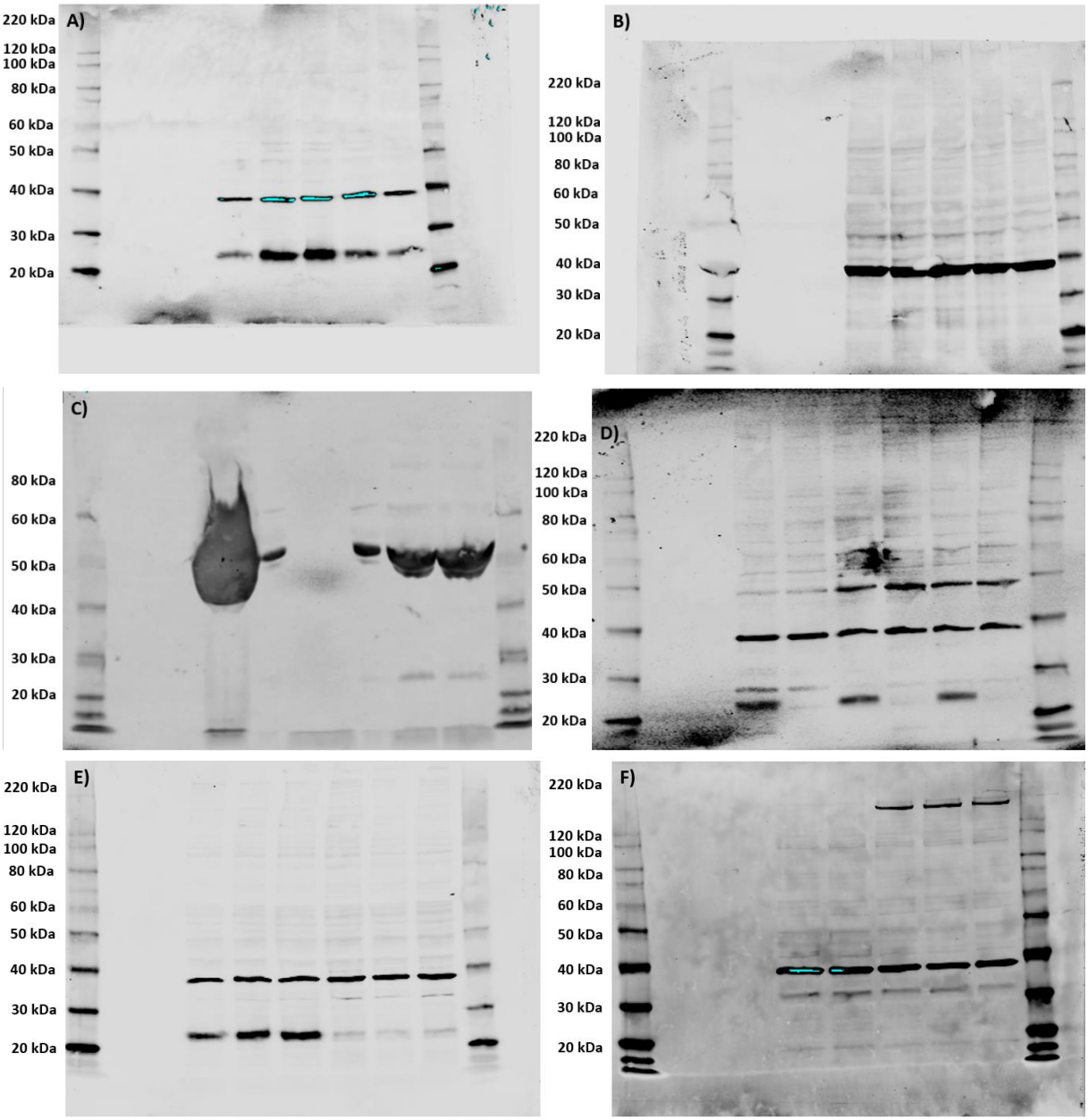

Figure 3: Western blots depicted with MagicMark™ XP Western Protein Standard. **A)** HT-29 cells transfected by Lipofectamine 2000 and CRISPR/Cas9 LCN2 KO plasmids **B)** Organoids transfected by Accell Delivery Media and Accell GAPDH positive control siRNA **C)** FCS, HT-29 cell supernatants (48.- and 72. Hrs.) (10% FCS) and McCoy's 5a base medium tested for unknown band at 50 kDa **D)** HT-29 cells transfected by RNAiMAX and ON-TARGETplus LCN2 siRNA **E)** Verification of xCELLigence protein knockdown; HT-29 transfected by RNAiMAX and ON-TARGETplus LCN2 siRNA, compared to Allstars Negative Control siRNA. **F)** HT-29 cells transduced with Cas9-lentiviral particles.

xCELLigence (÷FCS)

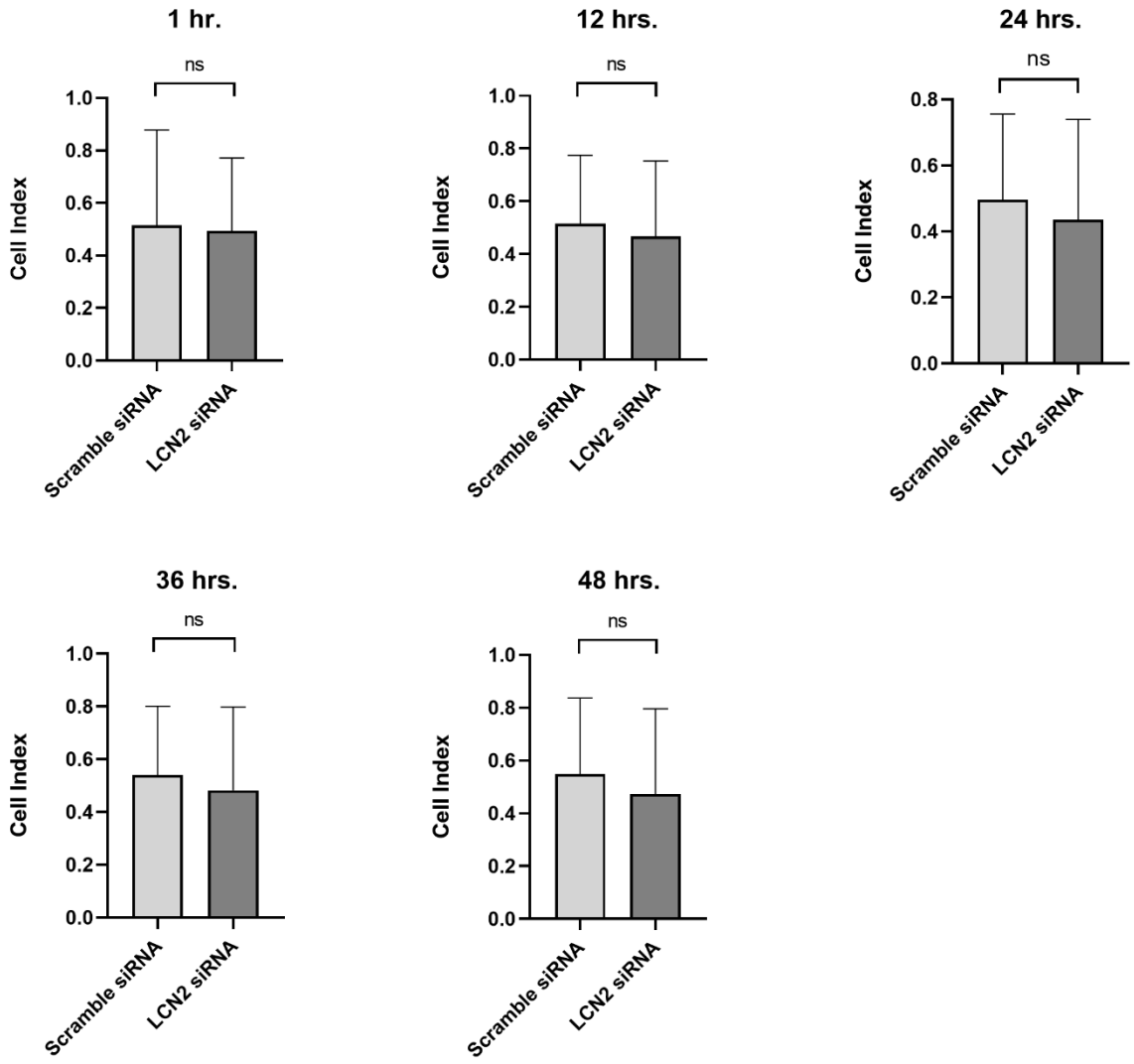

Figure 4: Cellular impedance measured at chosen timepoints (1-, 12-, 24-, 36-, 48 hrs.) for HT-29 cells treated with LCN2 and Scramble siRNA (12,5 nM) in the absence of FCS. The results were non-significant.

Appendix 6 – Media and Buffers

Cell Line Culture Media

Table 1: HT-29 culture medium

Constituent		Volume (total 50 mL tube)
McCoy's 5a base medium		45 mL
FCS		5 mL
Gentamicin		50 µl

Table 2: HEK293T culture medium

Constituent	Volume (total 50 mL tube)
DMEM base medium	45 mL
FCS	5 mL
Penicillin-Streptomycin	500 µl

Intestinal Organoid Culture Media and Buffers

Table 3: Minigut-A

Constituent	Concentration	Amount
Wnt-3A conditioned medium		500 mL
BSA	1 %	5 g
GlutaMAX 100X	1x	5 mL
HEPES 1M	10mM	5 mL
Pen- Strep (10,000 U/mL)	100U/mL	5 mL
N2 Supplement 100x	1x	5 mL
B27 Supplement 50x	1x	10 mL

Table 4: Minigut-B

Constituent	Concentration	Amount
Advanced DMEM/ F12		1000
BSA	1 %	10
GlutaMAX 100X	1x	10
HEPES 1M	10mM	10
Pen- Strep (10,000 U/mL)	100U/mL	10
N2 Supplement 100x	1x	10
B27 Supplement 50x	1x	20

Table 5: R-spondin conditioned medium

Constituent	Concentration	Amount
R-spondin conditioned medium		500 mL
BSA	1 %	5 g
GlutaMAX 100X	1x	5 mL
HEPES 1M	10mM	5 mL
Pen- Strep (10,000 U/mL)	100U/mL	5 mL
N2 Supplement 100x	1x	5 mL
B27 Supplement 50x	1x	10 mL

Table 6: Minigut-C

Constituent	Concentration	Amount
Minigut A	50 %	25 mL
Minigut B	30 %	15 mL
Nicotinamide stock	1:100	500 µL
N-Acetyl-L-cysteine stock	1:1000	50 µL
Noggin Protein stock	1:1000	50 µL
R- Spondin conditioned medium	20%	10 mL
A-83-01 stock	1:1000	50 µL
SB202190 stock	1:3000	16,67 µL
Human EGF stock	1:10000	5 µL
[Leu]15- Gastrin 1 stock	1:10000	5 µL

Table 7: Minigut-D for establishment

Constituent	Concentration	Amount
Minigut C	1:1	14 mL
CHIR99021 stock	1:4000	3,5 µL
Thiazovivin stock	1:4000	3,5 µL

Table 8: Minigut-E for passaging

Constituent	Concentration	Amount
Minigut C	1:1	15 mL
Y-27632	1:1000	15µL

Table 9: EDTA

Constituent	Concentration	Amount
Ultrapure ddH2O		100 mL
EDTA disodium dihydrate	0.5	18,61 g
NaOH pellets		1,8 g
NaOH 10M solution		? mL (adjust to pH 8)

Table 10: Chelating buffer

Constituent	Concentration	Amount
DPBS	1	500 mL
Sorbitol	2%	10 g
Sucrose	1%	5 g
BSA	1%	5 g
Genta/Ampho-B 500x	1x	1 mL

Bacterial Culture Media and Agar Plates

Table 11: LB-medium

Constituent	Amount
NaCl	5 g
Tryptone	5 g
Yeast extract	2,5 g
dH_2O	0.5 L

Table 12: LB-agar

Constituent	Amount
NaCl	5 g
Tryptone	5 g
Yeast extract	2,5 g
Agar	7,2 g
dH_2O	0.5 L

Western Blot Buffers

Table 13: Triton-X lysis buffer I

Constituent	Concentration (1X)	Volume (µl) per mL buffer	Per 10 mL
1M Tris-HCl, pH 7,5	50 mM	50 µl	500 µl
1 M NaCl	150 mM	150 µl	1500 µl
dH2O	-	800 µl	8000 µl

Table 14: Triton-X lysis buffer II

Constituent	Concentration (1X)	Volume (µl) per mL buffer	Per 10 mL
1M Tris-HCl, pH 7,5	50 mM	50 µl	500 µl
1 M NaCl	150 mM	150 µl	1500 µl
0,5 M EDTA	10 mM	20 µl	200 µl
Triton-X 100	1%	10 µl	100 µl
dH2O	-	770 µl	7700 µl

Table 15: Triton-X complete lysis buffer

Constituent	Concentration (1X)	Volume (µl) per mL
Buffer I or II (stock)	-	959 µl
1 M DTT	1 mM	1 µl
50xComplete	1x	20 µl
PIC2	1x	10 µl
PIC3	1x	10 µl

Table 16: MOPS running buffer

Reagent	Volume (mL)
dH2O	950
MOPS (20X)	50

Table 17: Transfer-buffer

Reagent	Volumes
dH2O	950 mL (1 gel)/ 850 (2 gels)
Transfer buffer NuPAGE (20X)	50 mL
meOH	100 mL (1 gel)/ 200 mL (2 gels)

Table 18: TBS-buffer

Reagent	Amount (g)	Volume
Tris	6,05	
NaCl	8,76	
dH2O	-	800 mL (final volume of 1000 after adjusting with HCl)
HCl		Adjust to pH 7.5

Table 19: TBS-Tween

Reagent	Volume
TBS	999 mL
Tween	1 mL

Other Buffers

Table 20: TE-buffer

Reagent	Amount
Tris 1 M pH 8	5 mL
EDTA 0.5 M pH 8	1 mL
dH_2O	494 mL

Table 21: TAE-buffer (50X)

Reagent	Amount
Tris base	242 g
EDTA 0.5 M pH 8.0	100 mL
Acetic acid	57.1 mL
dH_2O	To final volume of 1L

Table 22: Paraformaldehyde (PFA) for fixation

Reagent	Amount
PFA 4%	20 mL
Sucrose 2%	0,4 g

Appendix 7 – Reagents, Manufacturers and Cat.no

Table 1: Table showing all the reagents utilized in the present thesis, with information about manufacturer and catalogue number.

Kit/reagent	Manufacturer	Catalogue no
Cell culture		
Phosphate buffer saline	Sigma Aldrich, St. Louis, MO, USA	D8537-500ML
McCoy's 5a	Sigma Aldrich, St. Louis, MO, USA	M9309
Dulbecco's Modified Eagle Medium	Life Technologies, Carlsbad, CA, USA	31966-021
RPMI 1640	Life Technologies, Carlsbad, CA, USA	31870-025
Gentamicin	Sigma Aldrich, St. Louis, MO, USA	G1397-10ML
Penicillin-Streptomycin	Sigma Aldrich, St. Louis, MO, USA	P0781
Trypsin/EDTA	Lonza, Walkersville, MD, USA	BE17-161E
Organoid culture		
Advanced DMEM/F12	Life Technologies, Carlsbad, CA, USA	12634-010
Nicotinamide	Sigma Aldrich, St. Louis, MO, USA	N3376
N-Acetyl-L-Cysteine	Sigma Aldrich, St. Louis, MO, USA	A7250
A-83-01	Sigma Aldrich, St. Louis, MO, USA	A5480
SB202190	Sigma Aldrich, St. Louis, MO, USA	S7067
Y-27632	STEMCELL Technologies, Cambridge, UK	72307
EGF	PeproTech, Rocky Hill, USA	AF-100-15
Noggin	PeproTech, Rocky Hill, USA	120-10C
[Leu] 15 Gastrin-1	Sigma Aldrich, St. Louis, MO, USA	G9145
Bovine Serum Albumin	Sigma Aldrich, St. Louis, MO, USA	A7906-500G
GlutaMAX	Life Technologies, Carlsbad, CA, USA	35050038
HEPES	Life Technologies, Carlsbad, CA, USA	15630056
N2	Thermo Fischer Scientific, Waltham, MA USA	17502001
B27	Thermo Fischer Scientific, Waltham, MA USA	17504001
Sorbitol	Sigma Aldrich, St. Louis, MO, USA	S1876
Genta/Ampho-B 500x	Invitrogen, Carlsbad, CA, USA	R-015-10
CHIR99021	STEMCELL Technologies, Cambridge, UK	72054
Thiazovivin	STEMCELL Technologies, Cambridge, UK	72252
Matrigel	Corning Life Sciences, NY, USA	356234
Cell Recovery Solution	Corning Life Sciences, NY, USA	354253
Bacterial culture		
NaCl	Sigma Aldrich, St. Louis, MO, USA	1.06404.1000

Tryptone	Oxoid Limited, Hampshire, UK	LP0042
Yeast extract	Oxoid Limited, Hampshire, UK	LP0021
Agar Bacteriological	Oxoid Limited, Hampshire, UK	LP0011
SeaKem ® LE Agarose	Lonza, Basel, Switzerland	50004
Plasmid Isolation PureYield Miniprep	Promega, Madison, USA	A1222
Zymopure II Midiprep	Zymo Research, Tustin, USA	D4201
Gel Electrophoresis		
FastDigest Buffer (10X)	Thermo Fischer Scientific, Waltham, MA USA	B64
FastDigest EcoRI	Thermo Fischer Scientific, Waltham, MA USA	FD0274
FastDigest BamHI	Thermo Fischer Scientific, Waltham, MA USA	FD0054
FastDigest XbaI	Thermo Fischer Scientific, Waltham, MA USA	FD0685
Gelred® Nucleic Acid Gel Stain	Biotium, Landing Parkway Freemont, CA, USA	41003
Gel Loading Dye, Purple (6X)	New England Biolabs, County Road, MA, USA	B70245
READY-LOAD™ 1Kb Plus DNA Ladder	Invitrogen, Carlsbad, CA, USA	12308-011
Electroporation		
NEON™ Transfection System	Invitrogen, Carlsbad, CA, USA	MPK10096
Lipofection		
Lipofectamine 2000	Invitrogen, Carlsbad, CA, USA	11668019
Lipofectamine Stem Reagent	Invitrogen, Carlsbad, CA, USA	STEM00015
RNAiMAX	Invitrogen, Carlsbad, CA, USA	13778-075
Opti-MEM	Life Technologies, Carlsbad, CA, USA	31985-062
Accell Delivery Medium	Dharmacon, Lafayette, Colorado, USA	B-005000-100
Virus/Transduction		
HIV packaging mix	GeneCopoeia, Rockville, MD, USA	LT001-02
eGFP positive control plasmid	GeneCopoeia, Rockville, MD, USA	LT001-02
EndoFectin™ Lenti transfection reagent	GeneCopoeia, Rockville, MD, USA	LT001-03
TiterBoost™ reagent	GeneCopoeia, Rockville, MD, USA	LT001-04
Hexadimethrine Bromide	Sigma Aldrich, St. Louis, MO, USA	107689-10G
Western Blot		
Protein Assay Dye	Bio-Rad Laboratories, Hercules, CA, USA	5000006
MagicMark™ XP Western Protein Standard	Invitrogen, Carlsbad, CA, USA	LC5602
SeeBlue® Pre-Stained Standard (1x)	Life Technologies, Carlsbad, CA, USA	LC5625
NuPAGE® Transfer Buffer	Life Technologies, Carlsbad, CA, USA	NP0006-1
NuPAGE® MOPS SDS Running Buffer	Life Technologies, Carlsbad, CA, USA	NP0001

NuPAGE® LDS Sample Buffer	Invitrogen, Carlsbad, CA, USA	NP0008
NuPAGE® 4-12% Bis-Tris Gel	Invitrogen, Carlsbad, CA, USA	NP0321BOX
Plasmids and siRNAs		
pCas-Guide CRISPR vector 1 (KN207685G1)	OriGene, Rockville, MD, USA	KN207685G1 – EQBXOCL102
pCas-Guide CRISPR vector 1 (KN207685G2)	OriGene, Rockville, MD, USA	KN207685G2 – EQBYOCL102
GFP-puro Donor plasmid (KN207685)	OriGene, Rockville, MD, USA	KN207685D – EQBW1CL302
pScramble CRISPR vector	OriGene, Rockville, MD, USA	KN207688
pCMV-LifeAct	Ibidi, Gräfelfing, Germany	60101
Accell GAPDH siRNA	Dharmacon, Lafayette, Colorado, USA	D-001930-01-05
Accell red non targeting control siRNA	Dharmacon, Lafayette, Colorado, USA	D-001960-01-05
ON-TARGETplus LCN2 siRNA	Dharmacon, Lafayette, Colorado, USA	L-003679-00-0010
ON-TARGETplus GAPDH siRNA	Dharmacon, Lafayette, Colorado, USA	L-004253-00-0020
AllStars Negative Control siRNA	Qiagen, Hilden, Germany	1027280
CP-LvC9Nu-08 (Cas9)	GeneCopoeia, Rockville, MD, USA	CP-LvC9Nu-08
HCP301765-LvSG03-3-B-a (sgRNA for LCN2)	GeneCopoeia, Rockville, MD, USA	HCP301765-LvSG03-3-B-a
HCP301765-LvSG03-3-B-b (sgRNA for LCN2)	GeneCopoeia, Rockville, MD, USA	HCP301765-LvSG03-3-B-b
HCP301765-LvSG03-3-B-c (sgRNA for LCN2)	GeneCopoeia, Rockville, MD, USA	HCP301765-LvSG03-3-B-c
Antibodies		
GAPDH mouse mAb	Thermo Fischer Scientific, Waltham, MA USA	MA5-15738
NGAL rabbit mAb	Cell Signaling Technology, Danvers, MA, USA	D4M8L
CRISPR/Cas9 mouse mAb	Novous Biologicals, Briarwood Avenue, CO, USA	NBP2-36440
Goat anti-Mouse IgG (H+L) Secondary Antibody, DyLight 800	Invitrogen, Carlsbad, CA, USA	SA5-35521
Goat anti-Rabbit IgG (H+L) Secondary Antibody, DyLight 800	Invitrogen, Carlsbad, CA, USA	SA5--35571

Ingrid Aass Roseth

Genetic Engineering for Revealing Underlying Mechanisms of Inflammatory Bowel Diseases

NTNU
Norwegian University of
Science and Technology